Asymmetric synthesis of tetrahydroisoquinoline-fused spirooxindoles as Ras-GTP inhibitors that inhibit colon adenocarcinoma cell proliferation and invasion

Qian Zhao,[a] Cheng Peng,*[a] Hua Huang,[a] Shuai-Jiang Liu,[a] Ya-Jun Zhong,[a] Wei Huang,[a] Gu He*[b] and Bo Han*[a]

[a] *School of Pharmacy, Chengdu University of Traditional Chinese Medicine, Chengdu 611137, China. E-mail: pengcheng@cdutcm.edu.cn or hanbo@cdutcm.edu.cn*

[b] *State Key Laboratory of Biotherapy, West China Hospital, Sichuan University, Chengdu 610041, China. E-mail: hegu@scu.edu.cn*

Supporting Information

Table of Contents

1. Experimental details

1.1 General methods for synthesis

- Proton nuclear magnetic resonance (^{1}H NMR) spectra were recorded with Bruker Avance III 400 MHz spectrometers. Proton chemical shifts are reported in parts per million (δ scale), and are referenced using residual protium in the NMR solvent ($CDCl_3$: δ 7.26, DMSO-d_6: δ 2.50). Data are reported as follows: chemical shift [multiplicity (s = singlet, d = doublet, t = triplet, q = quartet, m = multiplet, br s = broad singlet), coupling constant(s) (Hz), integration].
- Carbon-13 nuclear magnetic resonance (^{13}C NMR) spectra were recorded with Bruker Avance 400 MHz spectrometers. Carbon chemical shifts are reported in parts per million (δ scale), and are referenced using the carbon resonances of the solvent ($CDCl_3$: δ 77.0, DMSO-d_6: δ 39.52). Data are reported as follows: chemical shift [multiplicity (if not singlet), assignment (C_q = fully substituted carbon)].
- High resolution mass spectra (HRMS) were recorded on a Waters SYNAPT G2 using an electrospray (ESI) ionization source.
- High Performance Liquid Chromatography (HPLC) was analyzed by chiral column in comparison with authentic racemates, using a Daicel Chiralpak AD-H Column (250 x 4.6 mm), Daicel Chiralpak OD-H Column (250 x 4.6 mm), Daicel Chiralpak IC-H Column (250 x 4.6 mm) or Daicel Chiralpak AS-H Column (250 x 4.6 mm). UV detection was performed at 220 nm or 254 nm.
- Optical rotation values were measured with instruments operating at λ = 589 nm, corresponding to the sodium D line at 25 ºC.
- Column chromatography was performed on silica gel (400-500 mesh) eluting with ethyl acetate and petroleum ether. TLC was performed on glass-backed silica plates. UV light and I_2 were used to visualize products.
- Melting points were determined on a Mel-Temp apparatus and are uncorrected.

1.2 Optimization of the model reaction (Table S1) [a]

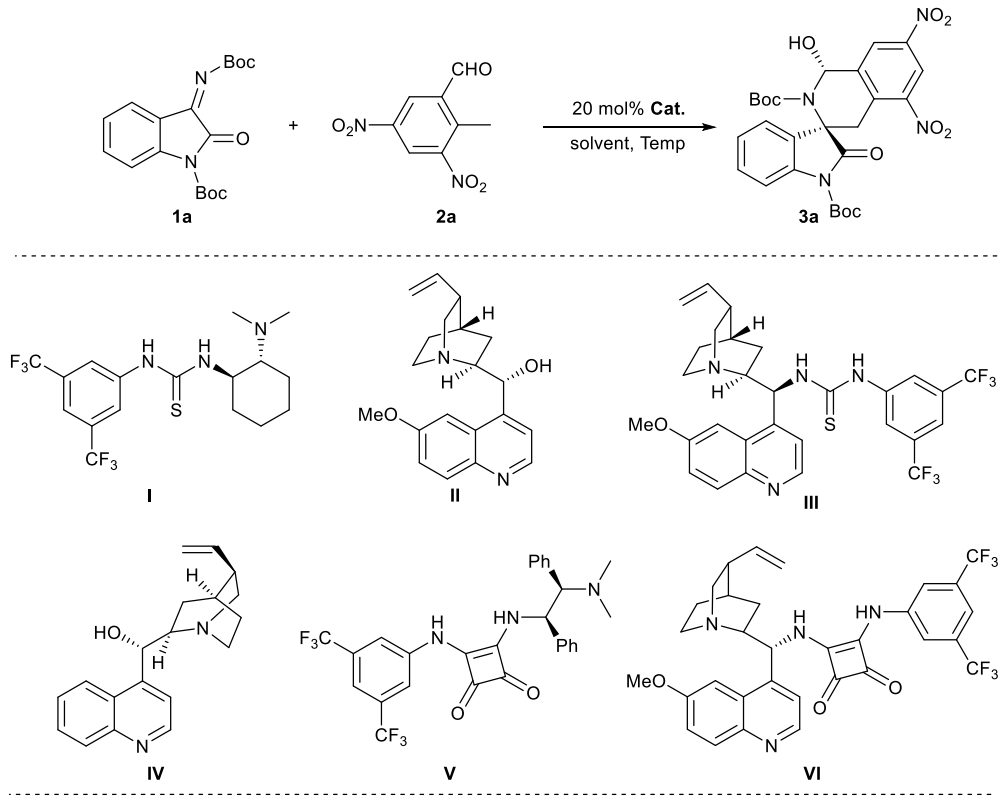

Entry	Cat.	Solvent	Yield[b]	dr[c]	*ee*[d]
1	**I**	Tol	55	65:35	70
2	**II**	Tol	57	70:30	62
3	**III**	Tol	62	55:45	55
4	**IV**	Tol	70	75:25	80
5	**V**	Tol	<10	-	-
6	**VI**	Tol	<10	-	-
7	**IV**	$CHCl_3$	n.r	-	-
8	**IV**	THF	66	78:22	78
9	**IV**	DCM	82	80:20	85
10	**IV**	MeCN	75	86:14	52
11[e]	**IV**	DCM	77	89:11	94

[a] Unless indicated otherwise, the reaction was performed with 0.25 mmol of **1a**, 0.3 mmol of **2a**, 0.05 mmol of catalyst (20 mmol%) in 2 mL solvent at 0 °C for certain time (monitored by TLC). [b] Yield of isolated **3a**. [c] Calculated based on ^{1}H NMR analysis of the crude reaction mixture. [d] Determined by HPLC using a chiral stationary phase. [e] Reaction was performed at -10 °C.

Initially, the model domino reaction of *N*-Boc-isatin ketimine **1a** and 2-methyl-3,5-dinitrobenzaldehyde **2a** proceeded smoothly in the present of Takemoto's bifunctional chiral thiourea catalyst (**I**), affording the desired product **3a** albeit in low yield (Table S1, entry 1). In order to improve the yield and stereoselectivity, more reaction parameters were screened. At first, we evaluated several chiral amine or bifunctional H-bonding catalysts (entry 2-6). Compared with **I**, quinine (**II**) and quinine-derivatived (**III**) didn't promote the stereoselectivity (entry 2-3), while cinchonine (**IV**) giving the desired product **3a** in a relatively good enantioselectivity (entry 4). Then, we switched catalyst to squaramides (**V** and **VI**), almost no desire product generated (entry 5-6). Improved results in terms of reactivity and selectivity were obtained, and catalyst **IV** was identified as the best choice (entry 5). Subsequent screening of solvents displayed that the reaction media had a significant effect on the reaction (entries 7-10). When the reaction was carried out in $CHCl_3$, no product was observed (entry 7). The solvents THF and MeCN gave only moderate yields (entry 8), and the use of MeCN resulted in a decrease of enantioselectivity (entry 10). To our satisfaction, good selectivity and yield were obtained in DCM (entry 9). We further lower the reaction temperature to -10 ^{o}C which led to a much better enantioselectivity (entry 11, 94 %), despite a slight decrease of the reaction yield, and this condition was chosen as the optimal one for further evaluation on the substrate scope.

1.3 Cell culture and cellular proliferation assay

Human colon adenocarcinoma cell lines Caco-2, HCT116, SW480 and SW620 were all derived from ATCC (American type culture collection) and cultured in our laboratory, the cells were incubated under sterile conditions at 37 °C and maintained in a humidified atmosphere 5 % CO_2 (v/v) with DMEM medium containing 10% fetal bovine serum (GIBCO, Waltham, MA, USA). MTT assays were performed to evaluate the compound's cell proliferation inhibitory activity on a panel of cancer cells. In general, cells were seeded into 96-well plates and treated with different concentrations of reagents for 48 hours. The MTT reagent (5 mg/ml) was added per well for 3 h at 37 °C. After that, MTT was removed and 150 μl DMSO was added to dissolve the formazan crystals. Then, optical density (OD) was measured at 570 nm of the solution. The control group consisted of untreated cells. The percentage of cell viability averaged from three separate experiments.

1.4 The HTRF based Ras-GTP binding assay

The His-tagged Ras protein with G12V mutation and GST-RalA-GDS Ras binding domain were produced in *E. coli* and purified as literature described. The *in vitro* binding inhibition assays of test compounds are using the HTRF based method provided by Cisbio Co. Ltd., in brief, the HTRF assay used a His-tagged Ras protein and the GST-tagged RalA-GDS (RalA guanine nucleotide dissociation stimulator) RBD domain and two HTRF detection reagents are added. The HTRF signal is proportional to the amount of interaction between GST-tagged RalA and His-tagged Ras protein, detailed experimental procedures are based on the manufacturer’s protocols.

1.5 Apoptosis assay by Flow Cytometry (FCM) and fluorescent microscopy

$5*10^3$ of HCT116 cells were seeded in six-well plates for 12 hours, and then treated with compound **3m** (0.5 or 2 μM, respectively) or vehicle for 24 hours. Cells were collected, then fixed with 75% ice-cold ethanol and stored at -20 °C for another one hour. Flow cytometry was used to detect the apoptosis-inducing effect of different micelles. HCT116 cells treated with compound **3m** or blank solvent (control) were gently trypsinized without EDTA and centrifuged at 2000 rpm for 5 minutes. Then, harvested cells were washed with 1.0 ml ice cold PBS and re-suspended in 500 μl 1×binding buffer, and incubated with 5 μl of Annexin V-FITC and 5 μl of propidium iodide (PI) for

15 min at room temperature. Followed by FCM (BD FACS Calibur, BD, USA) using the FL1 channel for Annexin V-FITC and the FL2 channel of PI. Detection of apoptosis include early (Annexin V+/PI-) and late apoptotic cells (Annexin V+/PI+). In addition, HCT116 cells were plated in six-well plates, grew and adhered for 24 hours, then incubated with 0.5 or 2 μM of compound **3m** for an additional 12 hours followed by Hoechst 33258 addition. The morphology of nuclei was visualized under an Olympus fluorescence microscope.

1.6 Wound healing and transwell assays

For wound healing assay, HCT116 cells were cultured in six-well microplates and scratch-wounded by sterilized pipettes. Then the cells were washed with PBS and cultured with normal saline or compound **3m**. After incubating for 24 h, pictures were taken by phase-contrast microscope. For transwell assay, HCT116 cells were cultured in 10-cm plates, and add fresh medium 18h before each assay. Cells were trypsinized, washed twice, and then resuspended in serum-free medium. The final cell density was determined by a hemocytometer. The lower wells of transwell chamber apparatus were loaded with DMEM containing 10% serum. A 200-μl cell suspension which containing 10,000 cells were added to each upper well. The loaded chamber was incubated for 24 h at 37°C, and then removed from the incubator and disassembled. Cells on the upper surface of the membrane were scraped, only the cells that have migrated through the membrane remained. The membrane was then fixed with methanol, stained with 0.1% crystal violet, and air dried. The number of cells is obtained by calculating the cells in each field, and data are presented as an average from five fields of triplicate wells for each test condition.

1.7 GST pull down assay and western blot analysis

In order to analyze the effects of compound **3m** on the binding of Ras-GTP and substrate RalA protein, HCT116 cells were seeded in six-plate dishes and cultured for 5 hours, after which cells were washed and lysed as described above. Lysates were cleared by centrifugation at 16,000 g for 5 min, and supernatants were incubated with 10μl of GST-tagged Ras-GTP bound to glutathione-Sepharose (GSH) beads for 1 h at 4°C with rocking as previously described. The beads were washed twice with lysis buffer, resuspended in Laemmli electrophoresis sample buffer,

resolved, and immunoblotted for activated RalA as described above. For WB assay, the different concentrations of drug treated cells were harvested and washed with cold 1×PBS. Total cell lysates were prepared in lysis RIPA buffer (Invitrogen, CA, USA) on ice for 30 min, followed by centrifugation at 13000 rpm for 30 min at 4°C. After collecting supernatant, protein concentration was determined by a bicinchoninic acid protein assay kit (Thermo, USA). The protein was resolved on a 10-15% SDS-PAGE, electro blotted onto nitrocellulose membranes, and then incubated with proper primary antibodies which were purchased from Cell Signaling Technology or Santa Cruz Biotechnology and secondary antibodies before visualization by chemiluminescence Kit (Millpore, USA).

1.8 Molecular docking

The molecular docking of **3m** and **3m'** to Ras-GTP protein were processed by the LibDock and CDOCKER modules of Accelrys Discovery Studio (version 3.5). The initial structures of **3m** and **3m'** were generated from the crystallized structure of **3m** and then minimized by Gaussian09 package at B3LYP/6-31*G level. Then the energy minimization of **3m** and **3m'** with Ras-GTP protein were performed by the CHARMm force field. All residues of Ras-GTP within 10 Å from the binding site of ligand were defined as the binding sphere. Additionally, Smart Minimizer and CAESAR (Conformer Algorithm based on Energy Screening and Recursive build-up) were applied for in situ ligand minimization and generating ligand conformations, respectively.

2. Asymmertric synthesis of THIQ-fused spirooxindole derivates

2.1 Procedure for the asymmetrics of 3

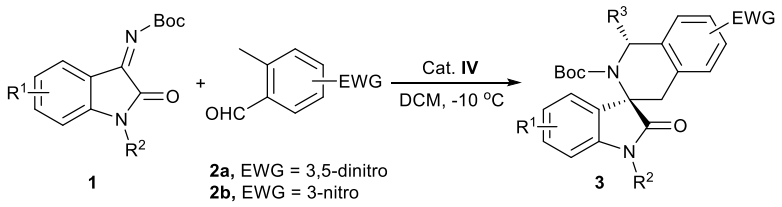

The reaction was carried out with ketimine **1** (0.25 mmol) and 2-methylbenzaldehyde **2** (0.3 mmol), catalyst **IV** (0.05 mmol) in DCM (2 mL) under an open atmosphere at -10 °C until the reaction was completed (monitored by TLC). Then the reaction mixture was concentrated and the residue was purified by flash chromatography on silica gel (petroleum ether/ethyl acetate = 12:1) to give THIQ-fused spirooxindole **3**, which was further analyzed by ^{1}H NMR, ^{13}C HMR, HRMS and chiral HPLC analysis.

di-tert-butyl(*1'R,3R*)-1'-hydroxy-5',7'-dinitro-2-oxo-1',4'-dihydro-2'H-spiro[indoline-3,3'-isoquinoline]-1,2'- dicarboxylate

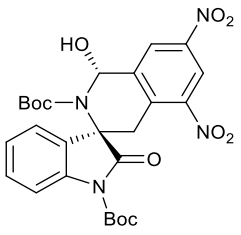

3a

Prepared according to the general procedure using *tert*-butyl-3-((tert-butoxycarbonyl)imino)-2-oxoindoline-1-carboxylate (86.6 mg, 0.25 mmol) and 2-methyl-3,5-dinitrobenzaldehydes (63.0 mg, 0.3 mmol). Purification of the crude product via column chromatography delivered **3a** as a white solid with 77% yield (106.8 mg). The dr value was calculated to be 89:11 by ^{1}H NMR analysis of the crude reaction mixture, and the enantiomeric excess was determined to be 94% by HPLC on Chiralpak OD-H column at 254nm (Hexane/isopropanol = 95/5, 1 mL/min), t_{major} = 17.50 min, t_{minor} = 22.79 min; $[\alpha]_D^{20}$ = -108.2 (C = 1.16, CH_2Cl_2); m.p. 152-153 °C.

NMR and HRMS data for the product **3a**:

^{1}H NMR (400 MHz, $CDCl_3$): δ = 8.87 (d, *J* = 2.0 Hz, 1H), 8.50 (d, *J* = 2.0 Hz, 1H), 7.93 (d, *J* = 8.0 Hz, 1H), 7.45 (d, *J* = 7.2 Hz, 1H), 7.41 (dd, *J* = 8.0, 1.6 Hz, 1H), 7.28-7.24 (m, 1H), 6.94 (d, *J* = 4.0 Hz, 1H), 4.56 (br s, 1H), 3.88 (d, *J* = 16.4 Hz, 1H), 3.78 (d, *J* = 16.4 Hz, 1H), 1.58 (s, 9H), 1.07 (s, 9H) ppm.

^{13}C NMR (100 MHz, $CDCl_3$): δ = 173.07, 153.6, 149.1, 148.1, 146.5, 141.7, 139.2, 135.3, 130.3, 129.8, 125.3, 125.1, 122.3, 120.4, 115.4, 84.8, 83.8, 62.0, 33.9, 28.0, 27.5 ppm.

HRMS (ESI): *m/z* calculated for $C_{26}H_{28}N_4O_{10}$+Na: 579.1703, found 579.1704.

di-tert-butyl(*1'R,3R*)-5-chloro-1'-hydroxy-5',7'-dinitro-2-oxo-1',4'-dihydro-2'H-spiro[indoline-3,3'- isoquinoline]-1,2'-dicarboxylate

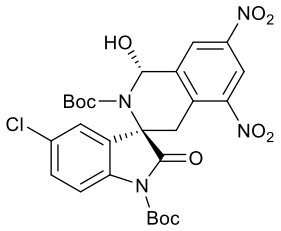

3b

Prepared according to the general procedure using *tert*-butyl-3-((tert-butoxycarbonyl) imino)-5-chloro-2-oxoindoline-1-carboxylate (95.2 mg, 0.25 mmol) and 2-methyl-3,5-dinitrobenzaldehydes (63.0 mg, 0.3 mmol). Purification of the crude product via column chromatography delivered **3b** as a white solid with 75% yield (110.3 mg). The dr value was calculated to be 86:14 by ^{1}H NMR analysis of the crude reaction mixture, and the enantiomeric excess was determined to be 94% by HPLC on Chiralpak AD-H column at 254nm (Hexane/isopropanol = 90/10, 1 mL/min), t_{minor} = 9.79 min, t_{major} = 11.56 min; $[\alpha]_D^{20}$ = -50.8 (C = 0.788, CH_2Cl_2); m.p. 174-175 °C.

NMR and HRMS data for the product **3b**:

^{1}H NMR (400 MHz, $CDCl_3$): δ = 8.88 (d, *J* = 2.4 Hz, 1H), 8.48 (d, *J* = 2.4 Hz, 1H), 7.90 (d, *J* = 8.8 Hz, 1H), 7.45 (d, *J* = 2.0 Hz, 1H), 7.40 (dd, *J* = 8.8, 2.4 Hz, 1H), 6.94 (d, *J* = 3.6 Hz, 1H), 4.51 (br s, 1H), 3.87 (d, *J* = 16.8 Hz, 1H), 3.79 (d, *J* = 16.8 Hz, 1H), 1.57 (s, 9H), 1.11 (s, 9H) ppm;

^{13}C NMR (100 MHz, $CDCl_3$): δ = 172.4, 153.2, 148.9, 148.4, 146.6, 141.7, 137.7, 134.8, 132.1, 130.8, 129.8, 125.0, 122.7, 120.5, 116.8, 85.2, 84.2, 61.8, 33.7, 28.0, 27.6 ppm;

HRMS (ESI): *m/z* calculated for $C_{26}H_{27}ClN_4O_{10}$+Na: 613.1313, found 613.1309.

di-tert-butyl(*1'R,3R*)-6-chloro-1'-hydroxy-5',7'-dinitro-2-oxo-1',4'-dihydro-2'H-spiro[indoline-3,3'- isoquinoline]-1,2'-dicarboxylate

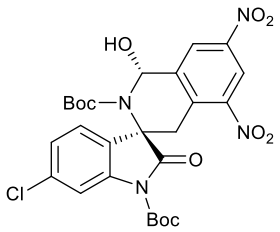

3c

Prepared according to the general procedure using *tert*-butyl- 3-((tert-butoxycarbonyl) imino)-6-chloro-2-oxoindoline-1-carboxylate (95.2 mg, 0.25 mmol) and 2-methyl-3,5-dinitrobenzaldehydes (63.0 mg, 0.3 mmol). Purification of the crude product via column chromatography delivered **3c** as a white solid with 80% yield (117.8 mg). The dr value was calculated to be 92:8 by ^{1}H NMR analysis of the crude reaction mixture, and the enantiomeric excess was determined to be 95% by HPLC on Chiralpak AD-H column at 254nm (Hexane/isopropanol = 90/10, 1 mL/min), t_{major} = 7.27 min, t_{minor} = 8.43 min; $[\alpha]_D^{20}$ = -90.2 (C = 0.244, CH_2Cl_2); m.p. 186-187 ºC.

NMR and HRMS data for the product **3c**:

^{1}H NMR (400 MHz, $CDCl_3$): δ = 8.88 (d, *J* = 2.0 Hz, 1H), 8.48 (d, *J* = 2.0 Hz, 1H), 8.02 (d, *J* = 2.0 Hz, 1H), 7.39 (d, *J* = 8.0 Hz, 1H), 7.28 (d, *J* = 2.0 Hz, 1H), 6.92 (d, *J* = 4.0 Hz, 1H), 4.29 (br s, 1H), 3.84 (d, *J* = 16.8 Hz, 1H), 3.77 (d, *J* = 16.8 Hz, 1H), 1.58 (s, 9H), 1.12 (s, 9H) ppm.

^{13}C NMR (100 MHz, $CDCl_3$): δ = 172.6, 153.3, 148.8, 148.4, 146.6, 141.6, 140.1, 135.6, 134.8, 128.7, 125.4, 125.0, 123.3, 120.5, 116.1, 85.4, 84.1, 61.7, 33.7, 28.0, 27.6 ppm.

HRMS (ESI): *m/z* calculated for $C_{26}H_{27}ClN_4O_{10}$+Na: 613.1313, found 613.1315.

di-tert-butyl(*1'R,3R*)-5-bromo-1'-hydroxy-5',7'-dinitro-2-oxo-1',4'-dihydro-2'H-spiro[indoline 3,3'- isoquinoline]-1,2'-dicarboxylate

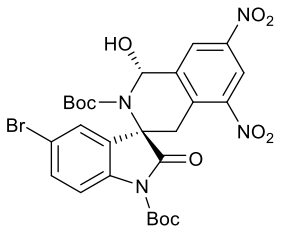

3d

Prepared according to the general procedure using *tert*-butyl-5-bromo 3-((tert-butoxycarbonyl) imino)-2-oxoindoline-1-carboxylate (106.3 mg, 0.25 mmol) and 2-methyl-3,5-dinitrobenzaldehydes (63.0 mg, 0.3 mmol). Purification of the crude product via column chromatography delivered **3d** as a white solid with 71% yield (112.2 mg). The dr value was calculated to be 88:12 by ^{1}H NMR analysis of the crude reaction mixture, and the enantiomeric excess was determined to be 97% by HPLC on Chiralpak AD-H column at 254nm (Hexane/isopropanol = 90/10, 1 mL/min), t_{minor} = 9.22 min, t_{major} = 11.22 min; $[\alpha]_D^{20}$ = -48.1 (C = 0.788, CH_2Cl_2); m.p. 103-105 ^{o}C.

NMR and HRMS data for the product **3d**:

^{1}H NMR (400 MHz, $CDCl_3$): δ = 8.88 (d, *J* = 2.0 Hz, 1H), 8.48 (d, *J* = 2.4 Hz, 1H), 7.85 (d, *J* = 8.8 Hz, 1H), 7.59 (d, *J* = 1.6 Hz, 1H), 7.56 (dd, *J* = 8.8, 2.4 Hz, 1H), 6.94 (d, *J* = 3.6 Hz, 1H), 4.50 (br s, 1H), 3.87 (d, *J* = 16.8 Hz, 1H), 3.79 (d, *J* = 16.8 Hz, 1H), 1.53 (s, 9H), 1.11 (s, 9H) ppm;

^{13}C NMR (100 MHz, $CDCl_3$): δ = 172.3, 153.2, 148.9, 148.4, 146.6, 141.7, 138.2, 134.8, 132.7, 132.4, 125.5, 125.0, 120.5, 118.2, 117.2, 85.3, 84.2, 61.8, 33.7, 28.00, 27.6 ppm;

HRMS (ESI): *m/z* calculated for $C_{26}H_{27}BrN_4O_{10}$+Na: 657.0808, found 657.0810.

<u>di-tert-butyl(*1'R,3R*)-6-bromo-1'-hydroxy-5',7'-dinitro-2-oxo-1',4'-dihydro-2'H-spiro[indoline-3,3'-isoquinoline]-1,2'-dicarboxylate</u>

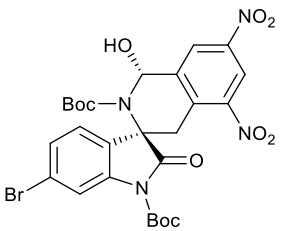

3e

Prepared according to the general procedure using *tert*-butyl-6-bromo 3-((tert-butoxycarbonyl) imino)-2-oxoindoline-1-carboxylate (106.3 mg, 0.25 mmol,) and 2-methyl-3,5-dinitrobenzaldehydes (63.0 mg, 0.3 mmol). Purification of the crude product via column chromatography delivered **3e** as a white solid with 78% yield (123.5 mg). The dr value was calculated to be 90:10 by ^{1}H NMR analysis of the crude reaction mixture, and the enantiomeric excess was determined to be 92% by HPLC on Chiralpak AD-H column at 254nm (Hexane/isopropanol = 90/10, 1 mL/min), t_{major} = 8.36 min, t_{minor} = 9.75 min. $[\alpha]_D^{20}$ = -60.5 (C = 0.352, CH_2Cl_2); m.p. 188-190 ºC.

NMR and HRMS data for the product **3e**:

^{1}H NMR (400 MHz, $CDCl_3$): δ = 8.88 (d, *J* = 2.0 Hz, 1H), 8.48 (d, *J* = 2.0 Hz, 1H), 8.18 (d, *J* = 5.6 Hz, 1H), 7.44 (d, *J* = 7.6, 1.6 Hz, 1H), 7.33 (d, *J* = 8.0 Hz, 1H), 6.93 (d, *J* = 4.0 Hz, 1H), 4.42 (br s, 1H), 3.84 (d, *J* = 16.8 Hz, 1H), 3.77 (d, *J* = 16.8 Hz, 1H), 1.58 (s, 9H), 1.12 (s, 9H) ppm.

^{13}C NMR (100 MHz, $CDCl_3$): δ = 172.5, 153.3, 148.8, 148.4, 146.5, 141.6, 140.2, 134.8, 129.2, 128.3, 125.0, 123.6, 123.4, 120.5, 118.9, 85.4, 84.2, 61.7, 33.6, 28.0, 27.6 ppm.

HRMS (ESI): *m/z* calculated for $C_{26}H_{27}BrN_4O_{10}$+Na: 657.0808, found 657.0812.

di-tert-butyl(*1'R,3R*)-5-fluoro-1'-hydroxy-5',7'-dinitro-2-oxo-1',4'-dihydro-2'H-spiro[indoline-3,3'- isoquinoline]-1,2'-dicarboxylate

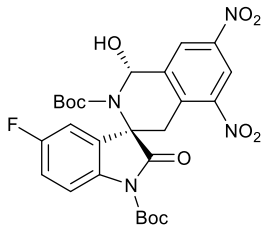

3f

Prepared according to the general procedure using *tert*-butyl- 3-((tert-butoxycarbonyl) imino)-5-fluoro-2-oxoindoline-1-carboxylate (91.1 mg, 0.25 mmol) and 2-methyl-3,5-dinitrobenzaldehydes (63.0 mg, 0.3 mmol). Purification of the crude product via column chromatography delivered **3f** as a white solid with 73% yield (104.7 mg). The dr value was calculated to be 88:12 by ^{1}H NMR analysis of the crude reaction mixture, and the enantiomeric excess was determined to be 95% by HPLC on Chiralpak AD-H column at 254nm

(Hexane/isopropanol = 90/10, 1 mL/min), t_{minor} = 7.97 min, t_{major} = 10.97 min; $[\alpha]_D^{20}$ = -35.8 (C = 0.062, CH_2Cl_2); m.p. 186-187 °C.

NMR and HRMS data for the product **3f**:

^{1}H NMR (400 MHz, $CDCl_3$): δ = 8.88 (d, *J* = 2.0 Hz, 1H), 8.49 (d, *J* = 2.0 Hz, 1H), 7.93 (dd, *J* = 8.8, 4.4 Hz, 1H), 7.21 (d, *J* = 2.0 Hz, 1H), 7.13 (td, *J* = 8.8, 2.8 Hz, 1H), 6.94 (d, *J* = 3.6 Hz, 1H), 4.55 (br s, 1H), 3.86 (d, *J* = 16.8 Hz, 1H), 3.80 (d, *J* = 16.8 Hz, 1H), 1.58 (s, 9H), 1.11 (s, 9H) ppm.

^{13}C NMR (100 MHz, $CDCl_3$): δ = 172.7, 160.4 (d, *J*=243.0), 153.3 (d, *J*=2.6), 149.0, 148.4, 146.6, 141.7, 135.1 (d, *J*=2.5), 134.8, 132.1 (d, *J*=7.2), 125.0, 120.5, 117.0 (d, *J*=7.5), 116.3 (d, *J*=227.0), 110.0 (d, *J*=245.0), 85.1, 84.2, 67.0, 33.7, 28.0, 27.5 ppm.

HRMS (ESI): m/z calculated for $C_{26}H_{27}FN_4O_{10}$+Na: 597.1609, found 597.1611.

di-tert-butyl(*1'R,3R*)-1'-hydroxy-5,5',7'-trinitro-2-oxo-1',4'-dihydro-2'H-spiro[indoline-3,3'-isoquinli-ne]-1,2'-dicarboxylate

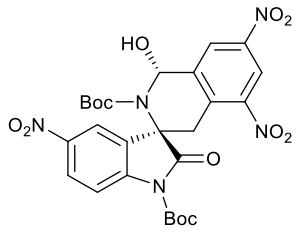

3g

Prepared according to the general procedure using *tert*-butyl-3-((tert-butoxycarbonyl)imino)-5-nitro-2-oxoindoline-1-carboxylate (97.9 mg, 0.25 mmol) and 2-methyl-3,5- dinitrobenzaldehydes (63.0 mg, 0.3 mmol). Purification of the crude product via column chromatography delivered **3g** as a white solid with 73% yield (109.3 mg). The dr value was calculated to be 85:15 by ^{1}H NMR analysis of the crude reaction mixture, and the enantiomeric excess was determined to be 94% by HPLC on Chiralpak AD-H column at 254nm (Hexane/isopropanol = 90/10, 1 mL/min), t_{minor} = 15.04 min, t_{major} = 20.46 min; $[\alpha]_D^{20}$ = -56.7 (C = 0.114, CH_2Cl_2); m.p. 125-126 °C.

NMR and HRMS data for the product **3g**:

^{1}H NMR (400 MHz, $CDCl_3$): δ = 8.89 (d, *J* = 2.0 Hz, 1H), 8.52 (d, *J* = 2.0 Hz, 1H), 8.37 (dd, *J* = 8.8, 2.4 Hz, 1H), 8.34 (d, *J* = 2.4 Hz, 1H), 8.15 (d, *J* = 8.8 Hz, 1H), 6.99 (s, 1H), 4.68 (br s, 1H), 3.93 (d, *J* = 16.8 Hz, 1H), 3.83 (d, *J* = 16.8 Hz, 1H), 1.59 (s, 9H), 1.10 (s, 9H) ppm.

^{13}C NMR (100 MHz, $CDCl_3$): δ = 172.2, 152.7, 148.6, 148.5, 146.7, 145.1, 144.4, 141.8, 134.2, 131.9, 126.0, 125.0, 120.6, 118.2, 115.7, 86.2, 84.5, 61.6, 33.3, 28.0, 27.6 ppm.

HRMS (ESI): *m/z* calculated for $C_{26}H_{27}N_5O_{12}$+Na: 624.1554, found 624.1551.

di-tert-butyl(*1'R,3R*)-5-methyl-1'-hydroxy-5',7'-dinitro-2-oxo-1',4'-dihydro-2'H-spiro[indoline-3,3'- isoquinoline]-1,2'-dicarboxylate

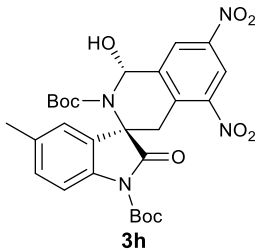

3h

Prepared according to the general procedure using *tert*-butyl- 3-((tert-butoxycarbonyl) imino)-5-methyl-2-oxoindoline-1-carboxylate (90.1mg, 0.25 mmol) and 2-methyl-3,5-dinitrobenzaldehydes (63.0 mg, 0.3 mmol). Purification of the crude product via column chromatography delivered **3h** as a white solid with 70% yield (100.5 mg). The dr value was calculated to be 87:13 by ^{1}H NMR analysis of the crude reaction mixture and the enantiomeric excess was determined to be 95% by HPLC on Chiralpak AD-H column at 254nm (Hexane/isopropanol = 90/10, 1 mL/min), t_{minor} = 6.80 min, t_{major} = 10.33 min; $[\alpha]_D^{20}$ = -25.4 (C=0.100, CH_2Cl_2); m.p. 157-158 °C.

NMR and HRMS data for the product **3h**:

^{1}H NMR (400 MHz, $CDCl_3$): δ = 8.87 (d, *J* = 2.4 Hz, 1H), 8.47 (d, *J* = 2.4 Hz, 1H), 7.79 (d, *J* = 8.0 Hz, 1H), 7.25-7.21 (m, 2H), 6.92 (d, *J* = 3.2 Hz, 1H), 4.40 (br s, 1H), 3.87 (d, *J* = 16.8 Hz, 1H), 3.76 (d, *J* = 16.8 Hz, 1H), 2.40 (s, 3H), 1.58 (s, 9H), 1.07 (s, 9H) ppm;

^{13}C NMR (100 MHz, $CDCl_3$): δ = 173.2, 153.7, 149.1, 148.4, 146.4, 141.7, 136.8, 135.4, 135.2, 130.2, 125.0, 122.8, 120.4, 115.3, 84.6, 83.7, 62.1, 34.0, 28.0, 27.5, 21.1 ppm;

ESI HRMS(m/z): calcd. for $C_{27}H_{30}N_4O_{10}$+Na 593.1860, found 593.1863.

tert-butyl(*1'R,3R*)-1-benzyl-1'-hydroxy-5',7'-dinitro-2-oxo-1',4'-dihydro-2'H-spiro[indoline-3,3'-isoquinoline]-2'-carboxylate

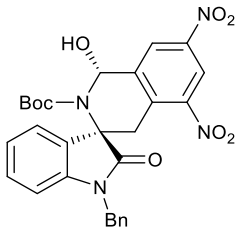

3i

Prepared according to the general procedure using *tert*-butyl-(1-benzyl-2-oxoindolin-3-ylidene) carbamate (84.1mg, 0.25 mmol) and 2-methyl-3,5-dinitrobenzaldehydes (63.0 mg, 0.3 mmol). Purification of the crude product via column chromatography delivered **3i** as a white solid with 74% yield (101.6 mg). The dr value was calculated to be 93:7 by ^{1}H NMR analysis of the crude reaction mixture, and the enantiomeric excess was determined to be 94% by HPLC on Chiralpak IC-H column at 254nm (Hexane/isopropanol = 80/20, 1 mL/min), t_{major} = 7.58 min, t_{minor} = 19.01 min; $[\alpha]_D^{20}$ = +26.3 (C = 0.140, CH_2Cl_2); m.p. 106-107 ºC.

NMR and HRMS data for the product **3i**:

^{1}H NMR (400 MHz, $CDCl_3$): δ = 8.87 (d, *J* = 2.0 Hz, 1H), 8.49 (d, *J* = 2.0 Hz, 1H), 7.41-7.35 (m, 3H), 7.32-7.27 (m, 4H), 7.15-7.11 (m, 1H), 6.98 (d, *J* = 4.0 Hz, 1H), 6.83 (d, *J* = 7.6 Hz, 1H), 5.18 (d, *J* = 15.2 Hz, 1H), 4.47 (br s, 1H), 4.36 (d, *J* = 15.2 Hz, 1H), 3.93 (d, *J* = 16.4 Hz, 1H), 3.77 (d, *J* = 16.0 Hz, 1H), 1.02 (s, 9H) ppm.

^{13}C NMR (100 MHz, $CDCl_3$): δ = 175.2, 153.8, 148.4, 146.4, 141.9, 141.8, 135.8, 135.5, 131.4, 129.4, 129.0, 128.0, 127.6, 125.0, 123.4, 122.1, 120.4, 109.4, 83.1, 62.2, 44.0, 33.7, 27.6 ppm.

HRMS (ESI): *m/z* calculated for $C_{28}H_{26}N_4O_8$+Na: 569.1648, found 569.1651.

tert-butyl(*1'R,3R*)-1-benzyl-5-chloro-1'-hydroxy-5',7'-dinitro-2-oxo-1',4'-dihydro-2'H-spiro[indoline-3,3'-isoquinoline]-2'-carboxylate

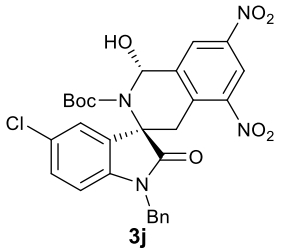

3j

Prepared according to the general procedure using *tert*-butyl-(1-benzyl-5-chloro-oxoindolin-3-ylidene) carbamate (92.7 mg, 0.25 mmol) and 2-methyl-3,5-dinitrobenzaldehydes (63.0 mg, 0.3 mmol). Purification of the crude product via column chromatography delivered **3j** as a white solid with 71% yield (102.8 mg). The dr value was calculated to be 90:10 by ^{1}H NMR analysis of the crude reaction mixture and the enantiomeric excess was determined to be 97% by HPLC on Chiralpak IC-H column at 254nm (Hexane/isopropanol = 80/20, 1 mL/min), t_{major} = 6.71 min, t_{minor} = 15.64 min; $[\alpha]_D^{20}$ = -26.6 (C = 0.380, CH_2Cl_2); m.p. 169-170ºC.

NMR and HRMS data for the product **3j**:

^{1}H NMR (400 MHz, $CDCl_3$): δ = 8.88 (d, *J* = 2.0 Hz, 1H), 8.50 (d, *J* = 2.4 Hz, 1H), 7.39-7.36 (m, 3H), 7.32-7.27 (m, 3H), 7.24 (d, *J* = 2.0 Hz, 1H), 6.98 (d, *J* = 4.0 Hz, 1H), 6.74 (d, *J* = 8.4 Hz, 1H), 5.17 (d, *J* = 15.2 Hz, 1H), 4.43 (br s, 1H), 4.35 (d, *J* = 12.8 Hz, 1H), 3.91 (d, *J* = 16.0 Hz, 1H), 3.78 (d, *J* = 16.0 Hz, 1H), 1.08 (s, 9H) ppm;

^{13}C NMR (100 MHz, $CDCl_3$): δ = 174.8, 153.2, 148.4, 146.5, 141.6, 140.4, 135.3, 135.1, 133.1, 129.2, 129.1, 128.9, 128.2, 127.5, 125.1, 122.7, 120.5, 110.5, 83.5, 62.1, 44.1, 33.4, 27.7 ppm;

HRMS (ESI): *m/z* calculated for $C_{28}H_{25}ClN_4O_8$+Na: 603.1259, found 603.1260.

tert-butyl(*1'R,3R*)-1-benzyl-6-chloro-1'-hydroxy-5',7'-dinitro-2-oxo-1',4'-dihydro-2'H-spiro[indoline-3,3'-isoquinoline]-2'-carboxylate

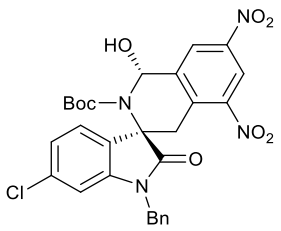

3k

Prepared according to the general procedure using *tert*-butyl-(1-benzyl- 6-chloro-oxoindolin-

3-ylidene) carbamate (92.7 mg, 0.25 mmol) and 2-methyl-3,5-dinitrobenzaldehydes (63.0 mg, 0.3 mmol). Purification of the crude product via column chromatography delivered **3k** as a white solid with 78% yield (112.6 mg). The dr value was calculated to be 92:8 by ^{1}H NMR analysis of the crude reaction mixture, and the enantiomeric excess was determined to be 93% by HPLC on Chiralpak IC-H column at 254nm (Hexane/isopropanol = 80/20, 1 mL/min), t_{major} = 6.36 min, t_{minor} = 12.42 min; $[\alpha]_D^{20}$ = +34.3 (C = 0.096, CH_2Cl_2); m.p. 153-155 °C.

NMR and HRMS data for the product **3k**:

^{1}H NMR (400 MHz, $CDCl_3$): δ = 8.88 (d, *J* = 2.0 Hz, 1H), 8.49 (d, *J* = 2.0 Hz, 1H), 7.41-7.36 (m, 2H), 7.34-7.29 (m, 4H), 7.11 (d, *J* = 8.0 Hz, 1H), 6.96 (d, *J* = 3.6 Hz, 1H), 6.82 (d, *J* = 1.6 Hz, 1H), 5.16 (d, *J* = 15.6 Hz, 1H), 4.34 (d, *J* = 14.0 Hz, 1H), 4.24 (br s, 1H), 3.89 (d, *J* = 16.4 Hz, 1H), 3.76 (d, *J* = 16.4 Hz, 1H), 1.08 (s, 9H) ppm.

^{13}C NMR (100 MHz, $CDCl_3$): δ = 175.1, 148.4, 146.5, 143.1, 141.6, 135.3, 135.2, 134.9, 129.2, 128.3, 127.5, 125.1, 123.3, 123.1, 120.5, 110.0, 83.4, 61.8, 44.1, 33.5, 27.7 ppm.

HRMS (ESI): *m/z* calculated for $C_{28}H_{25}ClN_4O_8$+Na: 603.1259, found 603.1256.

tert-butyl(*1'R,3R*)-1-benzyl-4-bromo-1'-hydroxy-5',7'-dinitro-2-oxo-1',4'-dihydro-2'H-spiro[indoline-3,3'-isoquinoline]-2'-carboxylate

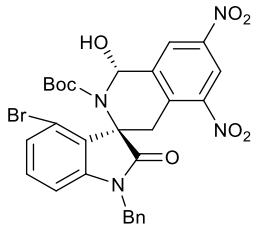

3l

Prepared according to the general procedure using *tert*-butyl-(1-benzyl- 4-bromo-oxoindolin-3-ylidene) carbamate (103.8 mg, 0.25 mmol) and 2-methyl-3,5-dinitrobenzaldehydes (63.0 mg, 0.3 mmol). Purification of the crude product via column chromatography delivered **3l** as a white solid with 54% yield (84.7 mg). The dr value was calculated to be 95:5 by ^{1}H NMR analysis of the crude reaction mixture, and the enantiomeric excess was determined to be 92% by HPLC on Chiralpak IC-H column at 254nm (Hexane/isopropanol = 80/20, 1 mL/min), t_{major} = 8.40, t_{minor} = 15.37 min; $[\alpha]_D^{20}$ = +51.5 (C=0.120, CH_2Cl_2); m.p. 147-148 °C.

NMR and HRMS data for the product **3l**:

^{1}H NMR (400 MHz, $CDCl_3$): δ = 8.87 (d, *J* = 2.0 Hz, 1H), 8.50 (d, *J* = 2.0 Hz, 1H), 7.36-7.28 (m, 3H), 7.23 (d, *J* = 8.8 Hz, 2H), 7.14 (t, *J* = 8.0 Hz, 1H), 6.96 (d, *J* = 2.0 Hz, 1H), 6.80 (d, *J* = 8.0 Hz, 1H), 4.93 (d, *J* = 15.2 Hz, 1H), 4.54 (d, *J* = 15.6 Hz, 1H) , 4.47 (d, *J* = 16.4 Hz, 1H), 3.90 (br s, 1H), 3.62 (d, *J* = 16.4 Hz, 1H), 3.49 (s, 1H), 0.99 (s, 9H) ppm;

^{13}C NMR (100 MHz, $CDCl_3$): δ = 174.4, 153.7, 148.7, 146.6, 143.6, 141.1, 135.2, 135.0, 130.5, 129.0, 128.2, 127.7, 127.5, 125.6, 120.5, 117.6, 108.9, 83.1, 79.0, 63.7, 44.2, 31.6, 27.5 ppm;

HRMS (ESI): *m/z* calculated for $C_{28}H_{25}BrN_4O_8$+Na: 647.0753, found 647.0754.

tert-butyl(*1'R,3R*)-1-benzyl-5-bromo-1'-hydroxy-5',7'-dinitro-2-oxo-1',4'-dihydro-2'H-spiro[indoline-3,3'-isoquinoline]-2'-carboxylate

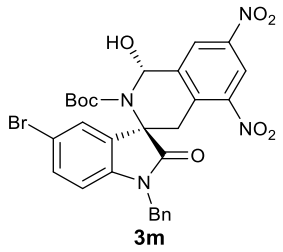

3m

Prepared according to the general procedure using *tert*-butyl-(1-benzyl- 5-bromo-oxoindolin-3-ylidene) carbamate (103.8 mg, 0.25 mmol) and 2-methyl-3,5-dinitrobenzaldehydes (63.0 mg, 0.3 mmol). Purification of the crude product via column chromatography delivered **3m** as a white solid with 70% yield (109.5 mg). The dr value was calculated to be 89:11 by ^{1}H NMR analysis of the crude reaction mixture, and the enantiomeric excess was determined to be 94% by HPLC on Chiralpak IC-H column at 254nm (Hexane/isopropanol = 80/20, 1 mL/min), t_{major} = 6.68 min, t_{minor} = 15.25 min; $[\alpha]_D^{20}$ = -25.3 (C=0.183, CH_2Cl_2); m.p. 146-147 °C.

NMR and HRMS data for the product **3m**:

^{1}H NMR (400 MHz, $CDCl_3$): δ = 8.88 (d, *J* = 2.4 Hz, 1H), 8.50 (d, *J* = 2.0 Hz, 1H), 7.51 (d, *J* = 1.6 Hz, 1H), 7.42-7.35 (m, 3H), 7.32-7.28 (m, 3H), 6.98 (d, *J* = 4.0 Hz, 1H), 6.70 (d, *J* = 8.0 Hz, 1H), 5.17 (d, *J* = 15.2 Hz, 1H), 4.35 (d, *J* = 12.0 Hz, 2H), 3.91 (d, *J* = 16.0 Hz, 1H), 3.78 (d, *J* = 16.0 Hz, 1H), 1.08 (s, 9H) ppm.

^{13}C NMR (100 MHz, $CDCl_3$): δ = 174.7, 153.3, 148.4, 146.5, 141.6, 140.9, 135.3, 135.0, 133.4, 132.1, 129.1, 128.2, 127.5, 125.4, 125.1, 120.5, 116.0, 111.0, 83.5, 62.0, 44.1, 33.4, 27.7 ppm.

HRMS (ESI): *m/z* calculated for $C_{28}H_{25}BrN_4O_8$+Na: 647.0753, found 647.0750.

tert-butyl(*1'R,3R*)-1-benzyl-6-bromo-1'-hydroxy-5',7'-dinitro-2-oxo-1',4'-dihydro-2'H-spiro[indoline-3,3'-isoquinoline]-2'-carboxylate

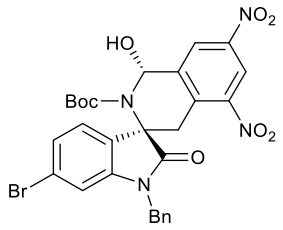

3n

Prepared according to the general procedure using *tert*-butyl-(1-benzyl- 6-bromo-oxoindolin-3-ylidene) carbamate (103.8 mg, 0.25 mmol) and 2-methyl-3,5-dinitrobenzaldehydes (63.0 mg, 0.3 mmol). Purification of the crude product via column chromatography delivered **3n** as a white solid with 76% yield (119.2 mg). The dr value was calculated to be 90:10 by ^{1}H NMR analysis of the crude reaction mixture, and the enantiomeric excess was determined to be 94% by HPLC on Chiralpak IC-H column at 254nm (Hexane/isopropanol = 80/20, 1 mL/min), t_{major} = 6.32 min, t_{minor} = 11.72 min; $[\alpha]_D^{20}$ = +8.3 (C=0.480, CH_2Cl_2); m.p. 175-177 °C.

NMR and HRMS data for the product **3n**:

^{1}H NMR (400 MHz, $CDCl_3$): δ = 8.88 (d, *J* = 2.4 Hz, 1H), 8.49 (d, *J* = 2.0 Hz, 1H), 7.41-7.36 (m, 2H), 7.34-7.25 (m, 5H), 6.96 (d, *J* = 6.8 Hz, 2H), 5.16 (d, *J* = 15.2 Hz, 1H), 4.47 (br s, 1H), 4.33 (d, *J* = 7.2 Hz, 1H), 3.89 (d, *J* = 16.4 Hz, 1H), 3.76 (d, *J* = 16.4 Hz, 1H), 1.07 (s, 9H) ppm;

^{13}C NMR (100 MHz, $CDCl_3$): δ = 175.0, 153.5, 148.4, 146.5, 143.2, 141.7, 135.3, 134.9, 129.2, 129.1, 128., 127.5, 126.2, 125.0, 123.5, 122.8, 120.4, 112.7, 83.4, 61.8, 44.1, 33.3, 27.7 ppm;

HRMS (ESI): *m/z* calculated for $C_{28}H_{25}BrN_4O_8$+Na: 647.0753, found 647.0751.

tert-butyl(*1'R,3R*)-1-benzyl-5-fluoro-1'-hydroxy-5',7'-dinitro-2-oxo-1',4'-dihydro-2'H-spiro[indoline-3,3'-isoquinoline]-2'-carboxylate

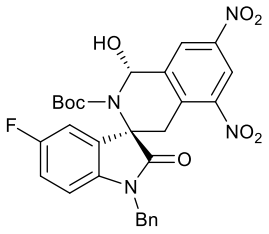

3o

Prepared according to the general procedure using *tert*-butyl-(1-benzyl- 5-fluoro-oxoindolin-3-ylidene) carbamate (88.6 mg, 0.25 mmol) and 2-methyl-3,5-dinitrobenzaldehydes (63.0 mg, 0.3 mmol). Purification of the crude product via column chromatography delivered **3o** as a white solid with 73% yield (102.7 mg). The dr value was calculated to be 88:12 by ^{1}H NMR analysis of the crude reaction mixture, and the enantiomeric excess was determined to be 92% by HPLC on Chiralpak IC-H column at 254nm (Hexane/isopropanol = 80/20, 1 mL/min), t_{major} = 6.67 min, t_{minor} = 15.34 min; $[\alpha]_D^{20}$ = +22.7 (C = 0.160, CH_2Cl_2); m.p. 156-158 ºC.

NMR and HRMS data for the product **3o**:

^{1}H NMR (400 MHz, $CDCl_3$): δ = 8.88 (d, *J* = 2.4 Hz, 1H), 8.50 (d, *J* = 2.4 Hz, 1H), 7.39-7.36 (m, 2H), 7.32-7.29 (m, 3H), 7.17 (d, *J* = 7.2, 2.4 Hz, 1H), 6.98 (td, *J* = 9.2, 2.8 Hz, 2H), 6.74 (dd, *J* = 8.4, 4.0 Hz, 1H), 5.19 (d, *J* = 15.2 Hz, 1H), 4.52 (br s, 1H), 4.33 (d, *J* = 15.2 Hz, 1H) , 3.90 (d, *J* = 16.0 Hz, 1H), 3.79 (d, *J* = 16.0 Hz, 1H), 1.07 (s, 9H) ppm.

^{13}C NMR (100 MHz, $CDCl_3$): δ = 175.0, 159.7 (d, *J*=241.0), 153.3, 148.4, 146.5, 141.7, 137.8 (d, *J*=2.0), 135.4, 135.2, 133.1 (d, *J*=7.0), 129.1, 128.2, 127.5, 125.1, 120.4, 115.5 (d, *J*=23.0), 110.4 (d, *J*=25.0), 110.2 (d, *J*=8.0), 83.4, 62.3, 44.1, 33.5, 27.7 ppm.

HRMS(ESI): *m/z* calculated for $C_{28}H_{25}FN_4O_8$+Na: 587.1554, found 587.1552.

tert-butyl(*1'R,3R*)-1-benzyl-4,6-difluoro-1'-hydroxy-5',7'-dinitro-2-oxo-1',4'-dihydro-2'H-spiro[indoline-3,3'-isoquinoline]-2'-carboxylate

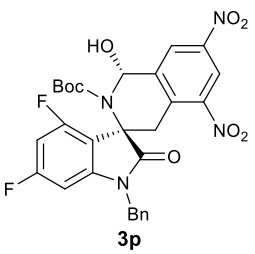

3p

Prepared according to the general procedure using *tert*-butyl-(1-benzyl- 4,6-difluoro-oxoindolin-3-ylidene) carbamate (93.1 mg, 0.25 mmol) and 2-methyl-3,5-dinitrobenzaldehydes (63.0 mg, 0.3 mmol). Purification of the crude product via column chromatography delivered **3p** as a white solid with 62% yield (90.7 mg). The dr value was calculated to be 92:8 by ^{1}H NMR analysis of the crude reaction mixture, and the enantiomeric excess was determined to be 96% by HPLC on Chiralpak IC-H column at 254nm (Hexane/isopropanol = 80/20, 1 mL/min), t_{major} = 7.05 min, t_{minor} = 11.40 min; $[\alpha]_D^{20}$ = +14.7 (C = 0.200, CH_2Cl_2); m.p. decomp. >201 °C.

NMR and HRMS data for the product **3p**:

^{1}H NMR (400 MHz, DMSO-*d*$_6$): δ = 8.80 (d, *J* = 2.0 Hz, 1H), 8.74 (d, *J* = 2.4 Hz, 1H), 7.35-7.29 (m, 5H), 7.15 (s, 1H), 6.99-6.94 (m, 3H), 4.94 (d, *J* = 15.2 Hz, 1H), 4.66 (d, *J* = 15.2 Hz, 1H) , 4.19 (d, *J* = 16.0 Hz, 1H), 3.37 (s, 1H), 1.06 (s, 9H) ppm.

^{13}C NMR (100 MHz, DMSO-*d*$_6$): δ = 175.1, 157.9 (d, *J*=235.0), 152.8, 151.8 (d, *J*=232.0), 148.8, 146.7, 145.2, 143.5, 136.4, 134.6, 129.1, 128.3, 128.1, 124.9, 120.0, 112.8 (d, *J*=24.0), 98.5 (d, *J*=26.0), 95.5 (d, *J*=25.0), 81.9, 76.8, 61.2, 43.6, 31.4, 27.9 ppm.

HRMS (ESI): *m/z* calculated for $C_{28}H_{24}F_2N_4O_8$+Na: 605.1460, found 605.1461.

tert-butyl(*1'R,3R*)-1-benzyl-5-methyl-1'-hydroxy-5',7'-dinitro-2-oxo-1',4'-dihydro-2'H-spiro[indoline-3,3'-isoquinoline]-2'-carboxylate

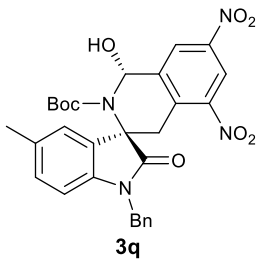

3q

Prepared according to the general procedure using *tert*-butyl-(1-benzyl- 5-methyl-oxoindolin-3-ylidene) carbamate (87.6 mg, 0.25 mmol) and 2-methyl-3,5-dinitrobenzaldehydes (63.0 mg, 0.3 mmol). Purification of the crude product via column chromatography delivered **3q** as a white solid with 70% yield (98.1 mg). The dr value was calculated to be 90:10 by ^{1}H NMR analysis of the crude reaction mixture, and the enantiomeric excess was determined to be 91% by HPLC on

Chiralpak IC-H column at 254nm (Hexane/isopropanol = 80/20, 1 mL/min), t_{major} = 7.37 min, t_{minor} = 19.44 min; $[\alpha]_D^{20}$ = +30.3 (C=0.064, CH_2Cl_2); m.p. 155-157 ºC.

NMR and HRMS data for the product **3q**:

^{1}H NMR (400 MHz, $CDCl_3$): δ = 8.87 (d, *J* = 2.4 Hz, 1H), 8.49 (d, *J* = 2.4 Hz, 1H), 7.38-7.34 (m, 2H), 7.31-7.29 (m, 3H), 7.20 (s, 1H), 7.08 (d, *J* = 8.0 Hz, 1H), 6.97 (d, *J* = 4.0 Hz, 1H), 6.70 (d, *J* = 8.0 Hz, 1H), 5.15 (d, *J* = 15.6 Hz, 1H), 4.34 (d, *J* = 15.2 Hz, 2H), 3.91 (d, *J* = 16.4 Hz, 1H), 3.75 (d, *J* = 16.4 Hz, 1H), 2.35 (s, 3H), 1.03 (s, 9H) ppm.

^{13}C NMR (100 MHz, $CDCl_3$): δ = 175.1, 153.8, 148.4, 146.4, 141.7, 139.5, 136.0, 135.6, 133.2, 131.4, 129.5, 129.0, 128.0, 127.6, 125.1, 122.8, 120.4, 109.2, 83.0, 62.2, 43.9, 33.8, 27.6 ppm.

HRMS (ESI): *m/z* calculated for $C_{29}H_{28}N_4O_8$+Na: 583.1805, found 583.1804.

tert-butyl(*1'R,3R*)-1-allyl-1'-hydroxy-5',7'-dinitro-2-oxo-1',4'-dihydro-2'H-spiro[indoline-3,3'-isoquinoline]-2'-carboxylate

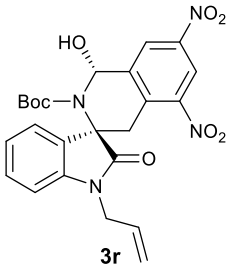

3r

Prepared according to the general procedure using *tert*-butyl-(1-allyl-oxoindolin-3-ylidene) carbamate (71.6 mg, 0.25 mmol) and 2-methyl-3,5-dinitrobenzaldehydes (63.0 mg, 0.3 mmol). Purification of the crude product via column chromatography delivered **3r** as a white solid with 78% yield (96.6 mg). The dr value was calculated to be 95:5 by ^{1}H NMR analysis of the crude reaction mixture, and the enantiomeric excess was determined to be 93% by HPLC on Chiralpak AD-H column at 254nm (Hexane/isopropanol = 80/20, 1 mL/min), t_{minor} = 8.73 min, t_{major} = 17.52 min; $[\alpha]_D^{20}$ = -48.8 (C = 0.500, CH_2Cl_2); m.p. 178-180 ºC.

NMR and HRMS data for the product **3r**:

^{1}H NMR (400 MHz, $CDCl_3$): δ = 8.86 (d, *J* = 2.0 Hz, 1H), 8.48 (d, *J* = 2.0 Hz, 1H), 7.40 (d, *J* = 7.2 Hz, 1H), 7.36 (td, *J* = 8.0, 1.2 Hz, 1H), 7.16 (t, *J* = 7.2 Hz, 1H), 6.94 (s, 1H), 6.89 (d, *J* = 7.6 Hz,

1H), 5.90-5.80 (m, 1H), 5.32-5.27 (m, 2H), 4.55 (dd, *J* = 16.0, 4.4 Hz, 1H), 4.29 (br s, 1H), 3.94-3.88 (m, 2H), 3.74 (d, *J* = 16.4 Hz, 1H), 1.06 (s, 9H) ppm.

^{13}C NMR (100 MHz, $CDCl_3$): δ = 174.8, 153.8, 148.3, 146.4, 142.1, 141.6, 135.9, 131.3, 131.0, 129.4, 125.1, 123.4, 122.1, 120.4, 118.1, 109.4, 83.1, 62.1, 42.5, 33.8, 27.7 ppm.

HRMS (ESI): *m/z* calculated for $C_{24}H_{24}N_4O_8$+Na: 519.1492, found 519.1490.

tert-butyl(*1'R,3R*)-1'-hydroxy-1-methyl-5',7'-dinitro-2-oxo-1',4'-dihydro-2'H-spiro[indoline-3, 3'- isoquinoline]-2'-carboxylate

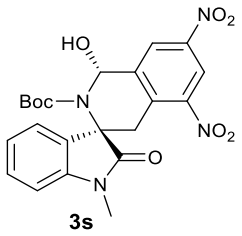

3s

Prepared according to the general procedure using *tert*-butyl-(1-methyl-oxoindolin-3-ylidene) carbamate (65.1mg, 0.25 mmol) and 2-methyl-3,5-dinitrobenzaldehydes (63.0 mg, 0.3 mmol). Purification of the crude product via column chromatography delivered **3s** as a white solid with 81% yield (95.6 mg). The dr value was calculated to be 90:10 by ^{1}H NMR analysis of the crude reaction mixture, and the enantiomeric excess was determined to be 94% by HPLC on Chiralpak AS-H column at 254nm (Hexane/isopropanol = 90/10, 1 mL/min), t_{minor} = 12.26 min, t_{major} = 17.90 min; $[\alpha]_D^{20}$ = -22.1 (C = 0.900, CH_2Cl_2); decomp. >178 ^oC.

NMR and HRMS data for the product **3s**:

^{1}H NMR (400 MHz, $CDCl_3$): δ = 8.83 (d, *J* = 2.4 Hz, 1H), 8.61 (d, *J* = 2.4 Hz, 1H), 7.24 (dd, *J* = 7.6, 1.2 Hz, 1H), 7.00 (s, 1H), 6.86 (d, *J* = 7.6 Hz, 1H), 6.76 (td, *J* = 7.6, 0.8 Hz, 1H), 5.96 (dd, *J* = 7.6, 0.4 Hz, 1H), 4.62 (br s, 1H), 3.39 (d, *J* = 16 Hz, 1H), 3.30 (s, 3H), 2.18 (s, 1H), 1.12 (s, 9H) ppm.

^{13}C NMR (100 MHz, $CDCl_3$): δ = 176.1, 153.2, 149.1, 146.6, 142.1, 142.0, 136.3, 130.5, 129.4, 125.2, 122.9, 120.5, 120.2, 108.9, 83.0, 62.7, 34.3, 27.8, 26.9 ppm.

HRMS (ESI): *m/z* calculated for $C_{22}H_{22}N_4O_8$+Na: 493.1335, found 493.1331.

di-tert-butyl(*1'R,3R*)-1'-hydroxy-5'-nitro-2-oxo-1',4'-dihydro-2'H-spiro[indoline-3,3'-isoquinoline]-1,2'-dicarboxylate

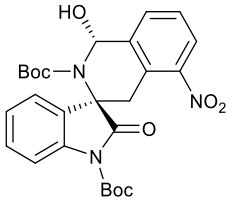

3t

Prepared according to the general procedure using *tert*-butyl 3-((tert-butoxycarbonyl)imino)-2-oxoindoline-1-carboxylate (86.6 mg, 0.25 mmol,) and 2-methyl-3-nitrobenzaldehydes (49.5 mg, 0.3 mmol). Purification of the crude product via column chromatography delivered **3t** as a white solid with 42% yield (53.3 mg). The dr value was calculated to be 96:4 by ^{1}H NMR analysis of the crude reaction mixture, and the enantiomeric excess was determined to be 89% by HPLC on Chiralpak AD-H column at 254nm (Hexane/isopropanol = 90/10, 1 mL/min), t_{minor} = 11.00 min, t_{major} = 16.79 min; $[\alpha]_D^{20}$ = -31.5 (C=0. 680, CH_2Cl_2). m.p. 169-171 °C.

NMR and HRMS data for the product **3t**:

^{1}H NMR (400 MHz, CDCl3): δ = 8.26 (d, *J* = 2.0 Hz, 1H), 8.20 (dd, *J* = 8.4, 2.4 Hz, 1H), 7.90 (d, *J* = 8.0 Hz, 1H), 7.44 (d, *J* = 7.2 Hz, 1H), 7.39 (td, *J* = 8.0, 1.2 Hz, 1H), 7.34 (d, *J* = 8.4 Hz, 1H), 7.24 (d, *J* = 7.6 Hz, 1H), 6.83 (d, *J* = 3.6 Hz, 1H), 4.19 (br s, 1H), 3.76 (d, *J* = 15.6 Hz, 1H), 2.99 (d, *J* = 16.0 Hz, 1H), 1.60 (s, 9H), 1.08 (s, 9H) ppm.

^{13}C NMR (100 MHz, CDCl3): δ = 173.4, 153.9, 149.4, 147.2, 139.3, 138.9, 137.8, 131.3, 129.3, 129.1, 125.2, 124.2, 122.4, 121.5, 115.1, 84.6, 83.3, 62.5, 38.2, 28.1, 27.5 ppm.

HRMS (ESI): *m/z* calculated for $C_{26}H_{29}N_3O_8$+Na: 534.1852, found 534.1853.

2.2 Procedure for the asymmetric synthesis of 3m'

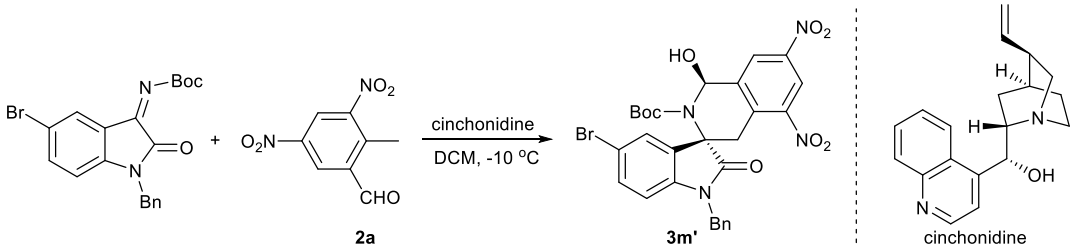

2a **3m'**

The reaction was carried out with *tert*-butyl-(1-benzyl-5-bromo-oxoindolin- 3-ylidene) carbamate (103.8 mg, 0.25 mmol) and 2-methyl-3,5-dinitrobenzaldehydes (63.0 mg, 0.3 mmol), catalyst cinchonidine (14.7 mg, 0.05 mmol) in DCM (2 mL) under an open atmosphere at -10 ºC. When the reaction was complete (based on TLC monitoring), the reaction mixture was concentrated and the residue was purified by flash chromatography on silica gel (petroleum ether/ethyl acetate = 12:1). The THIQ-fused spirooxindole **3m'** was obtained as a white solid in 72% yield (112.3 mg) after flash chromatography. The dr value was calculated to be 89:11 by ^{1}H NMR analysis of the crude reaction mixture, and the enantiomeric excess was determined to be 92% by HPLC on Chiralpak IC-H column at 254nm (Hexane/isopropanol = 80/20, 1 mL/min), t_{major} = 6.69 min, t_{minor} = 15.18 min; $[\alpha]_D^{20}$ = +22.6 (C=0.468, CH_2Cl_2); m.p. 135-136 ºC.

NMR and HRMS data for the product **3m'**:

^{1}H NMR (400 MHz, $CDCl_3$): δ = 8.89 (d, *J* = 2.0 Hz, 1H), 8.50 (d, *J* = 2.0 Hz, 1H), 7.50 (d, *J* = 2.0 Hz, 1H), 7.42-7.34 (m, 3H), 7.32-7.28 (m, 3H), 6.97 (d, *J* = 3.6 Hz, 1H), 6.69 (d, *J* = 8.4 Hz, 1H), 5.16 (d, *J* = 15.2 Hz, 1H), 4.35 (d, *J* = 12.8 Hz, 2H), 3.90 (d, *J* = 16.4 Hz, 1H), 3.78 (d, *J* = 16.0 Hz, 1H), 1.08 (s, 9H) ppm.

^{13}C NMR (100 MHz, $CDCl_3$): δ = 174.6, 153.2, 148.4, 146.5, 141.5, 140.9, 135.3, 135.0, 133.4, 132.1, 129.1, 128.2, 127.5, 125.4, 125.2, 120.5, 116.0, 111.0, 83.5, 62.0, 44.1, 33.5, 27.7 ppm.

HRMS (ESI): *m/z* calculated for $C_{28}H_{25}BrN_4O_8$+Na: 647.0753, found 647.0756.

2.3 Procedure for the asymmetric synthesis of 4

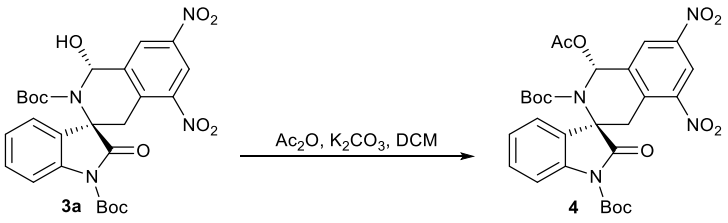

To a solution of **4** (61.2 mg, 0.11 mmol) in methylene chloride (2 mL) was added acetic anhydride (22.5 mg, 0.22 mmol) and K_2CO_3 (1.5 mg 0.011 mmol). The mixture was stirred at room temperature. When the reaction was complete (based on TLC monitoring), the reaction mixture was

concentrated and the residue was purified by flash chromatography on silica gel (petroleum ether/ethyl acetate = 10:1). The acetylated derivative **4** was obtained as a white solid in 87% yield (57.3 mg) after flash chromatography. The dr value was calculated to be 89:11 by ^{1}H NMR analysis of the crude reaction mixture, and enantiomeric excess was determined to be 91% by HPLC on Chiralpak OD-H column at 254nm (Hexane/isopropanol = 90/10, 1 mL/min): t_{major} = 7.52 min, t_{minor} = 9.43 min; $[\alpha]_D^{20}$ = -66.3 (C = 0.382, CH_2Cl_2), m.p. 181-182 °C.

NMR and HRMS data for the product **4**:

^{1}H NMR (400 MHz, $CDCl_3$): δ = 8.89 (d, *J* = 2.4 Hz, 1H), 8.71 (s, 1H), 7.96-7.94 (m, 1H), 7.85 (s, 1H), 7.45 (t, *J* = 7.2 Hz, 2H), 7.30 (t, *J* = 7.6 Hz, 1H), 3.87 (d, *J* = 17.2 Hz, 1H), 3.65 (d, *J* = 17.2 Hz, 1H), 2.18 (s, 3H), 1.58 (s, 9H), 1.07 (s, 9H) ppm.

^{13}C NMR (100 MHz, $CDCl_3$): δ = 172.7, 169.3, 152.1, 149.0, 148.3, 146.5, 139.3, 139.2, 135.11, 130.0, 126.7, 125.4, 122.1, 120.9, 115.5, 84.9, 84.3, 77.8, 61.9, 34.2, 28.0, 27.4, 21.2 ppm.

HRMS (ESI): *m/z* calculated for $C_{28}H_{30}N_4O_{11}$+Na: 621.1809, found 621.1808.

2.4 Procedure for the asymmetric synthesis of 5

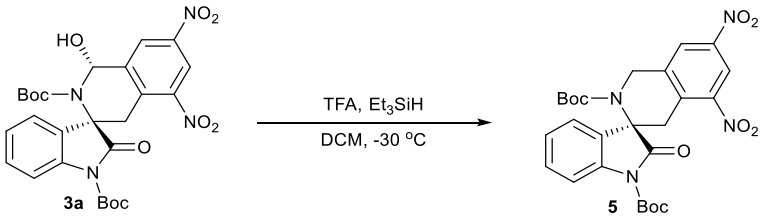

To a solution of **3a** (61.2 mg, 0.11 mmol) and triethyl silane (87 μl, 0.55 mmol) in DCM (3 mL) was added TFA (41 μl, 0.55 mmol). The mixture was stirred at -30 °C until the reaction completed (monitored by TLC). After quenching the reaction, the mixture was purified by flash chromatography on silica gel (petroleum ether/ethyl acetate = 15:1) to give **5** as a white solid in 86% yield (51.2 mg). The enantiomeric excess was determined to be 92% by HPLC on Chiralpak IC-H column at 254nm (Hexane/isopropanol = 90/10, 1 mL/min): t_{minor} = 34.46 min, t_{major} = 41.18 min; $[\alpha]_D^{20}$ = +35.6 (C = 0.074, CH_2Cl_2); m.p. 106-108 °C.

NMR and HRMS data for the product **5**:

^{1}H NMR (400 MHz, $CDCl_3$): δ = 8.83 (d, *J* = 2.4 Hz, 1H), 8.49 (d, *J* = 2.4 Hz, 1H), 7.89 (d, *J* = 8.0 Hz, 1H), 7.33 (td, *J* = 8.0, 1.2 Hz, 1H), 7.00 (td, *J* = 7.2, 0.4 Hz, 1H), 6.45 (dd, *J* = 7.2, 0.4 Hz, 1H), 5.10 (d, *J* = 15.6 Hz, 1H), 4.88 (d, *J* = 15.2 Hz, 1H), 3.65 (d, *J* = 16.0 Hz, 1H), 3.54 (d, *J* = 16.0 Hz, 1H), 1.64 (s, 9H), 1.11 (s, 9H) ppm.

^{13}C NMR (100 MHz, $CDCl_3$): δ = 173.8, 152.8, 149.0, 148.7, 146.6, 141.9, 138.6, 135.9, 130.1, 129.6, 124.9, 124.8, 120.9, 119.4, 115.5, 84.9, 82.9, 62.1, 45.1, 35.9, 28.1, 27.6 ppm.

HRMS (ESI): *m/z* calculated for $C_{26}H_{28}N_4O_9$+Na: 563.1754, found 563.1757.

2.5 Procedure for the asymmetric synthesis of 6

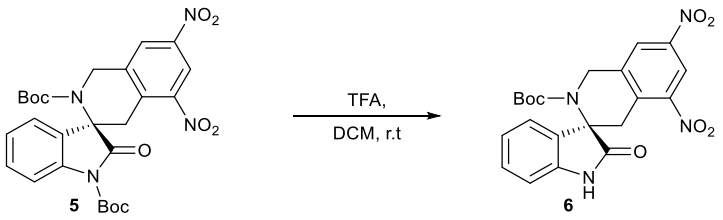

To a solution of **5** (0.1 mmol) in dry CH_2Cl_2 (2.0 mL) was added TFA (37 μl, 0. 5 mmol) in room temperature until the reaction was completed (monitored by TLC). After quenching the reaction, the mixture was purified by chromatography on silica gel (petroleum ether/ethyl acetate = 5:1) to give **6** as a white solid in 83% yield (36.4 mg). The enantiomeric excess was determined to be 96% by HPLC on Chiralpak AD-H column at 254nm (Hexane/isopropanol = 90/10, 1 mL/min), t_{minor} = 13.32 min, t_{major} = 16.80 min; $[\alpha]_D^{20}$ = +32.8 (C = 0.800, CH_2Cl_2); m.p. 178-179 °C.

NMR and HRMS data for the product **6**:

^{1}H NMR (400 MHz, $CDCl_3$): δ = 8.83 (d, *J* = 2.4 Hz, 1H), 8.50 (d, *J* = 2.4 Hz, 1H), 8.20 (s, 1H), 7.24 (t, *J* = 7.6 Hz, 1H), 6.90-6.88 (m, 2H), 6.43 (d, *J* = 7.6 Hz, 1H), 5.09 (d, *J* = 15.2 Hz, 1H), 4.90 (d, *J* = 15.2 Hz, 1H), 3.65 (d, *J* = 15.6 Hz, 1H), 3.53 (d, *J* = 16.0 Hz, 1H), 1.17 (s, 9H) ppm.

^{13}C NMR (100 MHz, $CDCl_3$): δ =177.6, 153.0, 148.7, 146.5, 141.8, 139.5, 136.4, 131.5, 129.4, 124.9, 123.0, 121.4, 119.4, 110.6, 82.6, 62.3, 45.1, 35.5, 27.7 ppm.

HRMS (ESI): *m/z* calculated for $C_{21}H_{20}N_4O_7$+Na: 463.1230, found 463.1227

2.6 Procedure for the asymmetric synthesis of 7

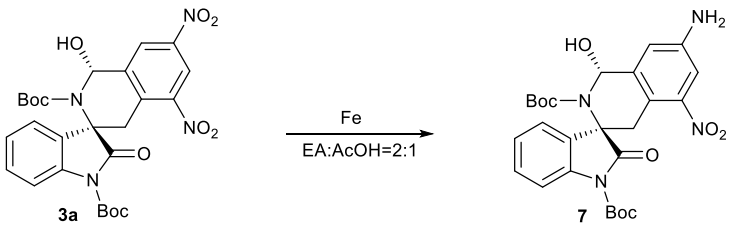

To a solution of **7** (61.2 mg, 0.11 mmol) in ethyl acetate (1 mL) and AcOH (0.5 mL) was added reduced iron powder (30.7 mg, 0.55 mmol) in room temperature until the reaction was completed (monitored by TLC). The solid particle were filtered off. The filtrate was washed with water and extracted with ethyl acetate. The organic layer was dried over anhydrous Na_2SO_4, concentrated and purified by chromatography on silica gel (petroleum ether/ethyl acetate = 3:1) to give **7** as a yellow solid in 75% yield (43.2 mg). The dr value was calculated to be 89:11 by ^{1}H NMR analysis of the crude reaction mixture, and the enantiomeric excess was determined to be 94% by HPLC on Chiralpak AD-H column at 254nm (Hexane/isopropanol = 90/10, 1 mL/min): t_{minor} = 21.31 min, t_{major} = 26.18 min; $[\alpha]_D^{20}$ = -39.1 (C = 0.430, CH_2Cl_2); m.p. 197-198 °C.

NMR and HRMS data for the product **7**:

^{1}H NMR (400 MHz, DMSO-*d*$_6$): δ = 7.76 (d, *J* = 8.0 Hz, 1H), 7.49 (d, *J* = 7.2 Hz, 1H), 7.42 (t, *J* = 7.6 Hz, 1H), 7.30 (t, *J* = 7.2 Hz, 1H), 7.10 (d, *J* = 2.4 Hz, 1H), 6.96 (d, *J* = 3.2 Hz, 1H), 6.93 (t, *J* = 2.0 Hz, 1H), 6.44 (d, *J* = 3.6 Hz, 1H), 5.83 (s, 1H), 3.50 (d, *J* = 16.0 Hz, 1H), 3.25 (d, *J* = 16.0 Hz, 1H), 3.18 (s, 1H), 1.53 (s, 9H), 0.98 (s, 9H) ppm.

^{13}C NMR (100 MHz, DMSO-*d*$_6$): δ = 173.5, 152.83, 149.2, 149.1, 149.0, 141.9, 138.7, 129.3, 125.3, 123.0, 116.7, 114.8, 113.0, 107.6, 84.2, 81.6, 62.3, 33.2, 31.4, 28.1, 22.5 ppm.

HRMS (ESI): *m/z* calculated for $C_{26}H_{30}N_4O_8$+Na: 549.1961, found 549.1962.

3. Crystal data of 3q

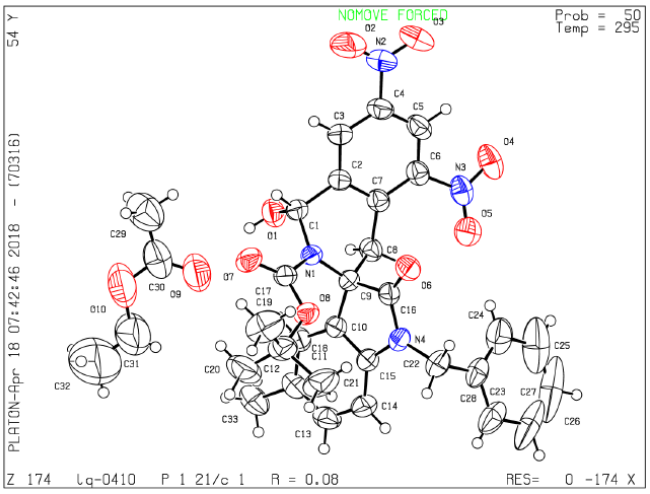

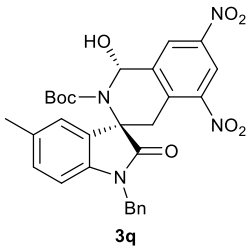

3q

Empirical formula	$C_{33}H_{36}N_4O_{10}$
Formula weight	648.66
Temperature/K	295.12(15)
Crystal system	monoclinic
Space group	$P2_1/c$
a/Å	10.4543(2)
b/Å	13.8322(3)
c/Å	23.1289(5)
α/°	90
β/°	90.3385(17)
γ/°	90
Volume/Å^3	3344.52(12)
Z	4
ρ_{calc}g/cm^3	1.288
μ/mm^{-1}	0.804
F(000)	1368.0
Crystal size/mm^3	0.7 × 0.45 × 0.35
Radiation	CuKα (λ = 1.54184)
2Θ range for data collection/°	8.458 to 145.004
Index ranges	$-12 \le h \le 10$, $-16 \le k \le 17$, $-28 \le l \le 23$
Reflections collected	12960
Independent reflections	6464 [R_{int} = 0.0267, R_{sigma} = 0.0316]
Data/restraints/parameters	6464/0/431
Goodness-of-fit on F^2	1.033
Final R indexes [I>=2σ (I)]	R_1 = 0.0782, wR_2 = 0.2011
Final R indexes [all data]	R_1 = 0.0875, wR_2 = 0.2138
Largest diff. peak/hole / e Å^{-3}	0.41/-0.54

4. EDC calculation (Figure S1)

In order to determine the absolute configuration of **3q**, a theoretical calculation of the electronic circular dichroism (ECD) spectra was carried out by means of the TD-DFT method. This technique has been successfully employed to predict ECD spectra and to assign the absolute configuration of organic molecules.

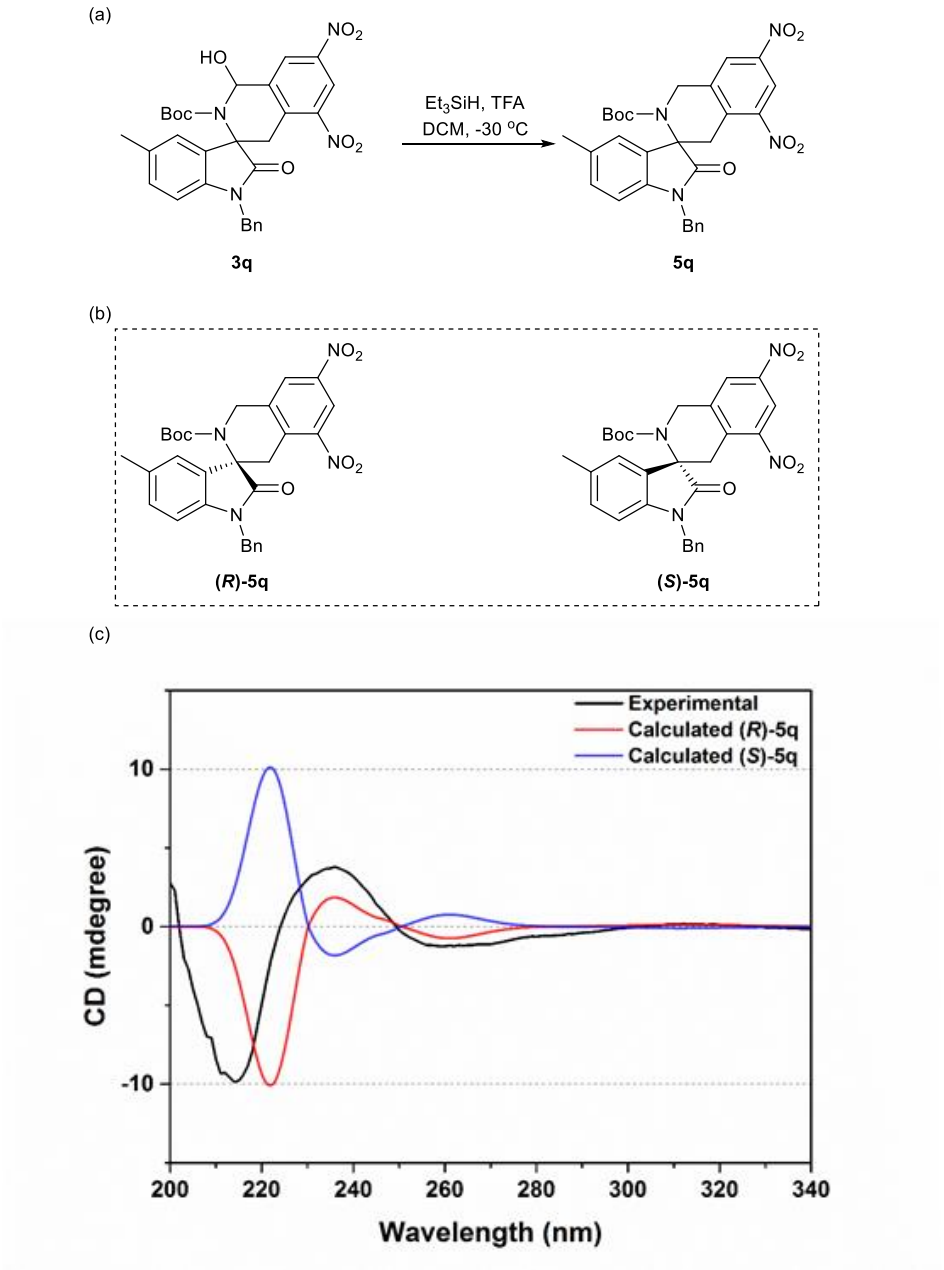

Figure S1. (a) Procedure for the synthesis of **5q**; (b) Two conformations of compound **5q**; (c) Calculated ECD spectra for the two conformations of compound **5q** and the experimental data.

At first, compound **3q** was dehydroxylated to **5q** (Figure S1a), and the global energy minimum structures of the two probable configurations (Figure S1b: (*R*)-**5q** and (*S*)-**5q**) of **5q** were submitted to ECD calculations by using TD-DFT method at B3LYP/aug-cc-pVDZ level. Frequency calculations were then carried out to verify the stability of these conformers and also gave a relevant percentage of the population for subsequent ECD investigations. Finally, the Boltzmann-averaged ECD calculation results were proceeded by the Multiwfn 3.4 software and compared with the experimental data (Figure S1c). The calculated ECD spectrum of (*R*)-**5q** was in good agreement both the sign and shape of the experimental result. Thus absolute configuration of **5q** could thus be reliably assigned to *R*. Meanwhile, the absolute configuration of **3q** was assigned to *R,R*.

CD spectra were recorded on a JASCO J-815 Spectropolarimeter, using CH_3OH as solvent. After the conformation search, fully optimization and imaginary frequency check by using Gaussian09 package and DFT method at B3LYP/6-311G* level. All the quantum chemical computations have been carried out with Gaussian09 software (Gaussian, Inc., Pittsburgh, PA, 2006). The input geometries of 5q was built based on relative configuration of 3q, and conformational search was then performed using the simulated annealing method and MMFF94 force field with the Sybly-X 1.3 software. The 31 corresponding conformers were further optimized with the DFT method at the B3LYP/6-311G* level. There were 16 representative energy minimum conformers without imaginary frequencies (by frequency analysis check) were shifted to TDDFT calculations by B3LYP functional and the aug-cc-pVDZ basis set. The overall calculated ECD spectra were then generated by Boltzmann-weighting of the 16 representative conformers using Multiwfn 3.4 software.

Reference: T. Lu, F. Chen, *J. Comput. Chem.*, **2012**, *33*, 580.

5. NMR spectra and HPLC chromatograms

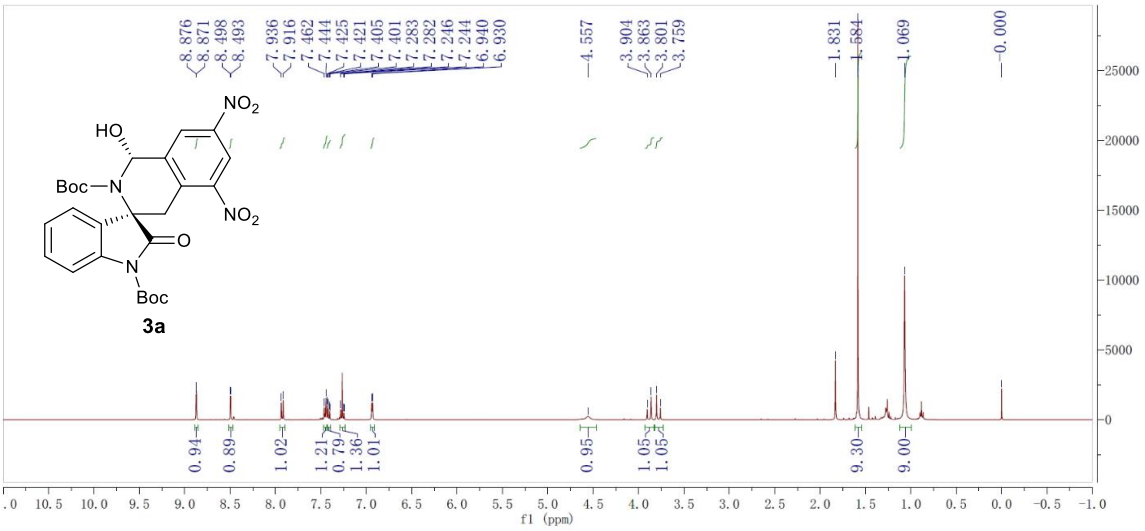

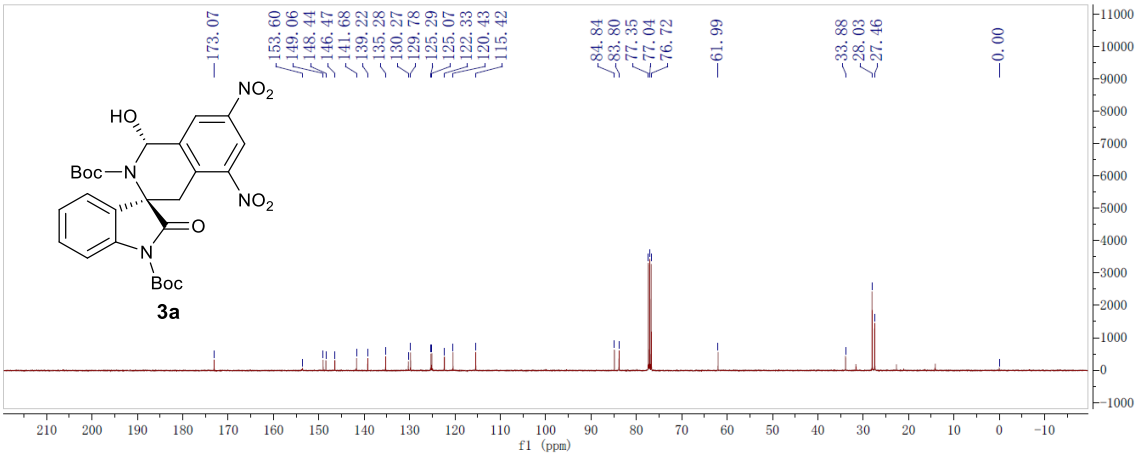

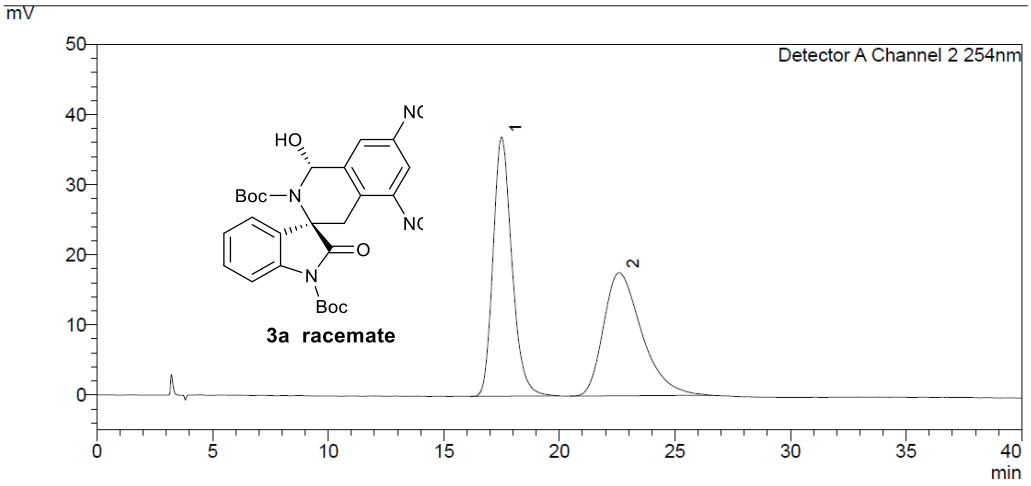

<Peak Table>

Detector A Channel 2 254nm

Peak#	Ret. Time	Area	Height	Conc.	Area%
1	17.500	2099102	36976	50.891	50.891
2	22.586	2025611	17574	49.109	49.109
Total		4124712	54550		100.000

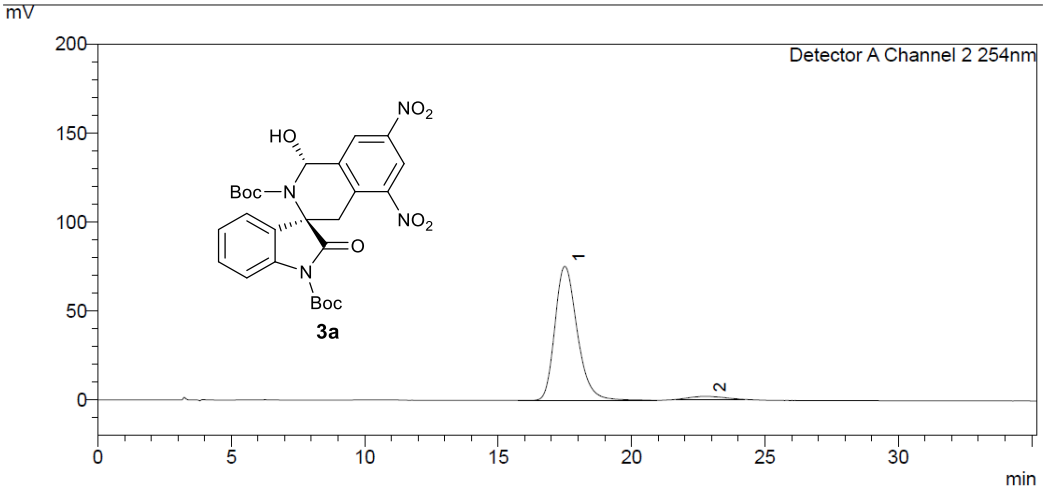

<Peak Table>

Detector A Channel 2 254nm

Peak#	Ret. Time	Area	Height	Conc.	Area%
1	17.500	4375285	75282	96.806	96.806
2	22.785	144367	1660	3.194	3.194
Total		4519653	76942		100.000

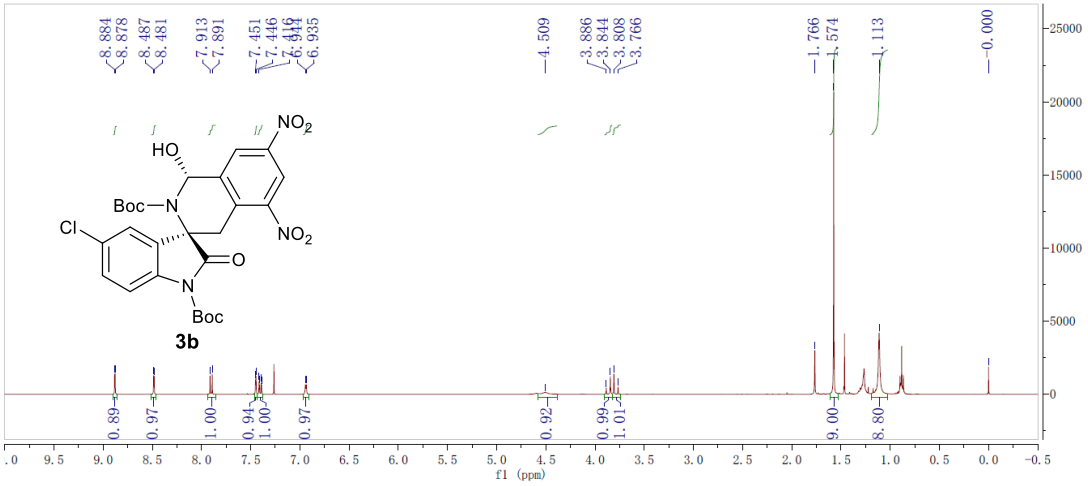
8.884
8.878
8.487
8.481
7.913
7.891
7.451
7.446
7.444
7.416
6.944
6.935
4.509
3.886
3.844
3.808
3.766
1.766
1.574
1.113
-0.000
NO2
HO
Boc
N
Cl
O
NO2
N
Boc
3b
0.89
0.97
1.00
0.94
1.00
0.97
0.92
0.99
1.01
9.00
8.80
f1 (ppm)

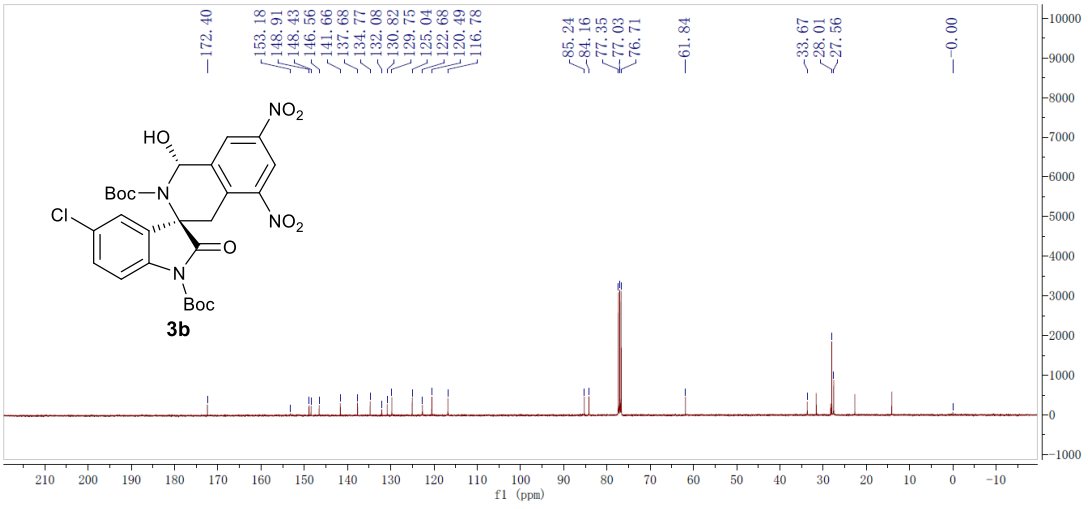
172.40
153.18
148.91
148.43
146.56
141.66
137.68
134.77
132.08
130.82
129.75
125.04
122.68
120.49
116.78
85.24
84.16
77.35
77.03
76.71
61.84
33.67
28.01
27.56
0.00
NO2
HO
Boc
N
Cl
O
NO2
N
Boc
3b
f1 (ppm)

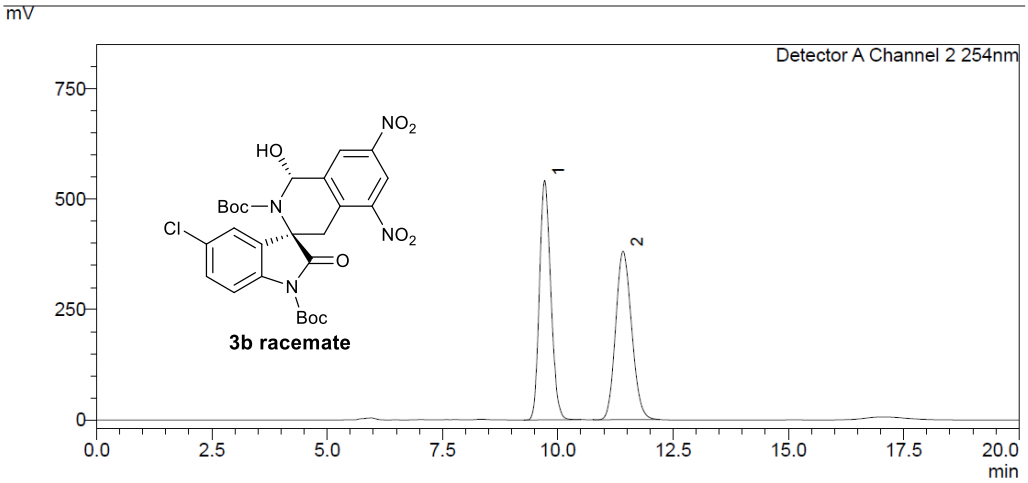

<Peak Table>

Detector A Channel 2 254nm

Peak#	Ret. Time	Area	Height	Conc.	Area%
1	9.715	9289492	542059	50.182	50.182
2	11.416	9222226	381393	49.818	49.818
Total		18511718	923452		100.000

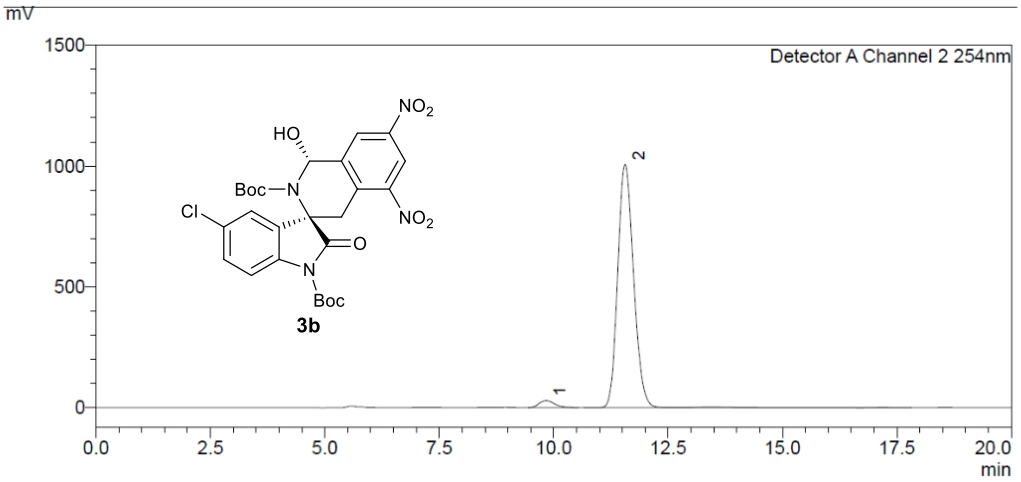

<Peak Table>

Detector A Channel 2 254nm

Peak#	Ret. Time	Area	Height	Conc.	Area%
1	9.794	736731	69394	2.922	2.922
2	11.560	24477594	1006532	97.078	97.078
Total		25214326	1075926		100.000

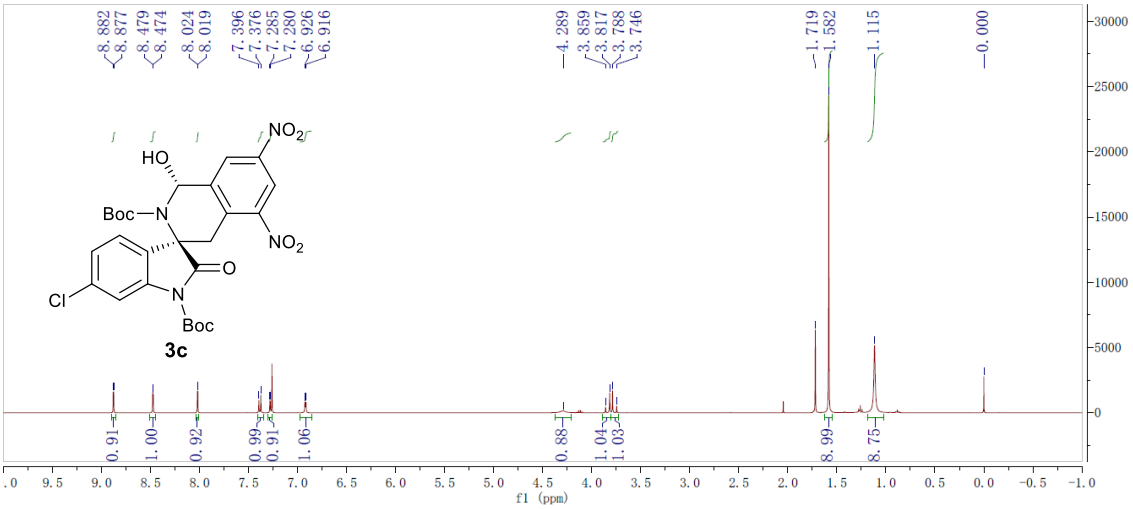
8.882
8.877
8.479
8.474
8.024
8.019
7.396
7.376
7.285
7.280
6.926
6.916
4.289
3.859
3.817
3.788
3.746
1.719
1.582
1.115
0.000
NO2
HO
Boc
N
NO2
O
Cl
N
Boc
3c
0.91
1.00
0.92
0.99
0.91
1.06
0.88
1.04
1.03
8.99
8.75
f1 (ppm)

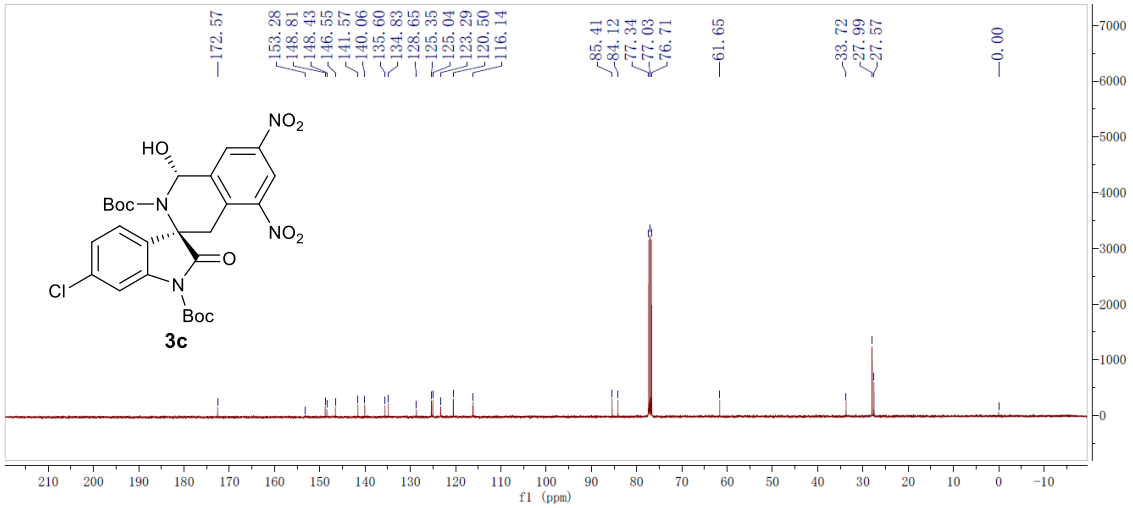
172.57
153.28
148.81
148.43
146.55
141.57
140.06
135.60
134.83
128.65
125.35
125.04
123.29
120.50
116.14
85.41
84.12
77.34
77.03
76.71
61.65
33.72
27.99
27.57
0.00
NO2
HO
Boc
N
NO2
O
Cl
N
Boc
3c
f1 (ppm)

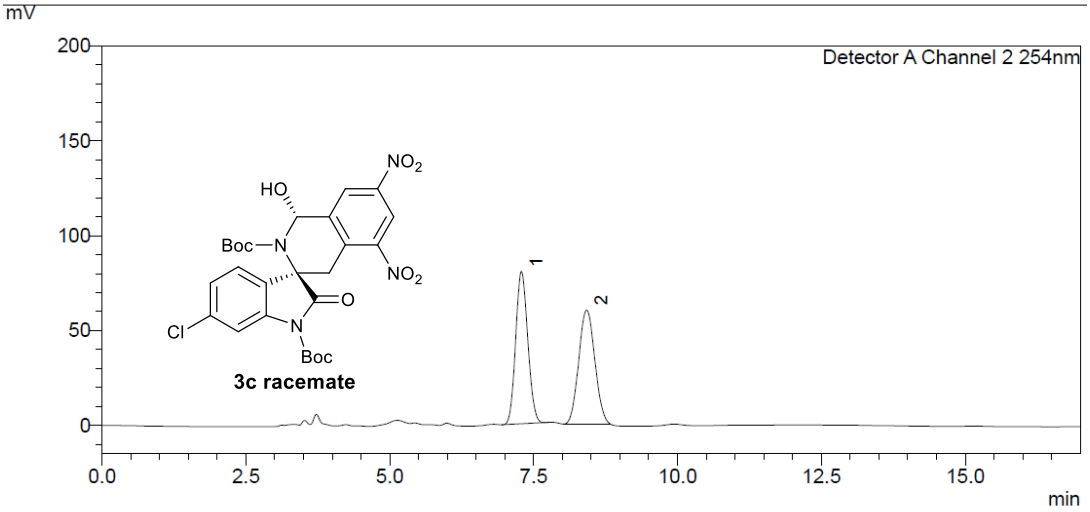

<Peak Table>

Detector A Channel 2 254nm

Peak#	Ret. Time	Area	Height	Conc.	Area%
1	7.288	1173514	80266	50.060	50.060
2	8.421	1170685	60110	49.940	49.940
Total		2344198	140376		100.000

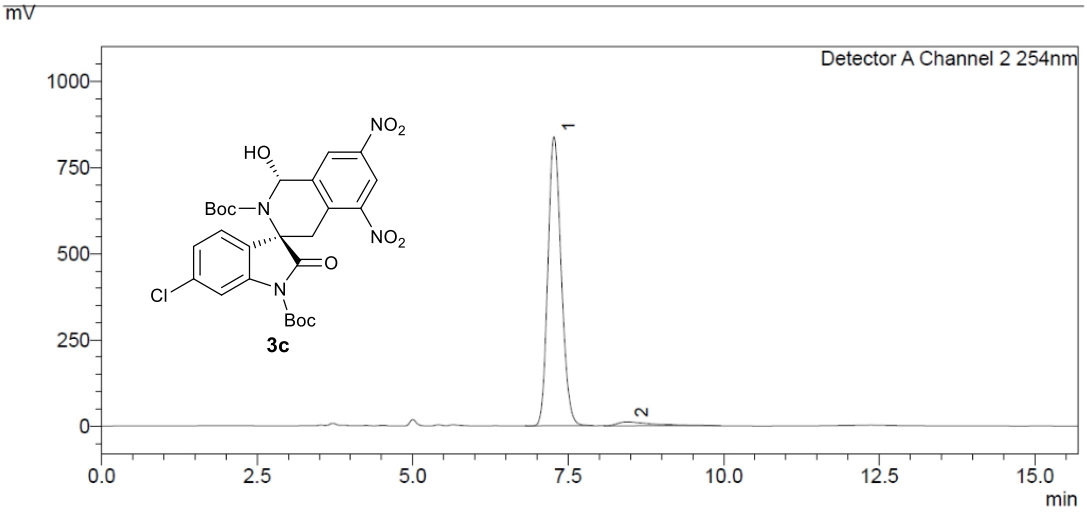

<Peak Table>

Detector A Channel 2 254nm

Peak#	Ret. Time	Area	Height	Conc.	Area%
1	7.273	12491165	838197	97.446	97.446
2	8.426	327375	28628	2.554	2.554
Total		12818540	866826		100.000

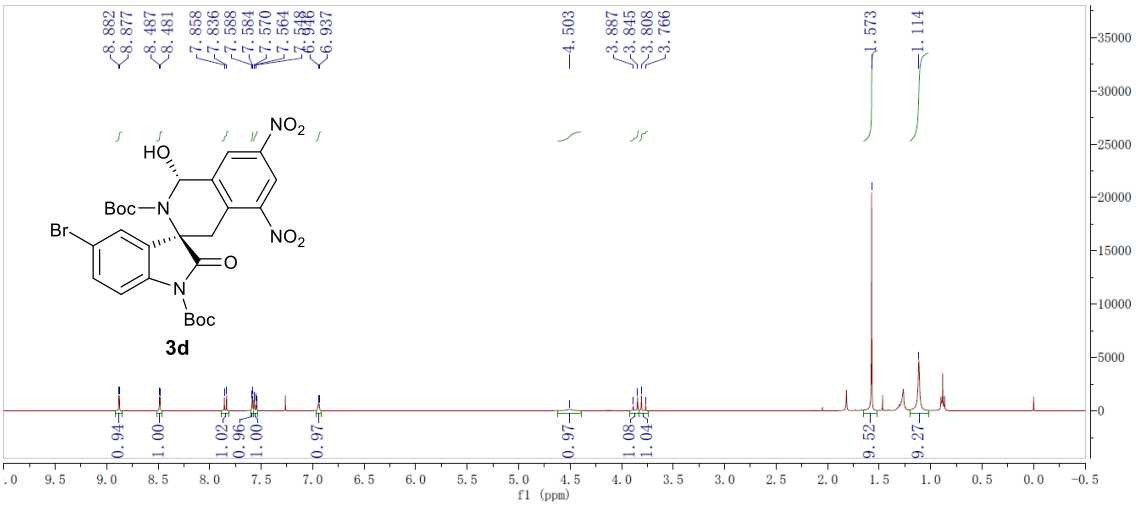
8.882
8.877
8.487
8.481
7.858
7.836
7.588
7.584
7.570
7.564
6.937
4.503
3.887
3.845
3.808
3.766
1.573
1.114
NO2
HO
Boc
N
Br
O
NO2
N
Boc
3d
0.94
1.00
1.02
0.96
1.00
0.97
0.97
1.08
1.04
9.52
9.27
f1 (ppm)

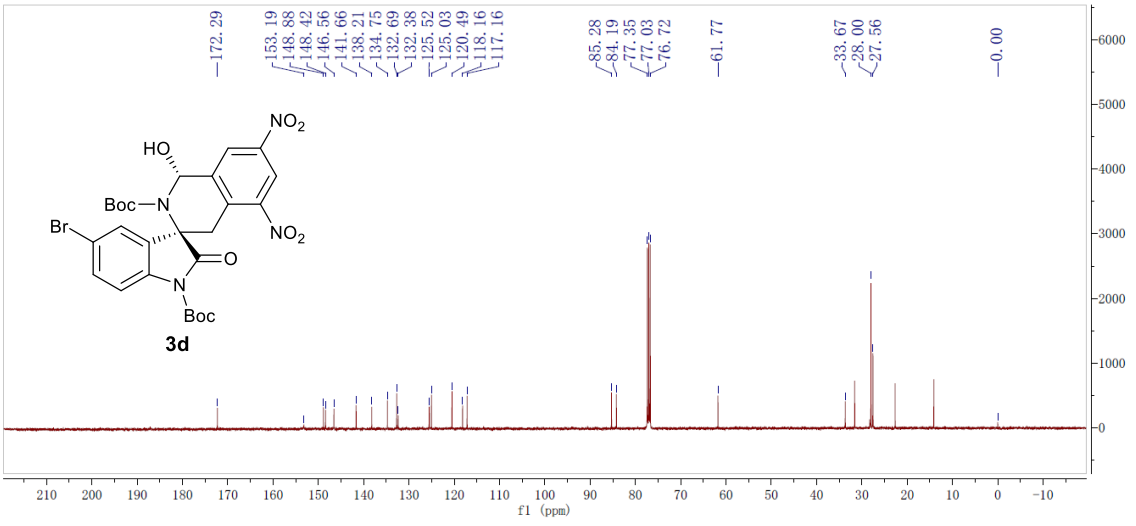
172.29
153.19
148.88
148.42
146.56
141.66
138.21
134.75
132.69
132.38
125.52
125.03
120.49
118.16
117.16
85.28
84.19
77.35
77.03
76.72
61.77
33.67
28.00
27.56
0.00
NO2
HO
Boc
N
Br
O
NO2
N
Boc
3d
f1 (ppm)

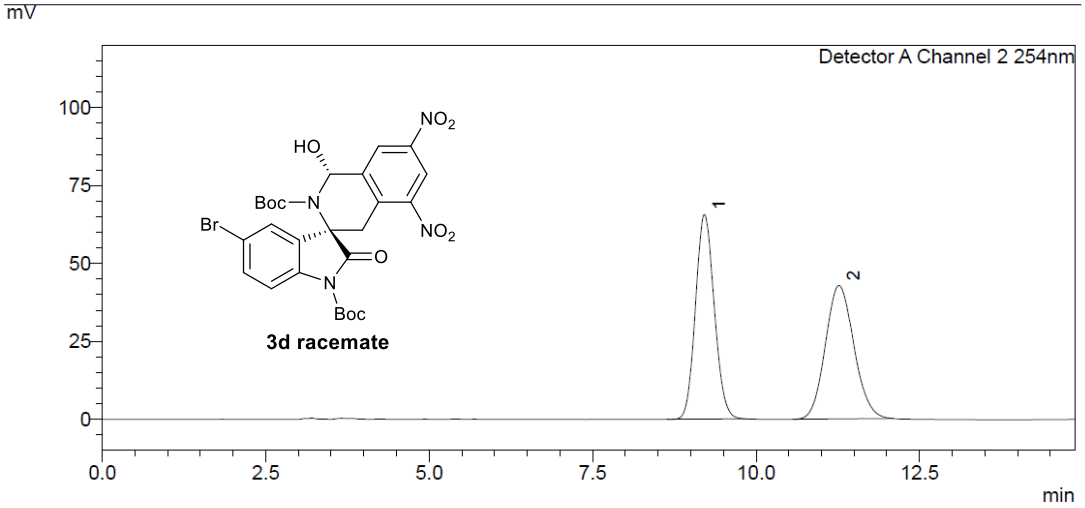

<Peak Table>

Detector A Channel 2 254nm

Peak#	Ret. Time	Area	Height	Conc.	Area%
1	9.209	1313567	65698	50.163	50.163
2	11.268	1305027	42838	49.837	49.837
Total		2618594	108536		100.000

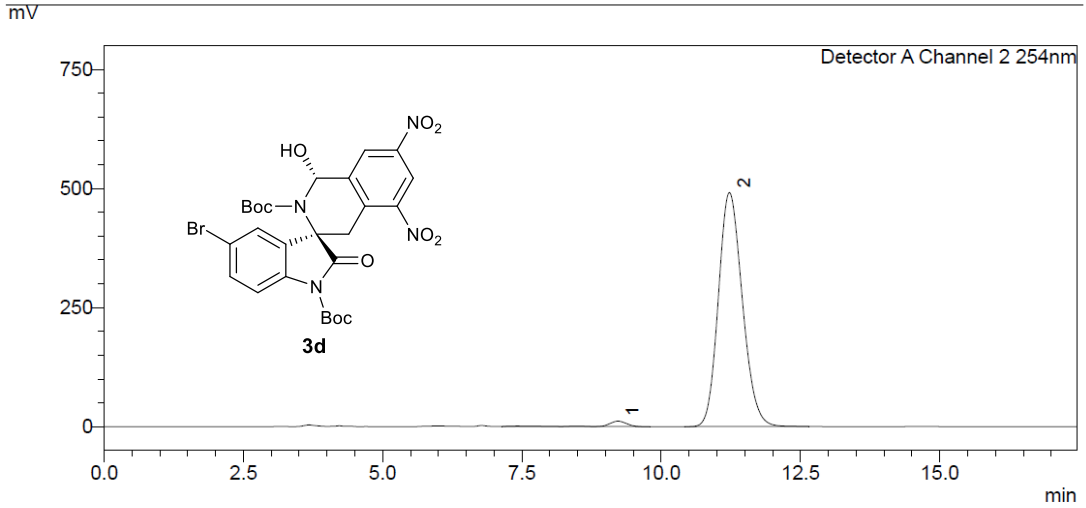

<Peak Table>

Detector A Channel 2 254nm

Peak#	Ret. Time	Area	Height	Conc.	Area%
1	9.223	257274	11617	1.722	1.722
2	11.224	14687158	491252	98.278	98.278
Total		14944431	502869		100.000

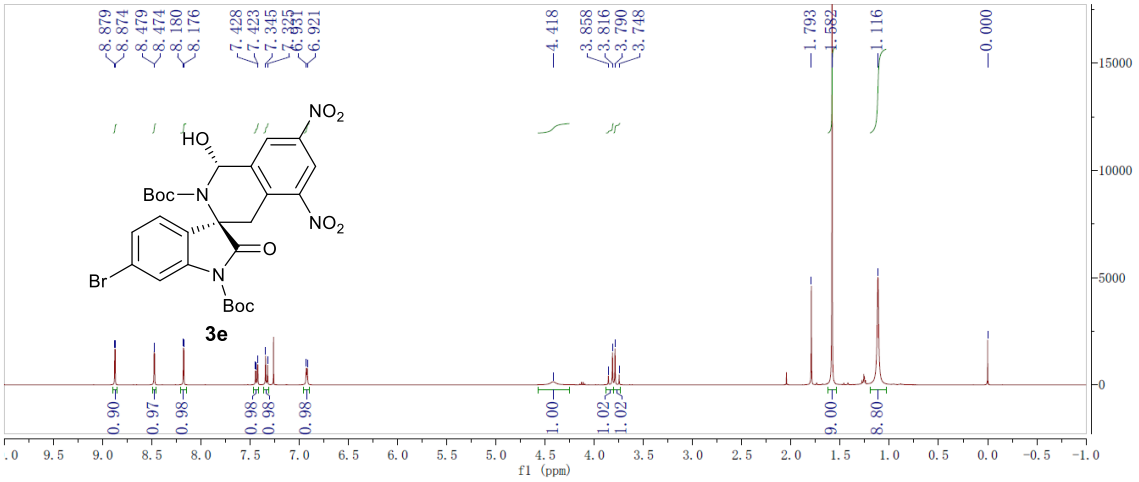
8.879
8.874
8.479
8.474
8.180
8.176
7.428
7.423
7.345
7.335
6.931
6.921
4.418
3.858
3.816
3.790
3.748
1.793
1.582
1.116
0.000
NO2
HO
Boc—N
NO2
O
Br
N
Boc
3e
0.90
0.97
0.98
0.98
0.98
0.98
1.00
1.02
1.02
9.00
8.80
f1 (ppm)

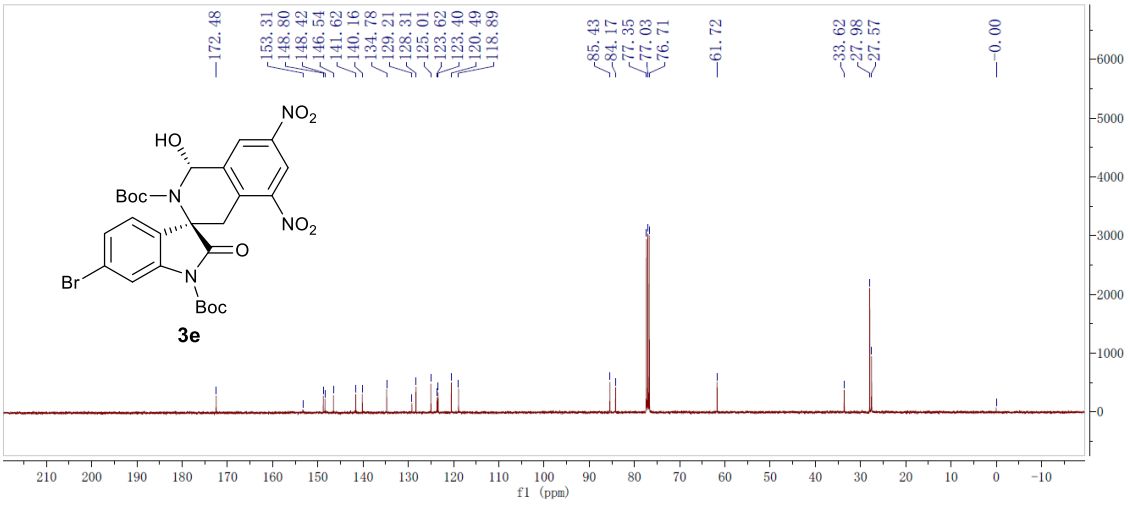
172.48
153.31
148.80
148.42
146.54
141.62
140.16
134.78
129.21
128.31
125.01
123.62
123.40
120.49
118.89
85.43
84.17
77.35
77.03
76.71
61.72
33.62
27.98
27.57
0.00
NO2
HO
Boc—N
NO2
O
Br
N
Boc
3e
f1 (ppm)

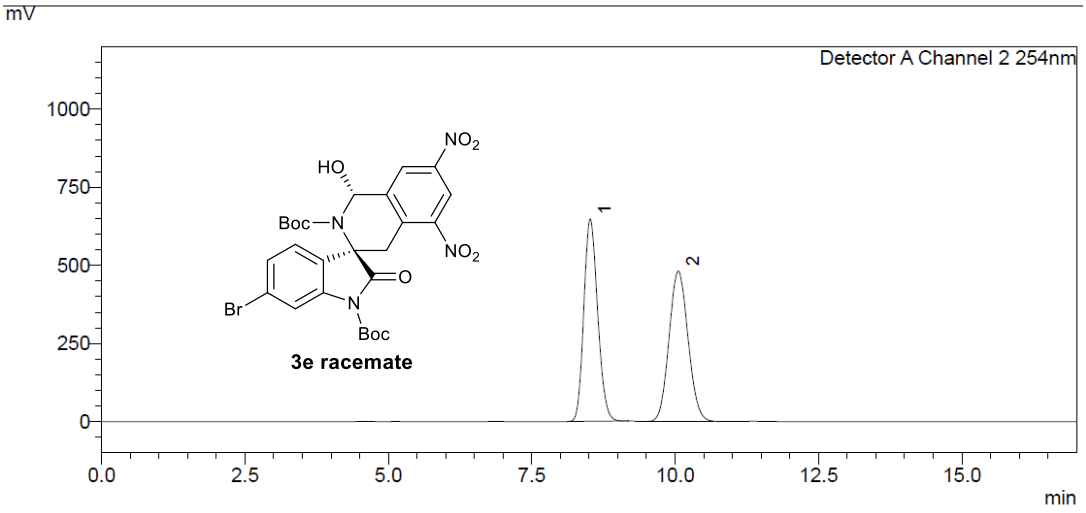

<Peak Table>

Detector A Channel 2 254nm

Peak#	Ret. Time	Area	Height	Conc.	Area%
1	8.520	10885307	647489	49.583	49.583
2	10.055	11068607	480588	50.417	50.417
Total		21953914	1128077		100.000

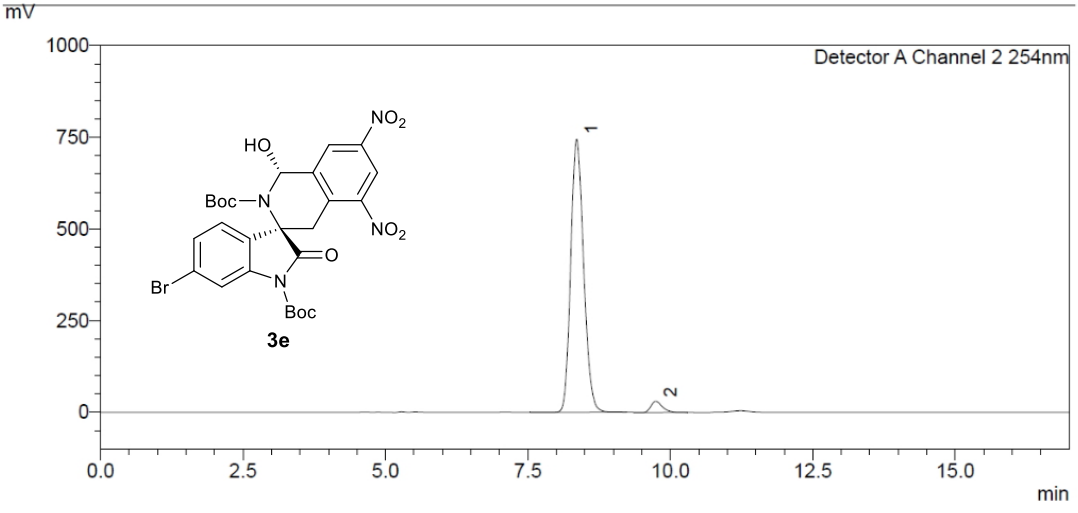

<Peak Table>

Detector A Channel 2 254nm

Peak#	Ret. Time	Area	Height	Conc.	Area%
1	8.356	11728881	744524	95.928	95.928
2	9.745	497822	35312	4.072	4.072
Total		12226703	779836		100.000

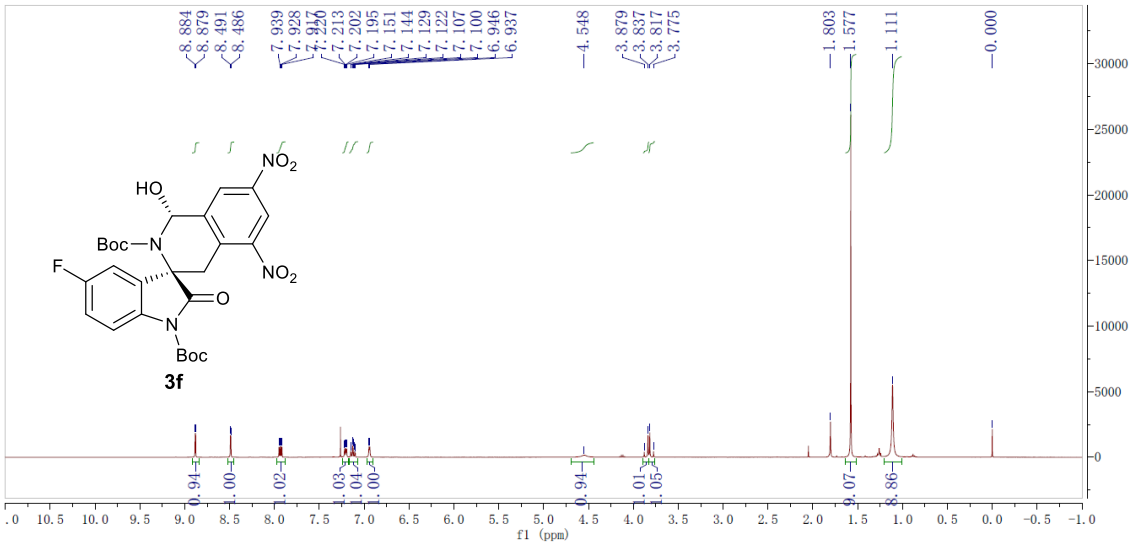
8.884
8.879
8.491
8.486
7.939
7.928
7.917
7.226
7.213
7.202
7.195
7.151
7.144
7.129
7.122
7.107
7.100
6.946
6.937
4.548
3.879
3.837
3.817
3.775
1.803
1.577
1.111
0.000
NO2
HO
Boc
N
F
O
N
Boc
NO2
3f
0.94
1.00
1.02
1.03
1.04
1.00
0.94
1.01
1.05
9.07
8.86
f1 (ppm)

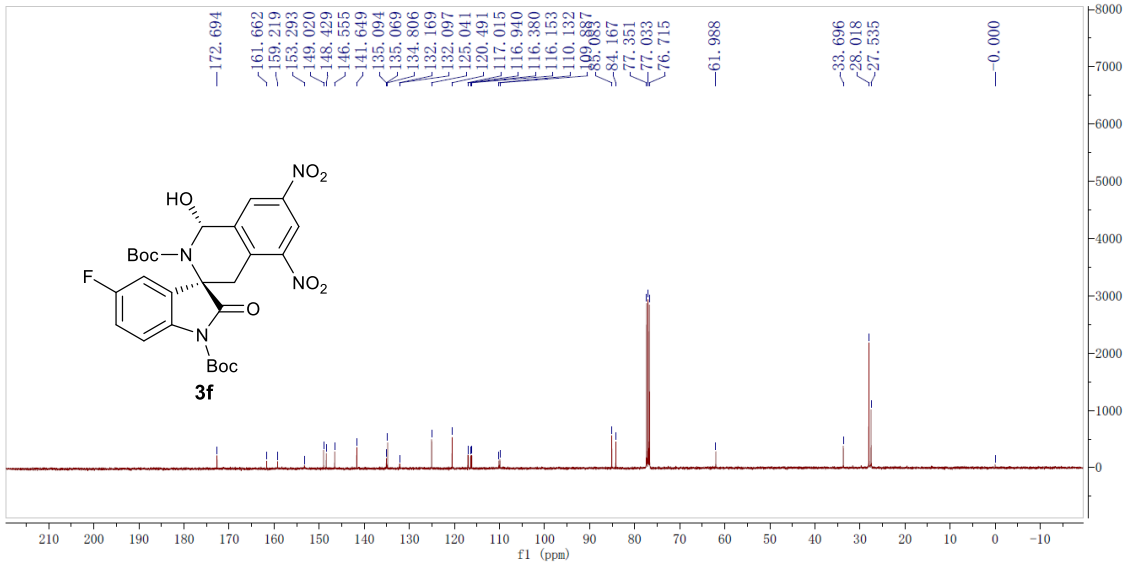
172.694
161.662
159.219
153.293
149.020
148.429
146.555
141.649
135.094
135.069
134.806
132.169
132.097
125.041
120.491
117.015
116.940
116.380
116.153
110.132
84.167
77.351
77.033
76.715
61.988
33.696
28.018
27.535
0.000
NO2
HO
Boc
N
F
O
N
Boc
NO2
3f
f1 (ppm)

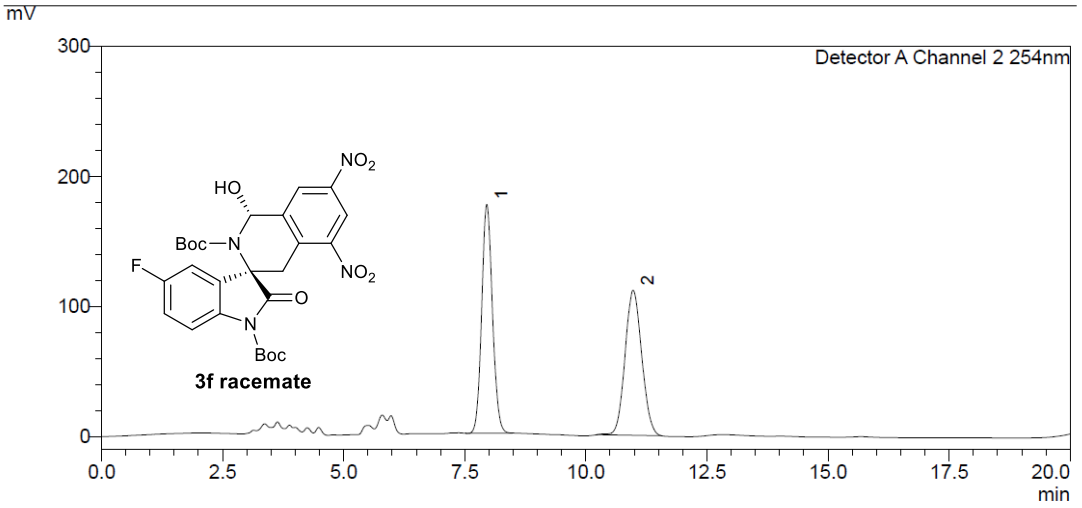

<Peak Table>

Detector A Channel 2 254nm

Peak#	Ret. Time	Area	Height	Conc.	Area%
1	7.954	2719630	175815	50.402	50.402
2	10.975	2676238	111432	49.598	49.598
Total		5395867	287247		100.000

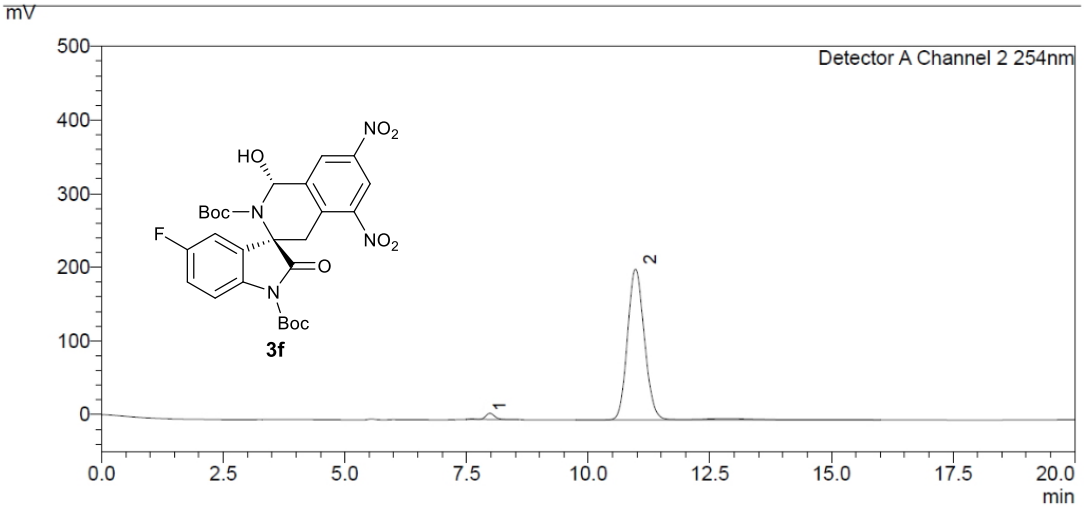

<Peak Table>

Detector A Channel 2 254nm

Peak#	Ret. Time	Area	Height	Conc.	Area%
1	7.970	137788	15924	2.614	2.614
2	10.972	5134343	204811	97.386	97.386
Total		5272132	220736		100.000

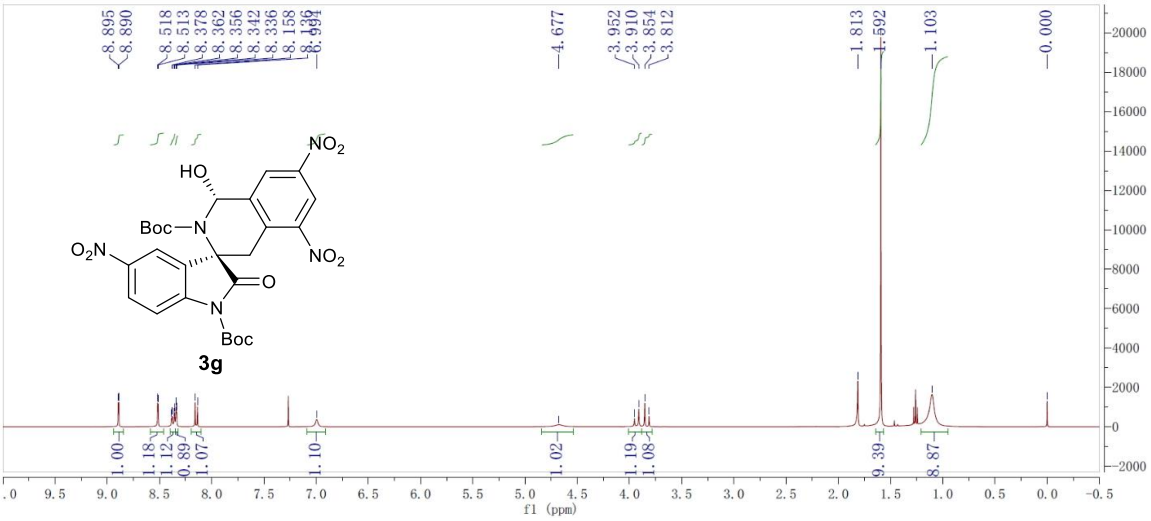
8.895
8.890
8.518
8.513
8.378
8.362
8.356
8.342
8.336
8.158
6.994
4.677
3.952
3.910
3.854
3.812
1.813
1.592
1.103
0.000
HO
Boc
N
O2N
NO2
NO2
O
N
Boc
3g
1.00
1.18
1.12
0.89
1.07
1.10
1.02
1.19
1.08
9.39
8.87
f1 (ppm)

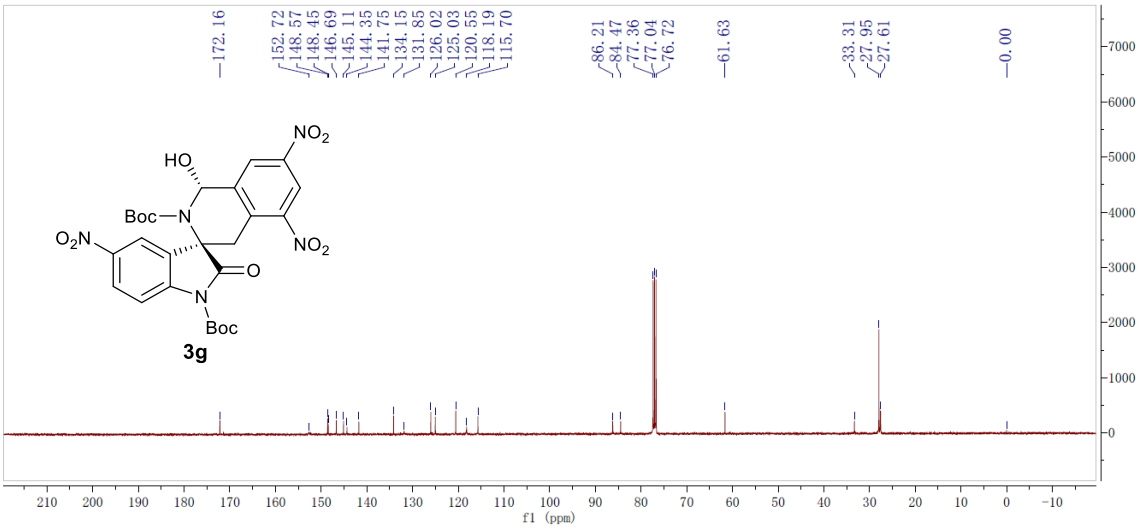
172.16
152.72
148.57
148.45
146.69
145.11
144.35
141.75
134.15
131.85
126.02
125.03
120.55
118.19
115.70
86.21
84.47
77.36
77.04
76.72
61.63
33.31
27.95
27.61
0.00
HO
Boc
N
O2N
NO2
NO2
O
N
Boc
3g
f1 (ppm)

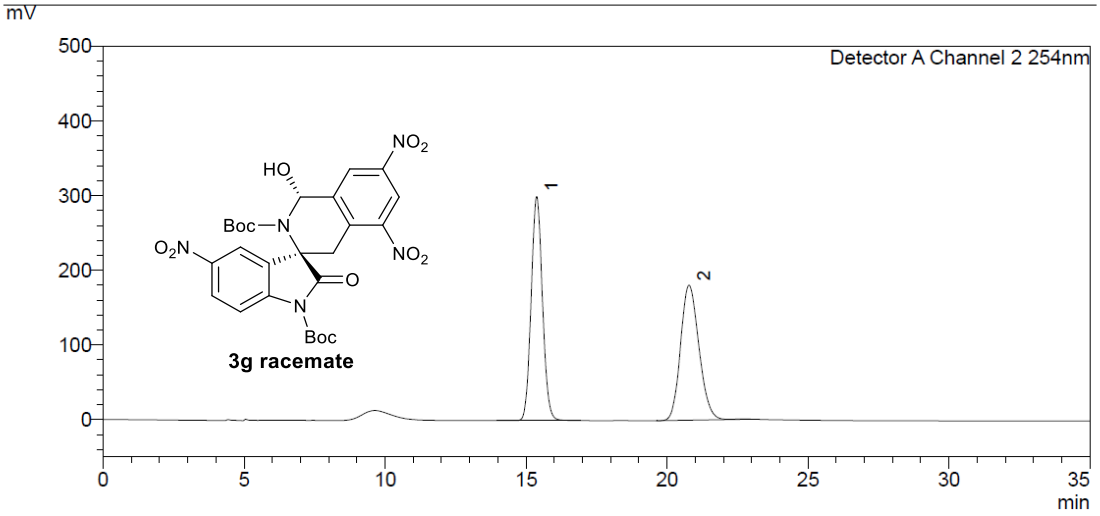

<Peak Table>

Detector A Channel 2 254nm

Peak#	Ret. Time	Area	Height	Conc.	Area%
1	15.376	8360948	300289	50.479	50.479
2	20.780	8202190	180827	49.521	49.521
Total		16563138	481117		100.000

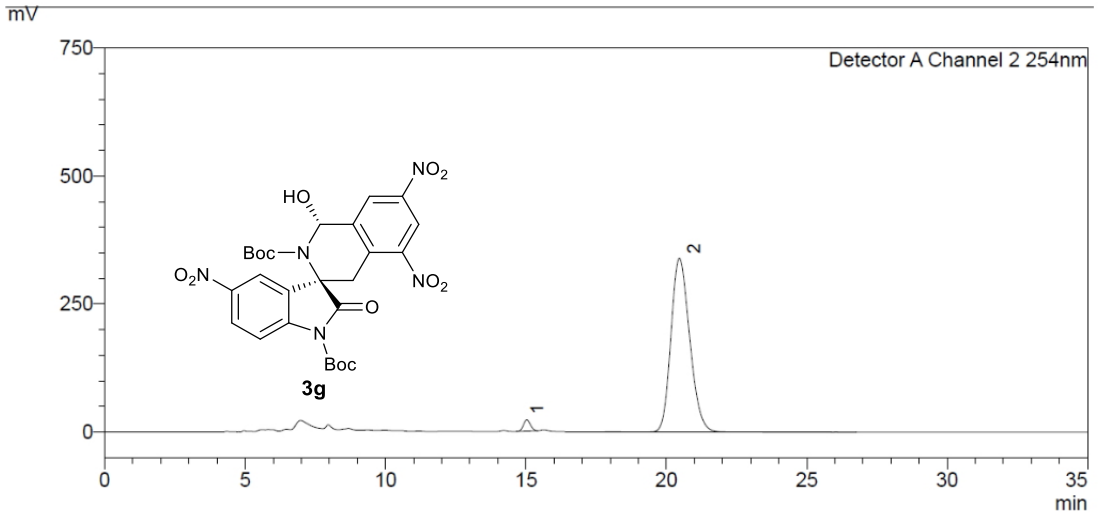

<Peak Table>

Detector A Channel 2 254nm

Peak#	Ret. Time	Area	Height	Conc.	Area%
1	15.041	475601	28644	2.924	2.924
2	20.464	15790136	339593	97.076	97.076
Total		16265737	368237		100.000

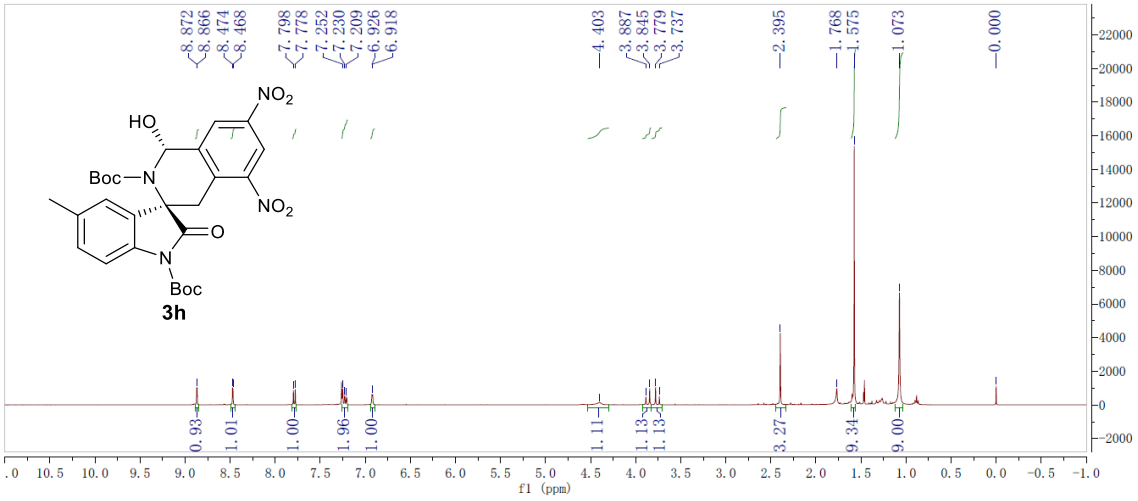
8.872
8.866
8.474
8.468
7.798
7.778
7.252
7.230
7.209
6.926
6.918
4.403
3.887
3.845
3.779
3.737
2.395
1.768
1.575
1.073
0.000
HO
Boc—N
NO2
NO2
O
N
Boc
3h
0.93
1.01
1.00
1.96
1.00
1.11
1.13
1.13
3.27
9.34
9.00
f1 (ppm)

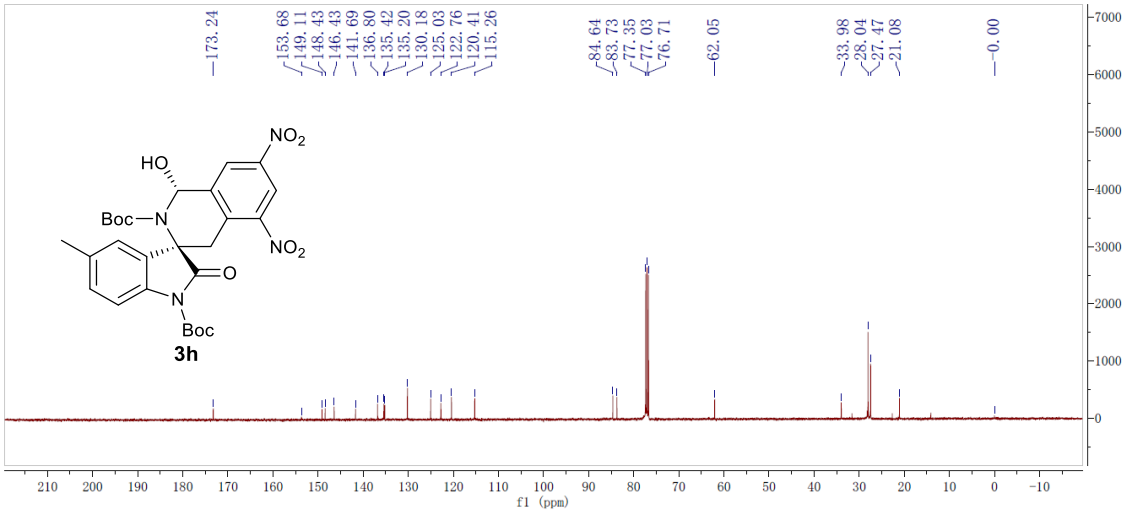
173.24
153.68
149.11
148.43
146.43
141.69
136.80
135.42
135.20
130.18
125.03
122.76
120.41
115.26
84.64
83.73
77.35
77.03
76.71
62.05
33.98
28.04
27.47
21.08
0.00
HO
Boc—N
NO2
NO2
O
N
Boc
3h
f1 (ppm)

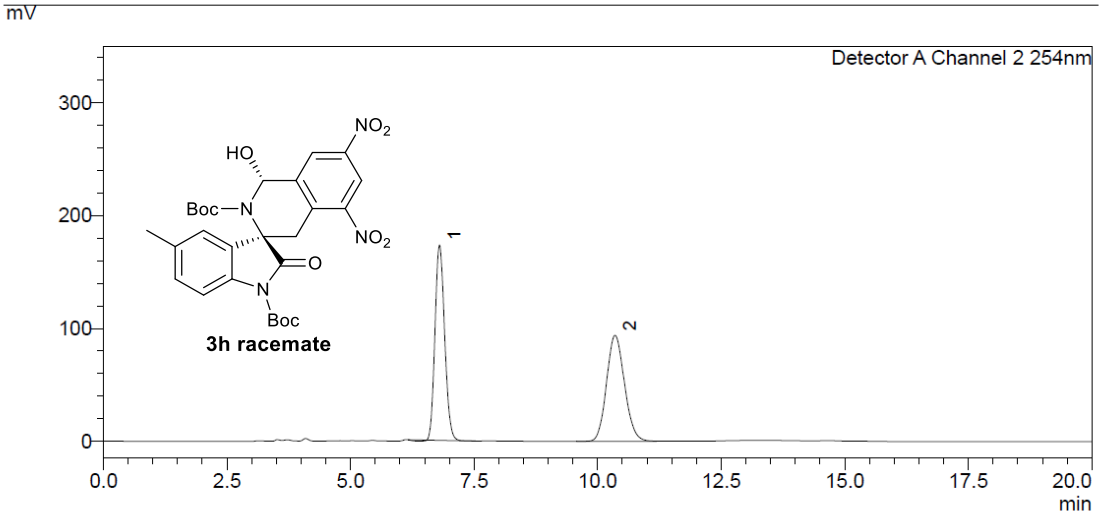

<Peak Table>

Detector A Channel 2 254nm

Peak#	Ret. Time	Area	Height	Conc.	Area%
1	6.800	2331229	173218	49.550	49.550
2	10.352	2373583	93943	50.450	50.450
Total		4704812	267161		100.000

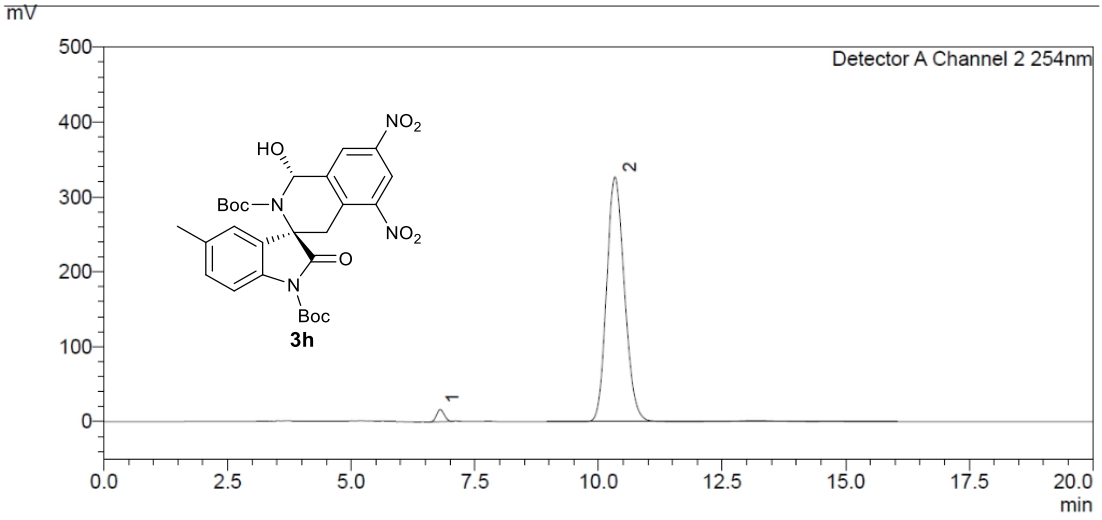

<Peak Table>

Detector A Channel 2 254nm

Peak#	Ret. Time	Area	Height	Conc.	Area%
1	6.803	231184	27230	2.710	2.710
2	10.333	8298670	326922	97.290	97.290
Total		8529854	354152		100.000

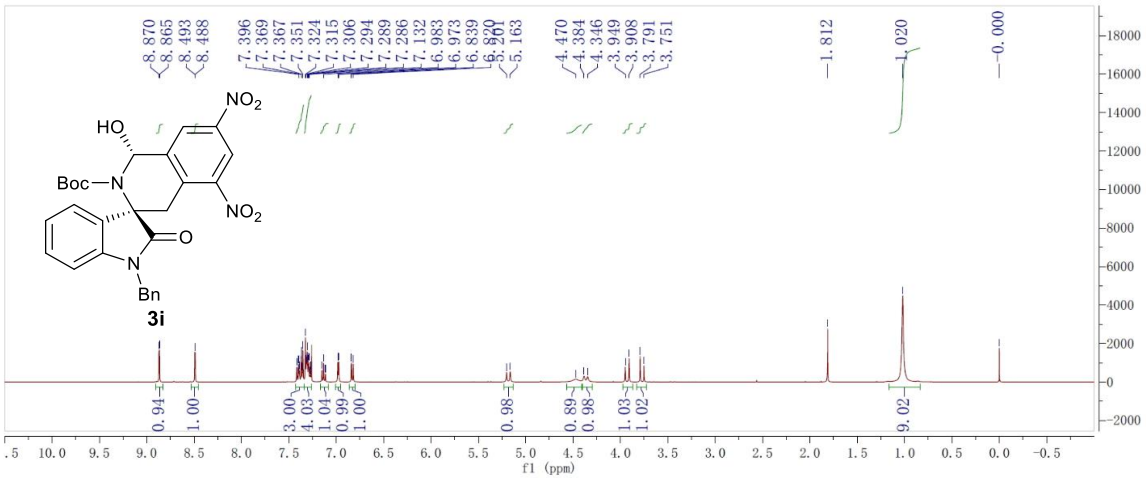
8.870
8.865
8.493
8.488
7.396
7.369
7.367
7.351
7.324
7.315
7.306
7.294
7.289
7.286
7.132
6.983
6.973
6.839
6.830
5.261
5.163
4.470
4.384
4.346
3.949
3.908
3.791
3.751
1.812
1.020
0.000
NO2
HO
Boc—N
NO2
O
N
Bn
3i
0.94
1.00
3.00
4.03
1.04
0.99
1.00
0.98
0.89
0.98
1.03
1.02
9.02
f1 (ppm)

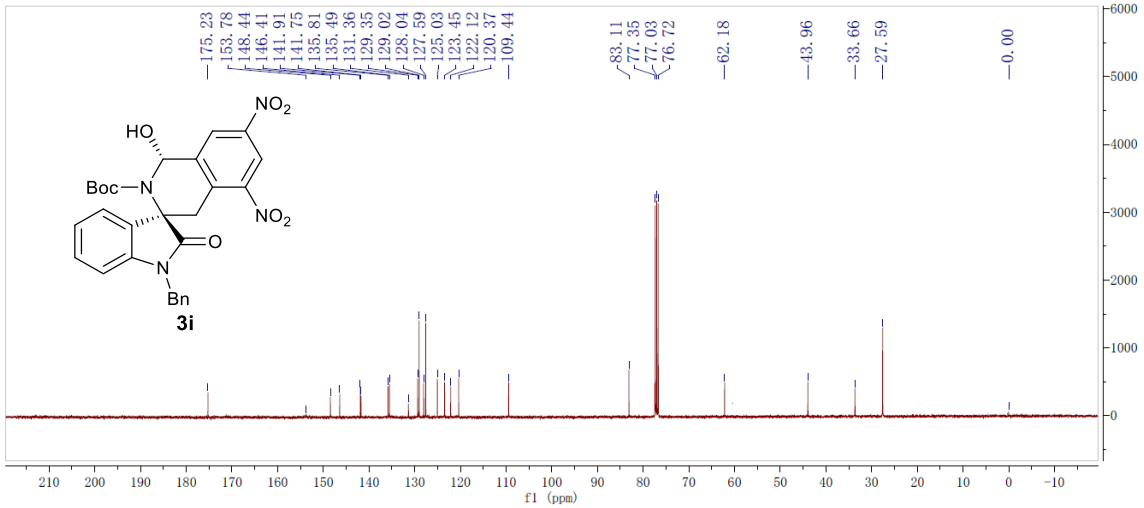
175.23
153.78
148.44
146.41
141.91
141.75
135.81
135.49
131.36
129.35
129.02
128.04
127.59
125.03
123.45
122.12
120.37
109.44
83.11
77.35
77.03
76.72
62.18
43.96
33.66
27.59
0.00
NO2
HO
Boc—N
NO2
O
N
Bn
3i
f1 (ppm)

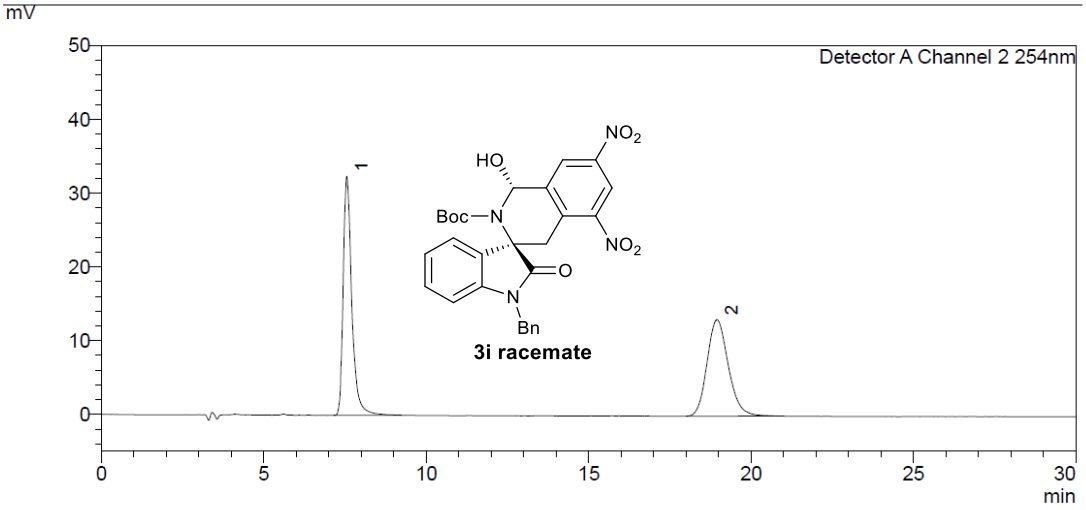

<Peak Table>

Detector A Channel 2 254nm

Peak#	Ret. Time	Area	Height	Conc.	Area%
1	7.550	597892	32414	50.133	50.133
2	18.947	594708	13108	49.867	49.867
Total		1192600	45522		100.000

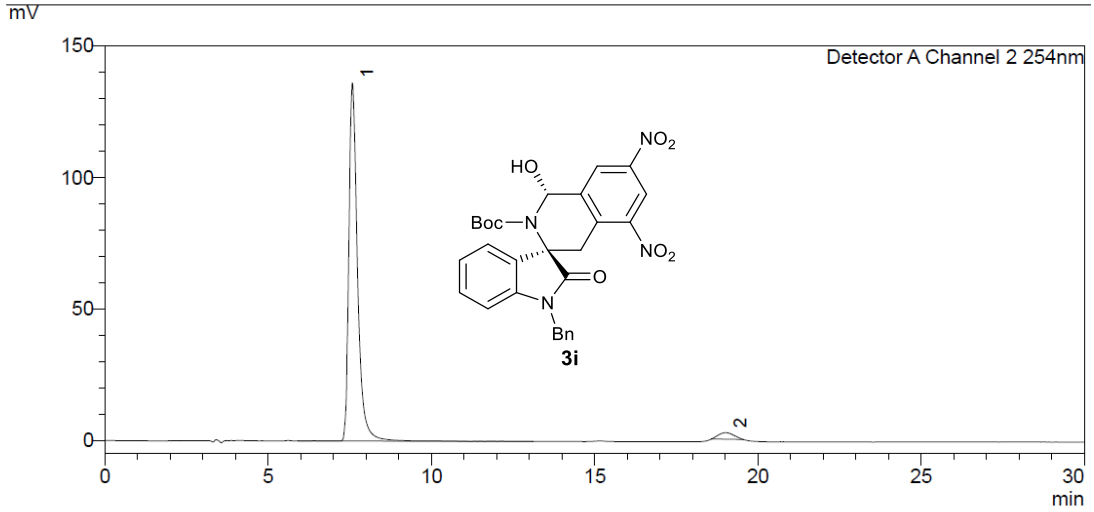

<Peak Table>

Detector A Channel 2 254nm

Peak#	Ret. Time	Area	Height	Conc.	Area%
1	7.575	2500398	136064	96.838	96.838
2	19.008	81647	2464	3.162	3.162
Total		2582045	138528		100.000

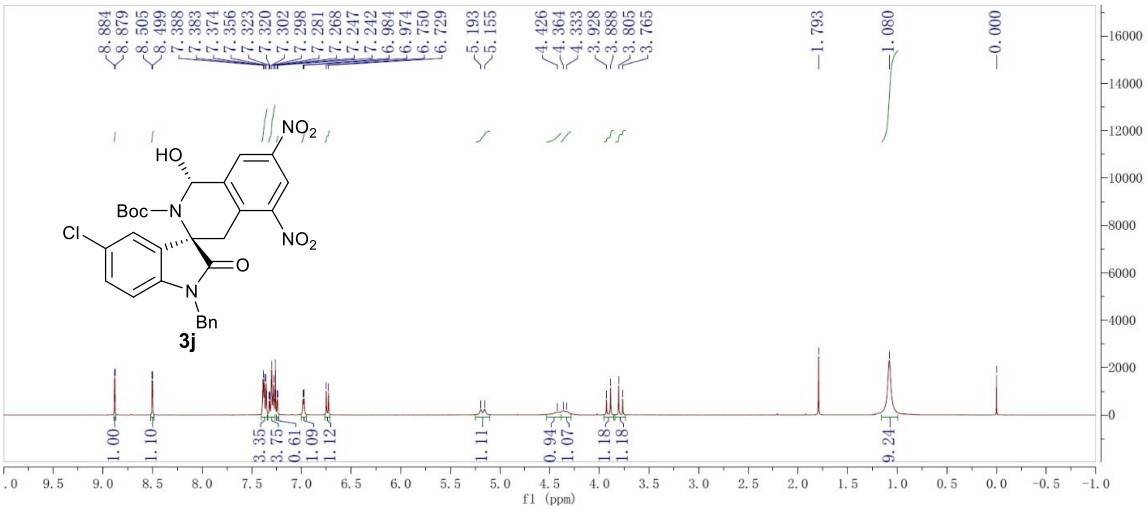
8.884
8.879
8.505
8.499
7.388
7.383
7.374
7.356
7.323
7.320
7.302
7.298
7.281
7.268
7.247
7.242
6.984
6.974
6.750
6.729
5.193
5.155
4.426
4.364
4.333
3.928
3.888
3.805
3.765
1.793
1.080
0.000
NO2
HO
Boc
N
Cl
NO2
O
N
Bn
3j
1.00
1.10
3.35
3.75
0.61
1.09
1.12
1.11
0.94
1.07
1.18
1.18
9.24
f1 (ppm)

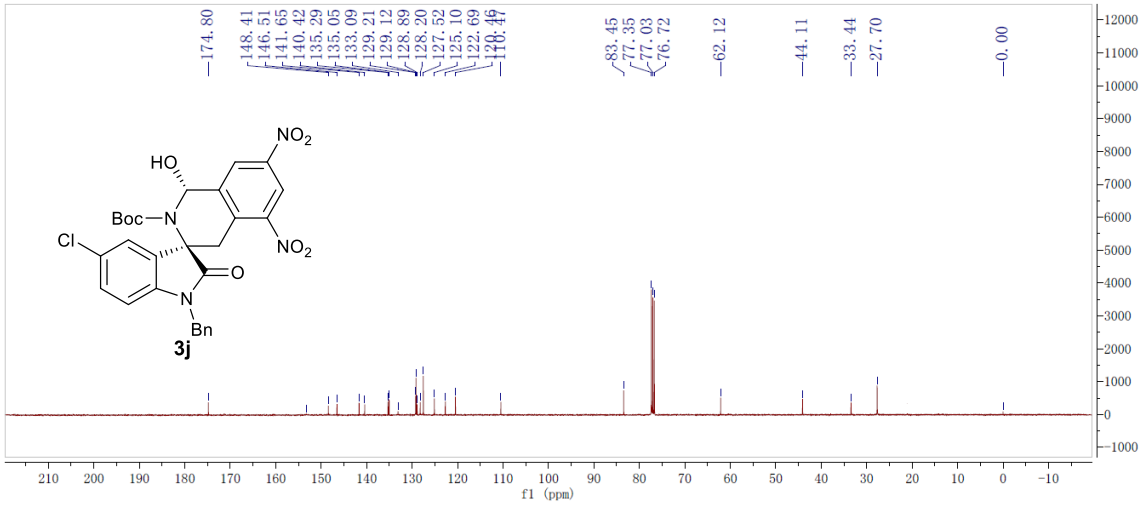
174.80
148.41
146.51
141.65
140.42
135.29
135.05
133.09
129.21
129.12
128.89
128.20
127.52
125.10
122.69
83.45
77.35
77.03
76.72
62.12
44.11
33.44
27.70
0.00
NO2
HO
Boc
N
Cl
NO2
O
N
Bn
3j
f1 (ppm)

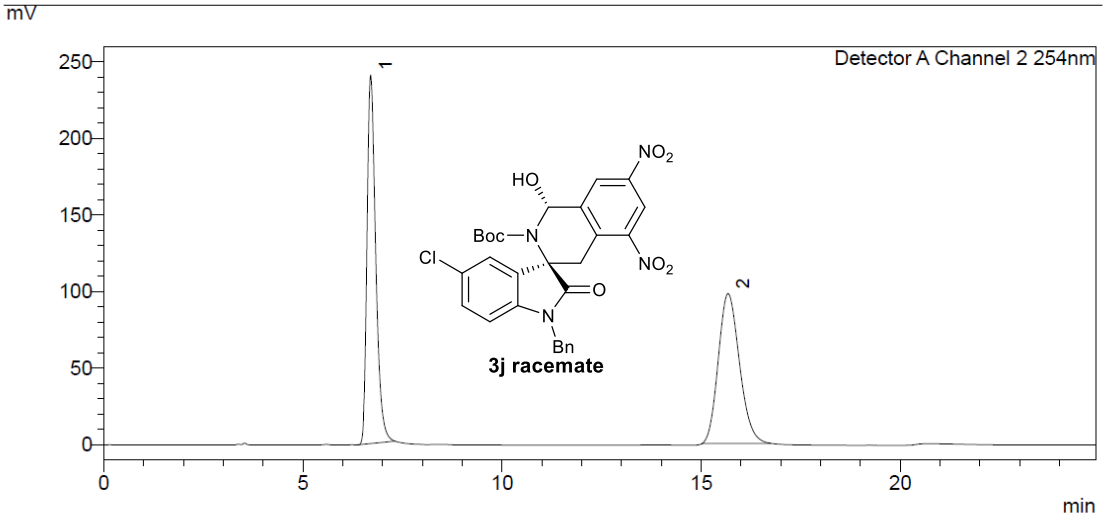

<Peak Table>

Detector A Channel 2 254nm

Peak#	Ret. Time	Area	Height	Conc.	Area%
1	6.699	3661440	240688	50.333	50.333
2	15.675	3613030	97785	49.667	49.667
Total		7274470	338473		100.000

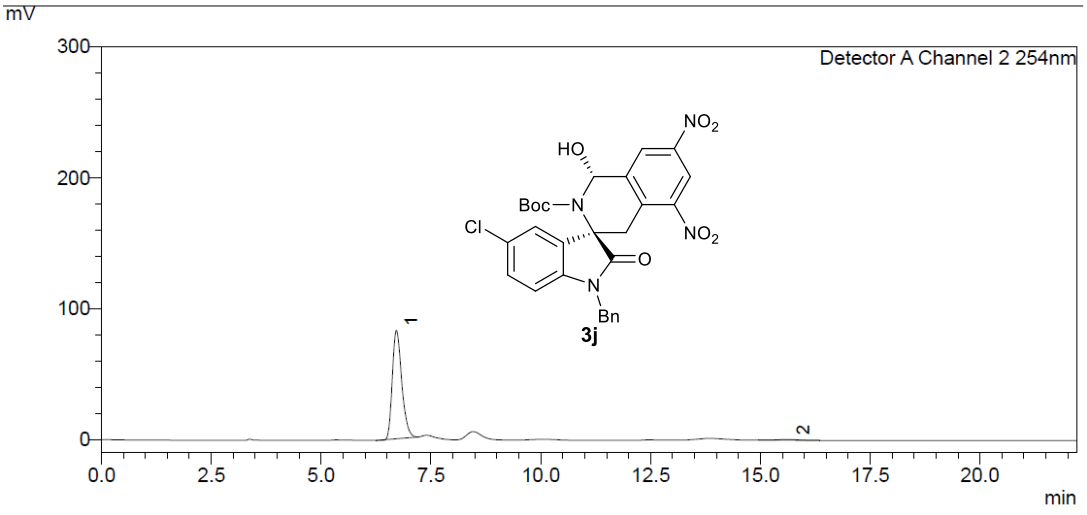

<Peak Table>

Detector A Channel 2 254nm

Peak#	Ret. Time	Area	Height	Conc.	Area%
1	6.714	1234178	82771	98.657	98.657
2	15.643	16803	486	1.343	1.343
Total		1250980	83257		100.000

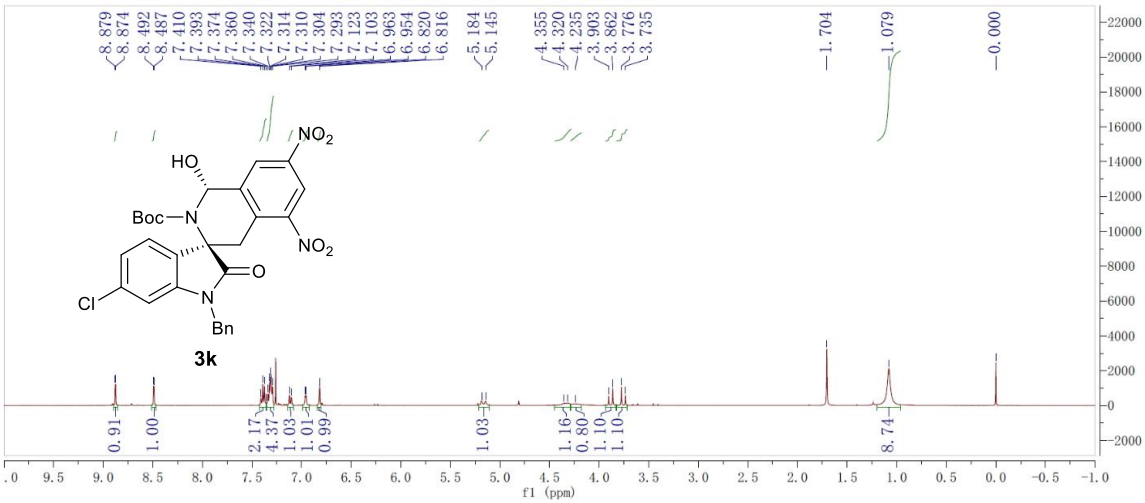
8.879
8.874
8.492
8.487
7.410
7.393
7.374
7.360
7.340
7.322
7.314
7.310
7.304
7.293
7.123
7.103
6.963
6.954
6.820
6.816
5.184
5.145
4.355
4.320
4.235
3.903
3.862
3.776
3.735
1.704
1.079
0.000
NO2
HO
Boc
N
NO2
O
Cl
N
Bn
3k
0.91
1.00
2.17
4.37
1.03
1.01
0.99
1.03
1.16
0.80
1.10
1.10
8.74
f1 (ppm)

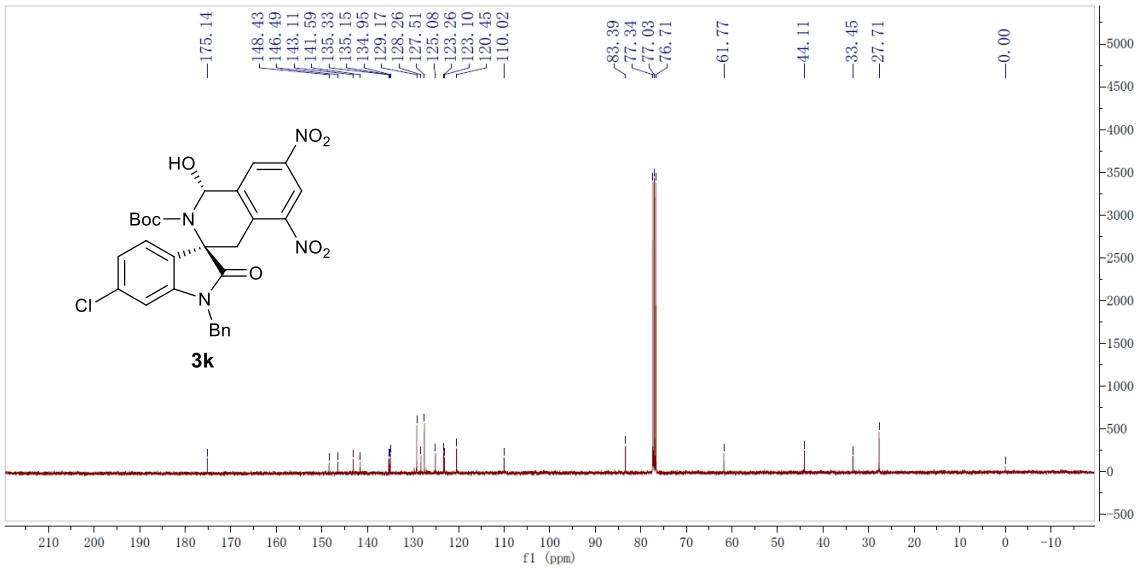
175.14
148.43
146.49
143.11
141.59
135.33
135.15
134.95
129.17
128.26
127.51
125.08
123.26
123.10
120.45
110.02
83.39
77.34
77.03
76.71
61.77
44.11
33.45
27.71
0.00
NO2
HO
Boc
N
NO2
O
Cl
N
Bn
3k
f1 (ppm)

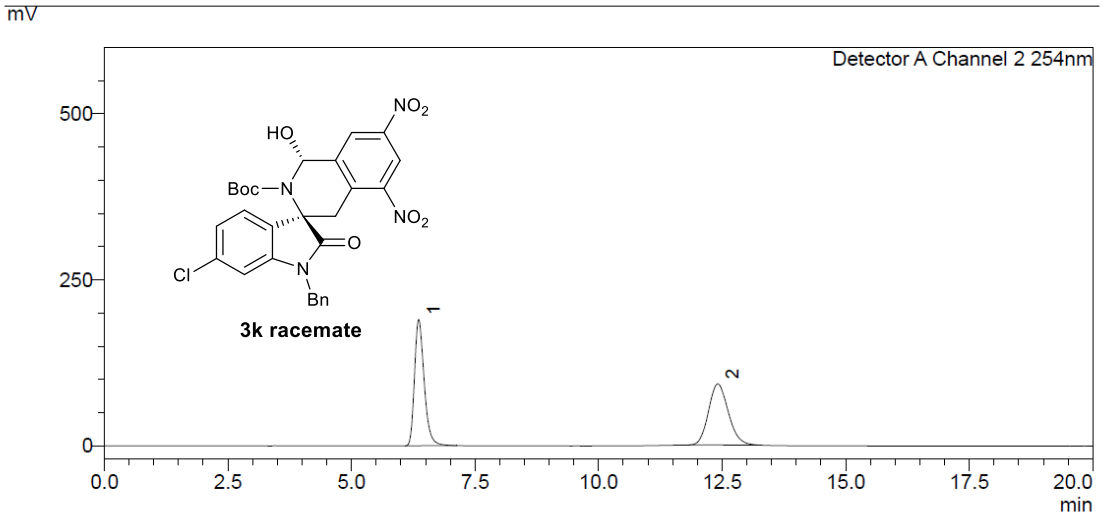

<Peak Table>

Detector A Channel 2 254nm

Peak#	Ret. Time	Area	Height	Conc.	Area%
1	6.361	2591367	190236	50.310	50.310
2	12.412	2559423	92015	49.690	49.690
Total		5150790	282251		100.000

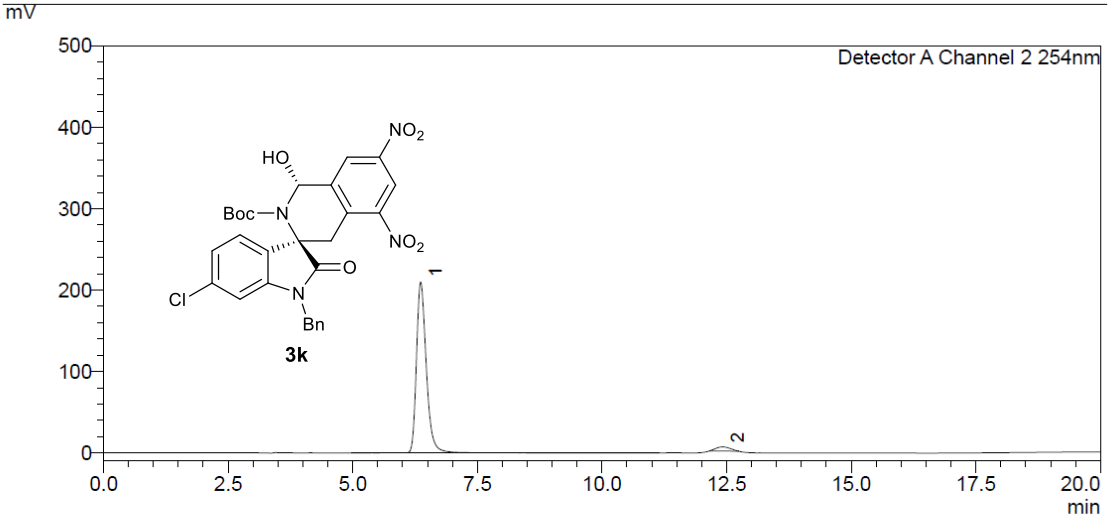

<Peak Table>

Detector A Channel 2 254nm

Peak#	Ret. Time	Area	Height	Conc.	Area%
1	6.364	2893237	210070	96.602	96.602
2	12.420	101785	5093	3.398	3.398
Total		2995022	215162		100.000

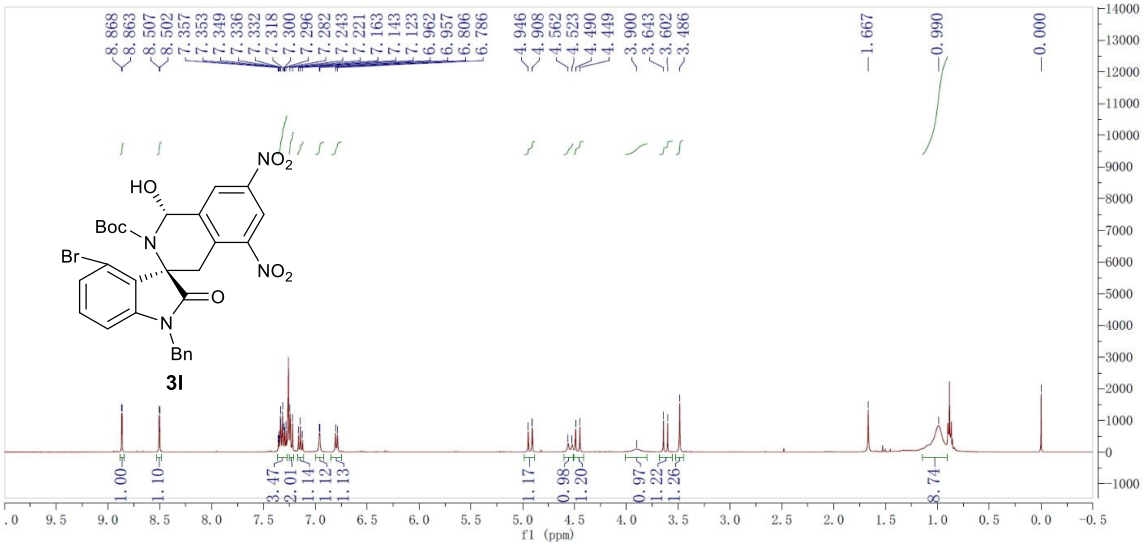
8.868
8.863
8.507
8.502
7.357
7.353
7.349
7.336
7.332
7.318
7.300
7.296
7.282
7.243
7.221
7.163
7.143
7.123
6.962
6.957
6.806
6.786
4.946
4.908
4.562
4.523
4.490
4.449
3.900
3.643
3.602
3.486
1.667
0.990
0.000
NO2
HO
Boc
N
Br
O
NO2
N
Bn
3l
1.00
1.10
3.47
2.01
1.14
1.12
1.13
1.17
0.98
1.20
0.97
1.22
1.26
8.74
f1 (ppm)

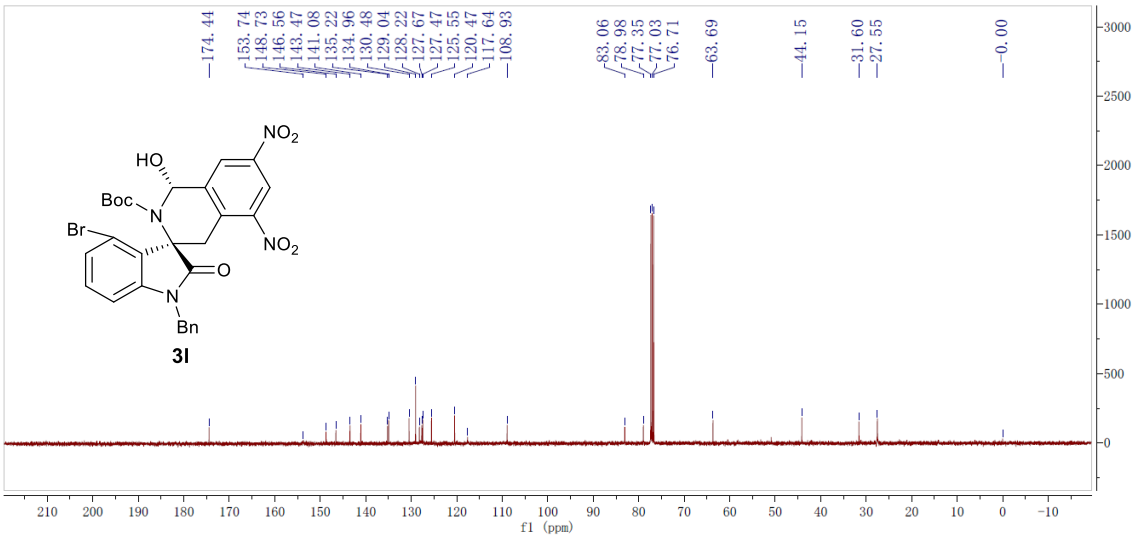
174.44
153.74
148.73
146.56
143.47
141.08
135.22
134.96
130.48
129.04
128.22
127.67
127.47
125.55
120.47
117.64
108.93
83.06
78.98
77.35
77.03
76.71
63.69
44.15
31.60
27.55
0.00
NO2
HO
Boc
N
Br
O
NO2
N
Bn
3l
f1 (ppm)

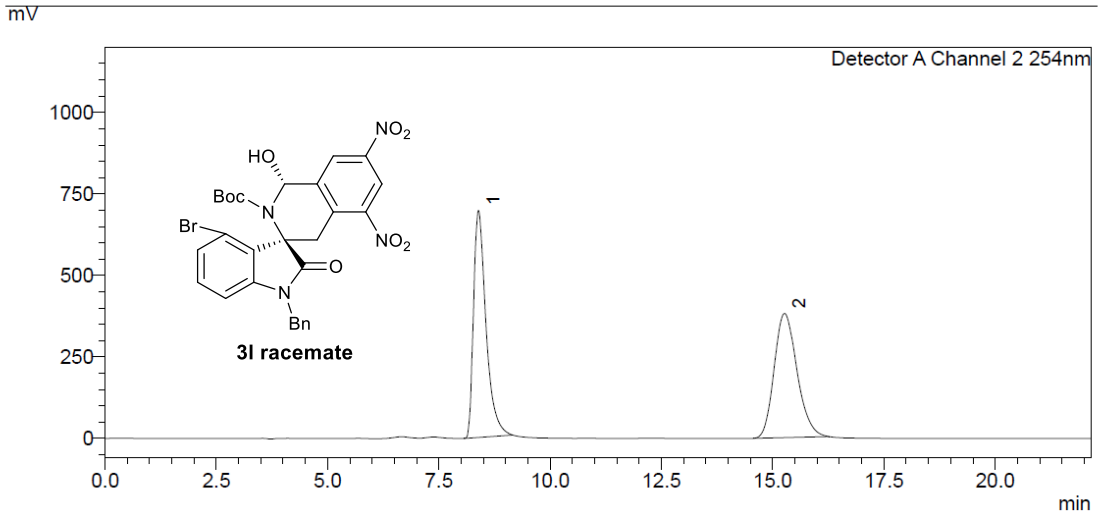

<Peak Table>

Detector A Channel 2 254nm

Peak#	Ret. Time	Area	Height	Conc.	Area%
1	8.390	13563266	696656	49.883	49.883
2	15.266	13627071	381228	50.117	50.117
Total		27190338	1077884		100.000

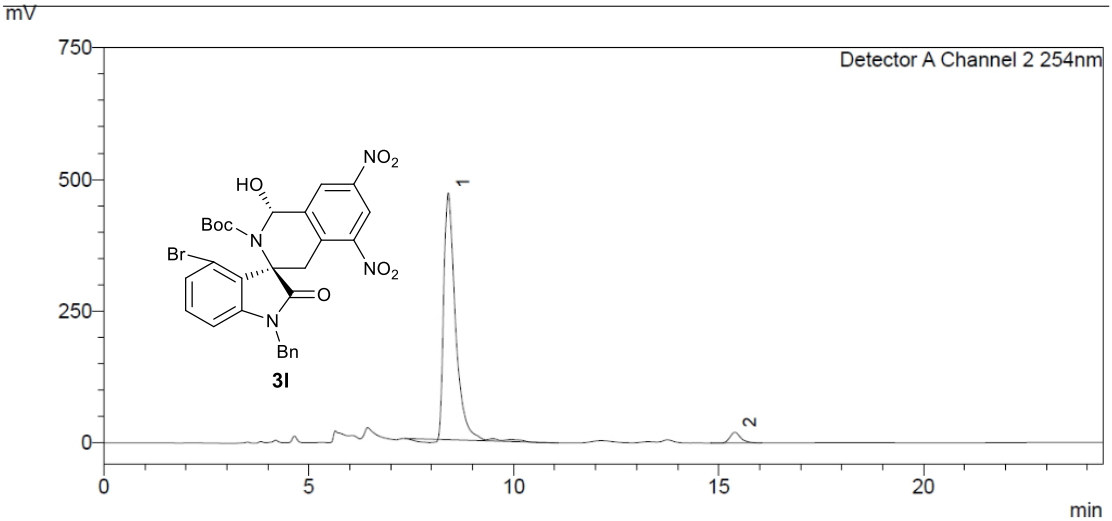

<Peak Table>

Detector A Channel 2 254nm

Peak#	Ret. Time	Area	Height	Conc.	Area%
1	8.400	9212593	468678	95.762	95.762
2	15.369	407658	38991	4.238	4.238
Total		9620252	507668		100.000

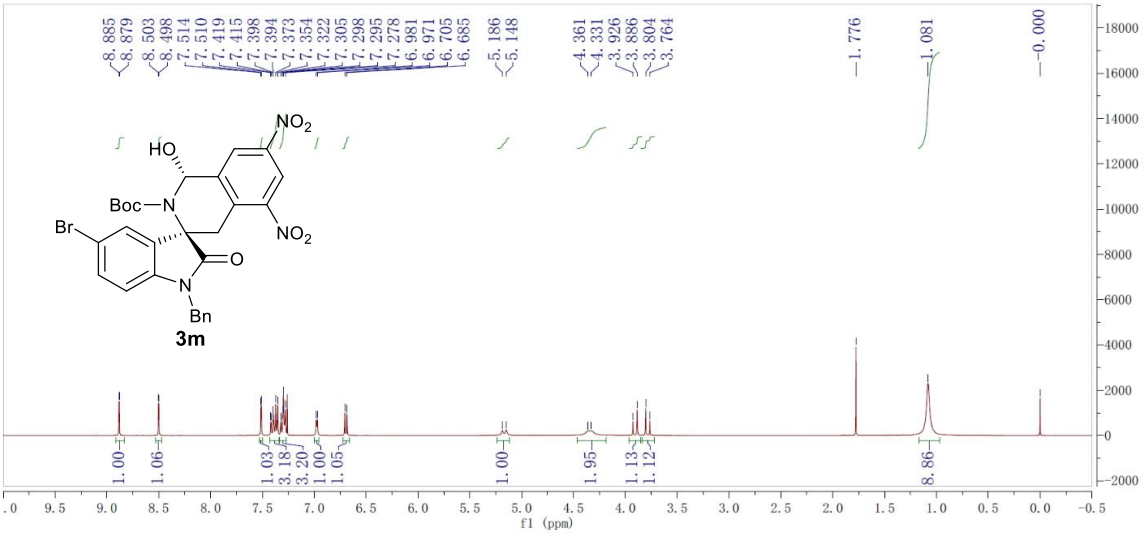
8.885
8.879
8.503
8.498
7.514
7.510
7.419
7.415
7.398
7.394
7.373
7.354
7.322
7.305
7.298
7.295
7.278
6.981
6.971
6.705
6.685
5.186
5.148
4.361
4.331
3.926
3.886
3.804
3.764
1.776
1.081
0.000
HO
Boc—N
Br
NO2
NO2
O
N
Bn
3m
1.00
1.06
1.03
3.18
3.20
1.00
1.05
1.00
1.95
1.13
1.12
8.86
f1 (ppm)

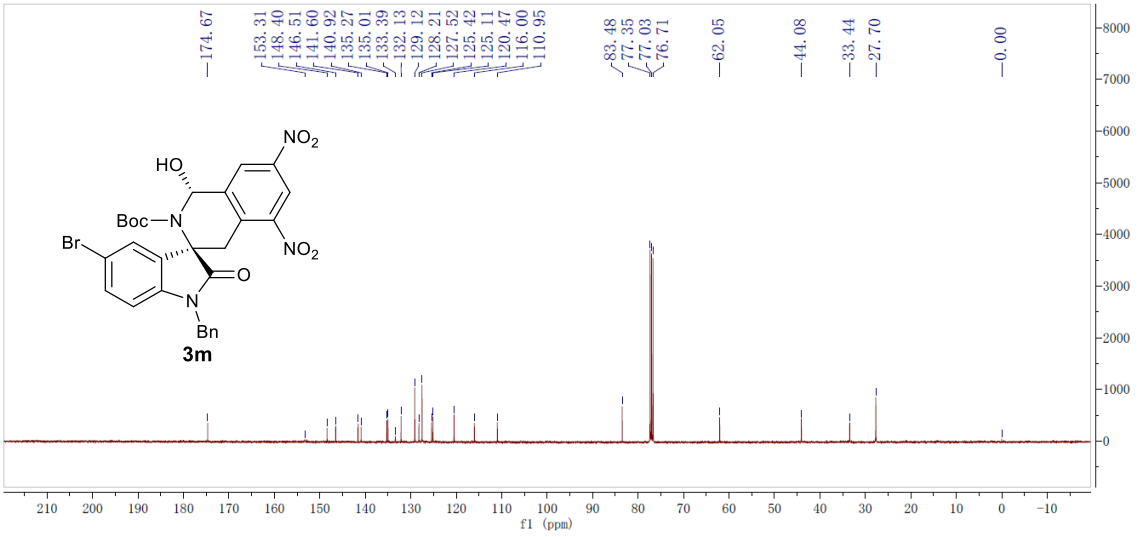
174.67
153.31
148.40
146.51
141.60
140.92
135.27
135.01
133.39
132.13
129.12
128.21
127.52
125.42
125.11
120.47
116.00
110.95
83.48
77.35
77.03
76.71
62.05
44.08
33.44
27.70
0.00
HO
Boc—N
Br
NO2
NO2
O
N
Bn
3m
f1 (ppm)

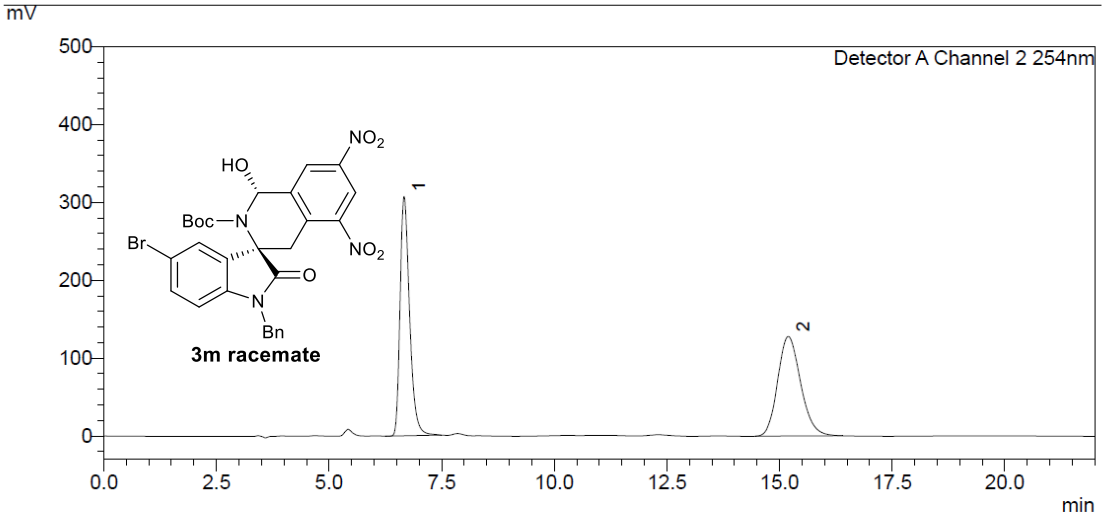

<Peak Table>

Detector A Channel 2 254nm

Peak#	Ret. Time	Area	Height	Conc.	Area%
1	6.665	4529323	307300	50.025	50.025
2	15.195	4524763	127851	49.975	49.975
Total		9054086	435152		100.000

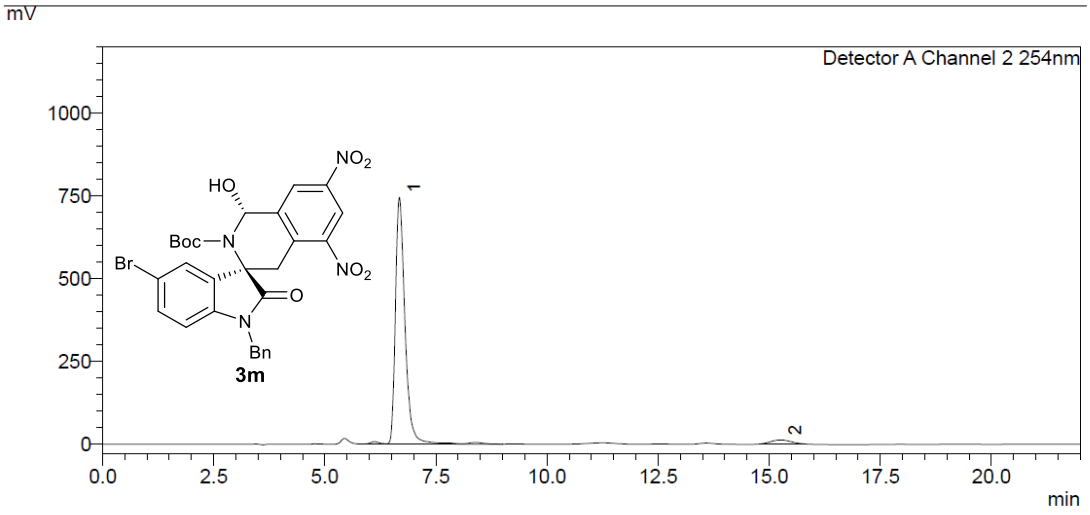

<Peak Table>

Detector A Channel 2 254nm

Peak#	Ret. Time	Area	Height	Conc.	Area%
1	6.678	11326959	744724	96.897	96.897
2	15.253	362764	11872	3.103	3.103
Total		11689723	756596		100.000

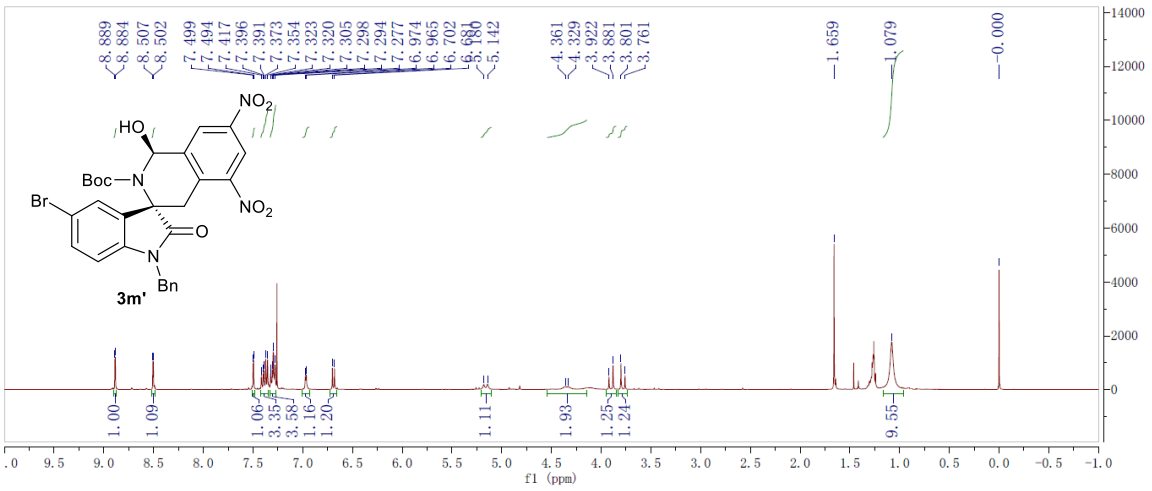
8.889
8.884
8.507
8.502
7.499
7.494
7.417
7.396
7.391
7.373
7.354
7.323
7.320
7.305
7.298
7.294
7.277
6.974
6.965
6.702
5.142
4.361
4.329
3.922
3.881
3.801
3.761
1.659
1.079
0.000
1.00
1.09
1.06
3.35
3.58
1.16
1.20
1.11
1.93
1.25
1.24
9.55
f1 (ppm)
HO
Boc
N
Br
NO2
NO2
O
N
Bn
3m'

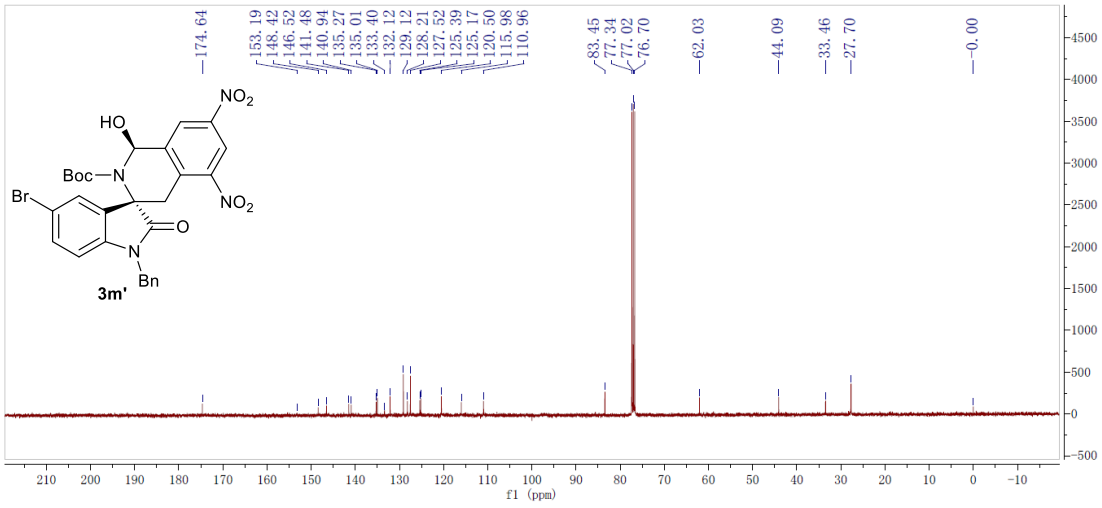
174.64
153.19
148.42
146.52
141.48
140.94
135.27
135.01
133.40
132.12
129.12
128.21
127.52
125.39
125.17
120.50
115.98
110.96
83.45
77.34
77.02
76.70
62.03
44.09
33.46
27.70
0.00
f1 (ppm)
HO
Boc
N
Br
NO2
NO2
O
N
Bn
3m'

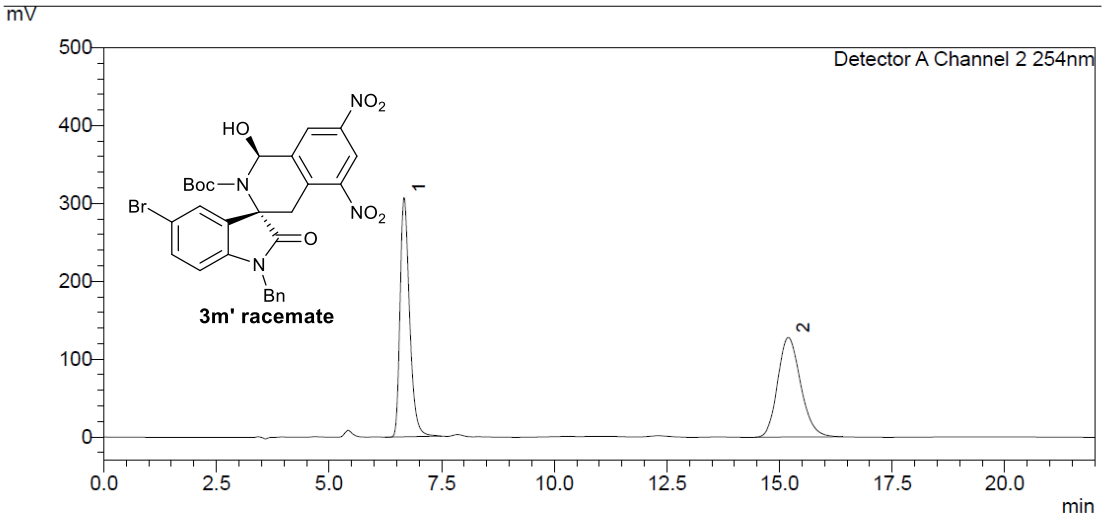

<Peak Table>

Detector A Channel 2 254nm

Peak#	Ret. Time	Area	Height	Conc.	Area%
1	6.665	4529323	307300	50.025	50.025
2	15.195	4524763	127851	49.975	49.975
Total		9054086	435152		100.000

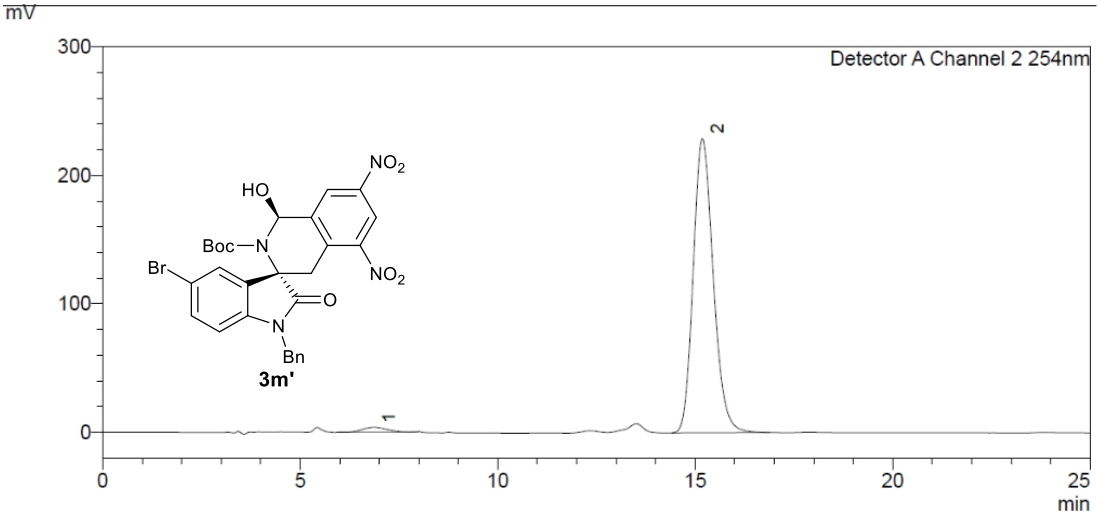

<Peak Table>

Detector A Channel 2 254nm

Peak#	Ret. Time	Area	Height	Conc.	Area%
1	6.693	331898	31727	3.940	3.940
2	15.183	8091785	228846	96.060	96.060
Total		8423683	260573		100.000

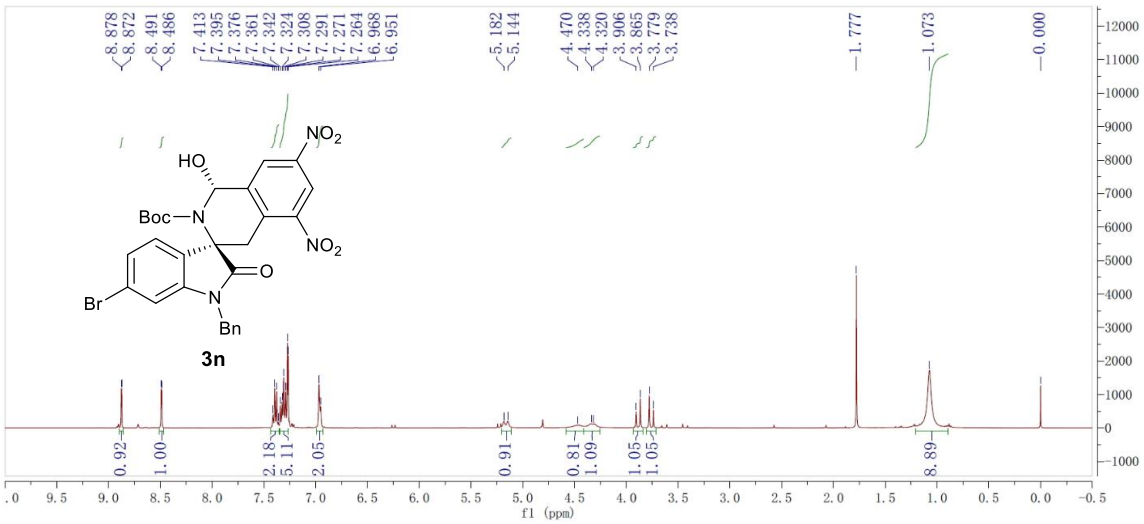
8.878
8.872
8.491
8.486
7.413
7.395
7.376
7.361
7.342
7.324
7.308
7.291
7.271
7.264
6.968
6.951
5.182
5.144
4.470
4.338
4.320
3.906
3.865
3.779
3.738
1.777
1.073
0.000
NO2
HO
Boc
N
NO2
O
Br
N
Bn
3n
0.92
1.00
2.18
5.11
2.05
0.91
0.81
1.09
1.05
1.05
8.89
f1 (ppm)

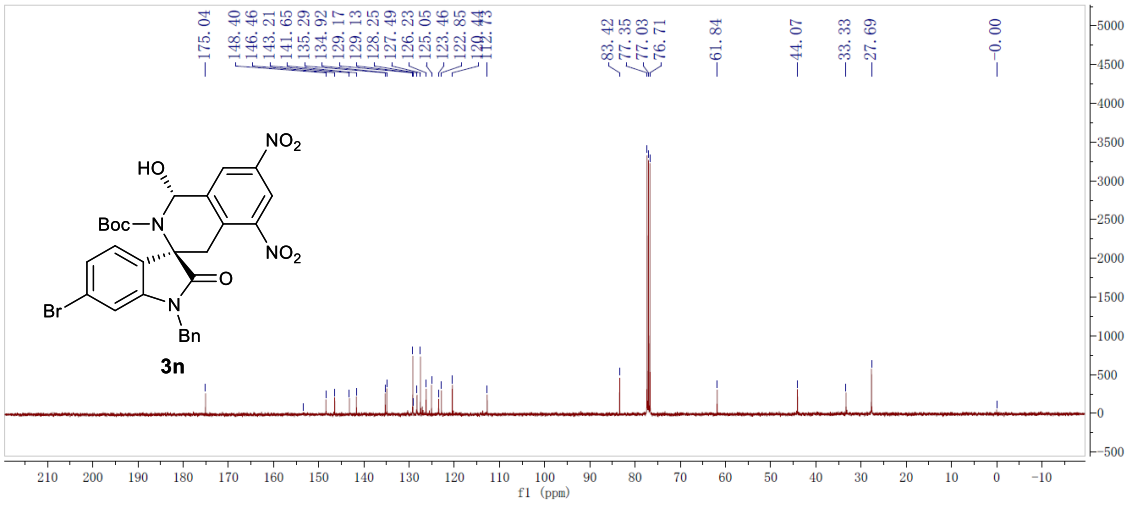
175.04
148.40
146.46
143.21
141.65
135.29
134.92
129.17
129.13
128.25
127.49
126.23
125.05
123.46
122.85
83.42
77.35
77.03
76.71
61.84
44.07
33.33
27.69
0.00
NO2
HO
Boc
N
NO2
O
Br
N
Bn
3n
f1 (ppm)

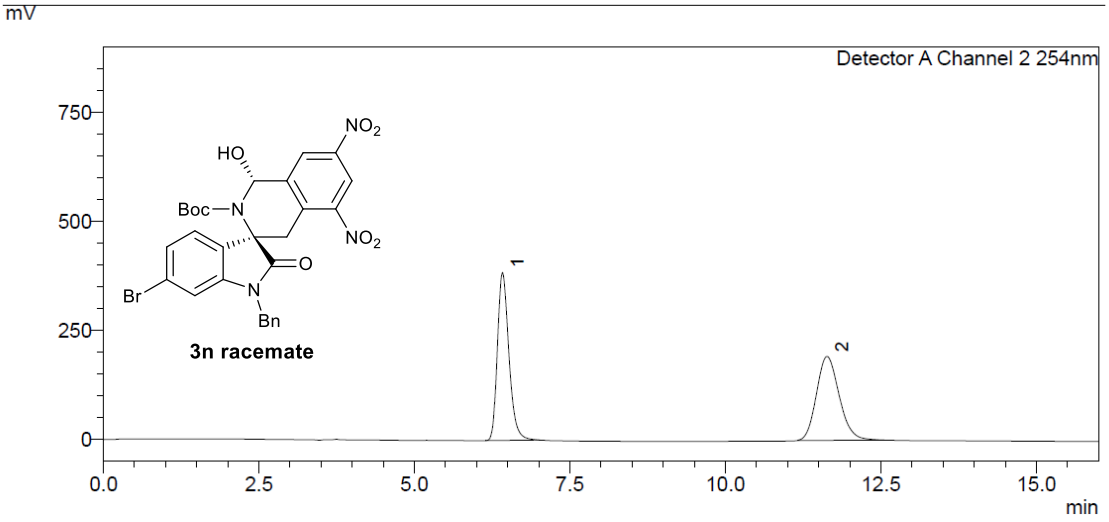

<Peak Table>

Detector A Channel 2 254nm

Peak#	Ret. Time	Area	Height	Conc.	Area%
1	6.417	4950428	384813	50.373	50.373
2	11.634	4877181	192207	49.627	49.627
Total		9827609	577020		100.000

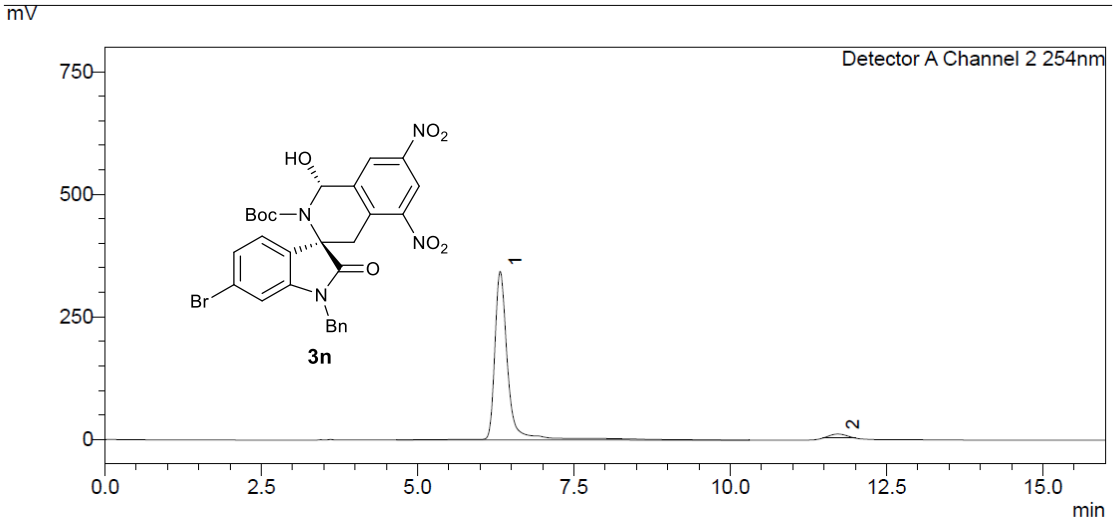

<Peak Table>

Detector A Channel 2 254nm

Peak#	Ret. Time	Area	Height	Conc.	Area%
1	6.321	5129193	343716	97.168	97.168
2	11.721	149468	8271	2.832	2.832
Total		5278662	351987		100.000

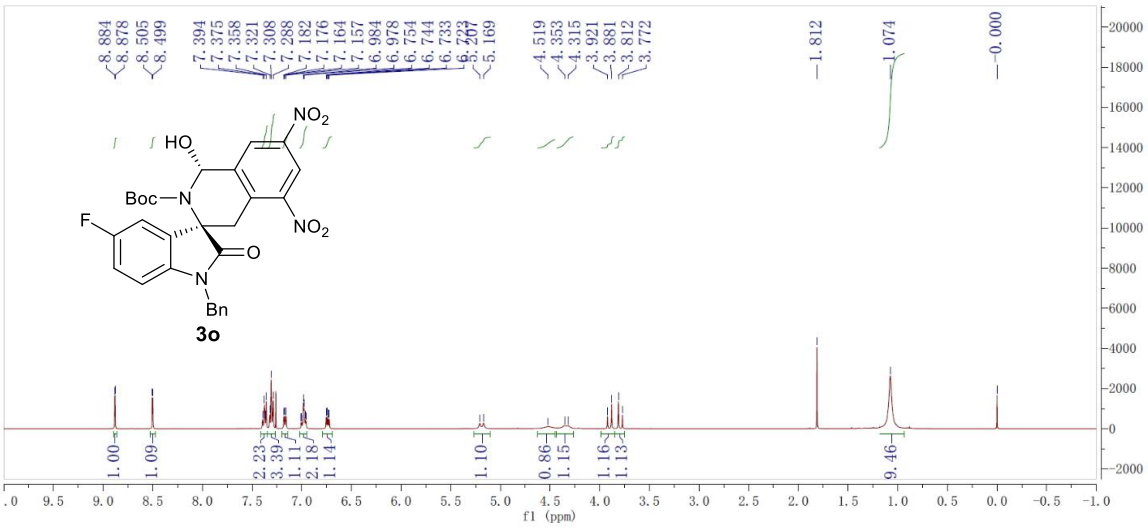
8.884
8.878
8.505
8.499
7.394
7.375
7.358
7.321
7.308
7.288
7.182
7.176
7.164
7.157
6.984
6.978
6.754
6.744
6.733
6.723
5.267
5.169
4.519
4.353
4.315
3.921
3.881
3.812
3.772
1.812
1.074
0.000
NO2
HO
Boc
N
F
O
N
Bn
NO2
3o
1.00
1.09
2.23
3.39
1.11
2.18
1.14
1.10
0.86
1.15
1.16
1.13
9.46
f1 (ppm)

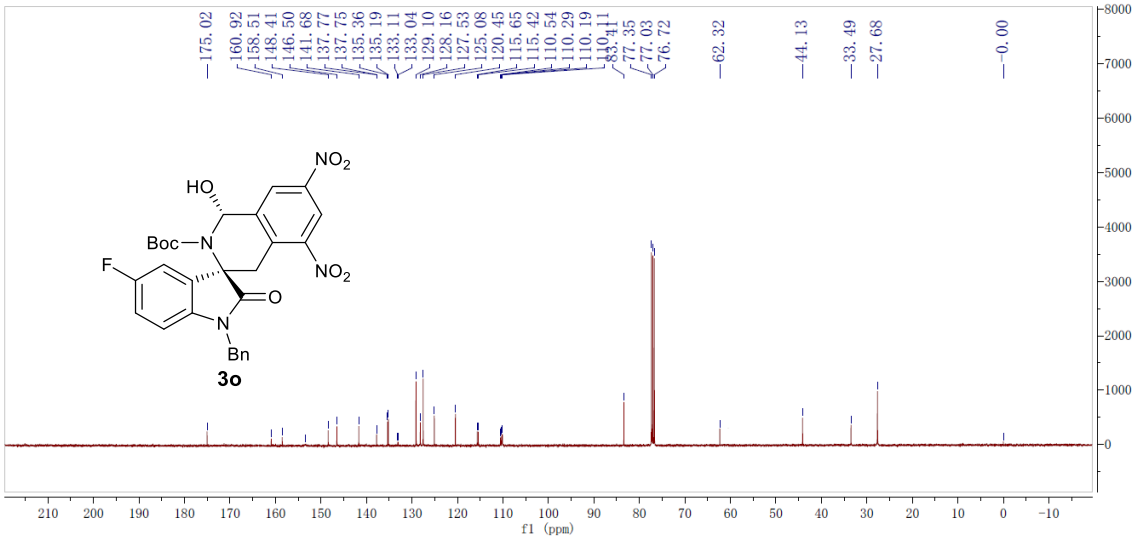
175.02
160.92
158.51
148.41
146.50
141.68
137.77
137.75
135.36
135.19
133.11
133.04
129.10
128.16
127.53
125.08
120.45
115.65
115.42
110.54
110.29
110.19
83.41
77.35
77.03
76.72
62.32
44.13
33.49
27.68
0.00
NO2
HO
Boc
N
F
O
N
Bn
NO2
3o
f1 (ppm)

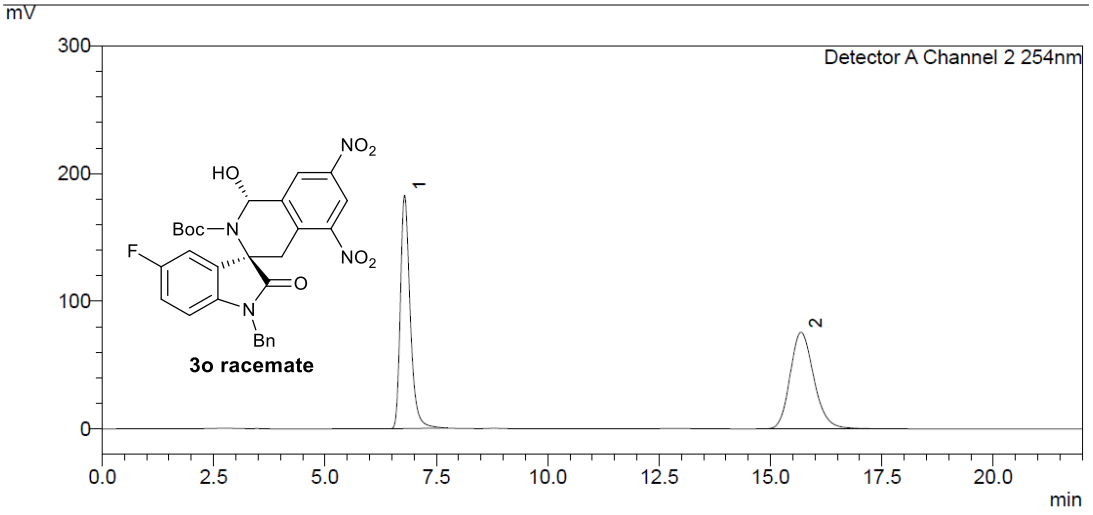

<Peak Table>

Detector A Channel 2 254nm

Peak#	Ret. Time	Area	Height	Conc.	Area%
1	6.787	2794509	182790	49.963	49.963
2	15.686	2798617	75673	50.037	50.037
Total		5593125	258463		100.000

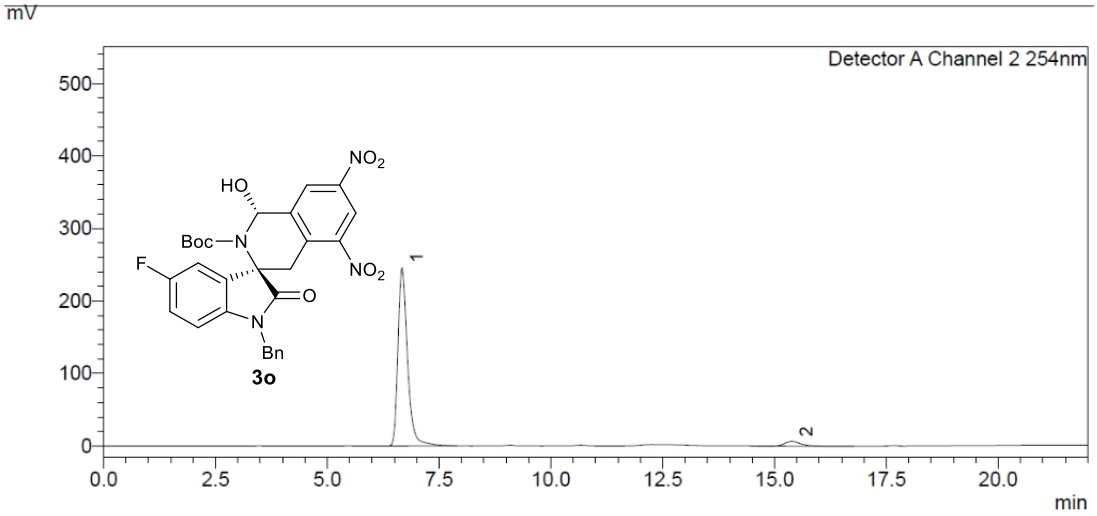

<Peak Table>

Detector A Channel 2 254nm

Peak#	Ret. Time	Area	Height	Conc.	Area%
1	6.672	3667496	245503	96.158	96.158
2	15.342	146551	5796	3.842	3.842
Total		3814047	251299		100.000

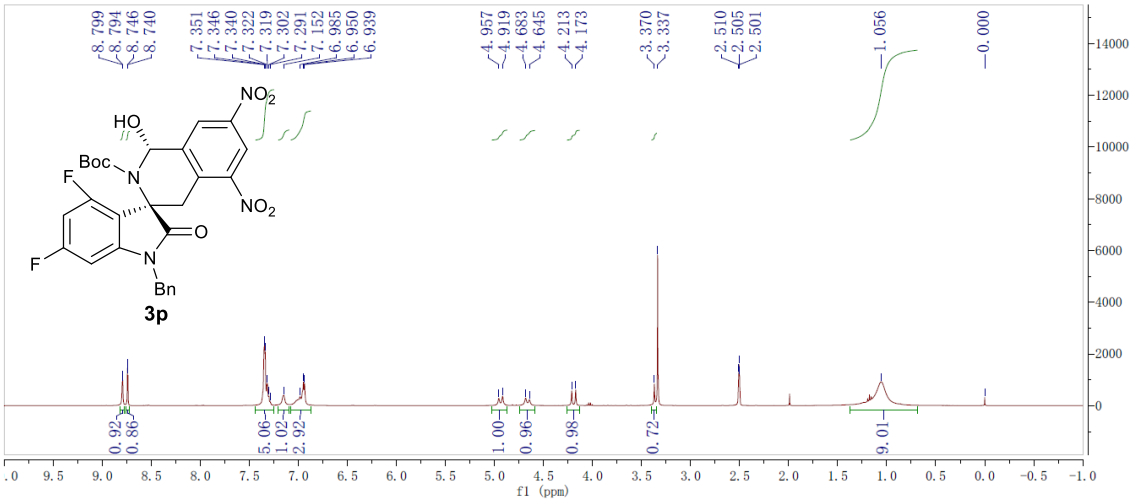
8.799
8.794
8.746
8.740
7.351
7.346
7.340
7.322
7.319
7.302
7.291
7.152
6.985
6.950
6.939
4.957
4.919
4.683
4.645
4.213
4.173
3.370
3.337
2.510
2.505
2.501
1.056
0.000
NO2
HO
Boc
N
F
O
NO2
F
N
Bn
3p
0.92
0.86
5.06
1.02
2.92
1.00
0.96
0.98
0.72
9.01
f1 (ppm)

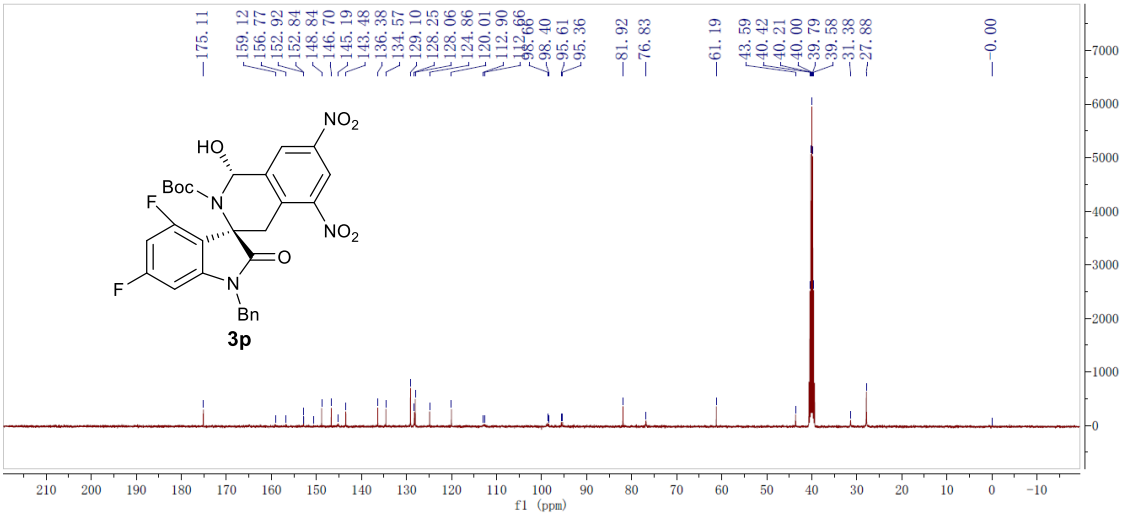
175.11
159.12
156.77
152.92
152.84
148.84
146.70
145.19
143.48
136.38
134.57
129.10
128.25
128.06
124.86
120.01
112.90
98.68
98.40
95.61
95.36
81.92
76.83
61.19
43.59
40.42
40.21
40.00
39.79
39.58
31.38
27.88
0.00
NO2
HO
Boc
N
F
O
NO2
F
N
Bn
3p
f1 (ppm)

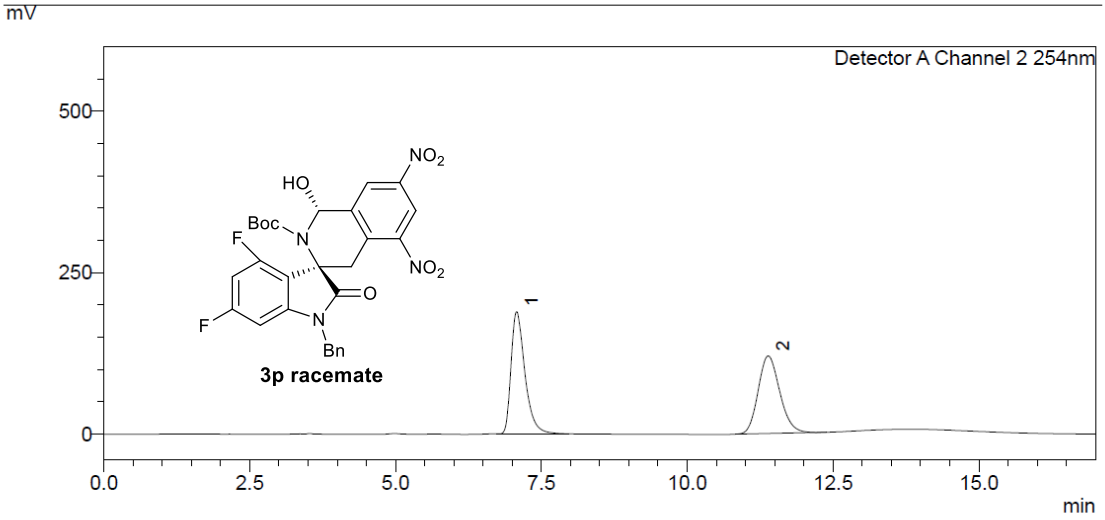

<Peak Table>

Detector A Channel 2 254nm

Peak#	Ret. Time	Area	Height	Conc.	Area%
1	7.077	3121513	189177	50.226	50.226
2	11.389	3093377	120093	49.774	49.774
Total		6214890	309270		100.000

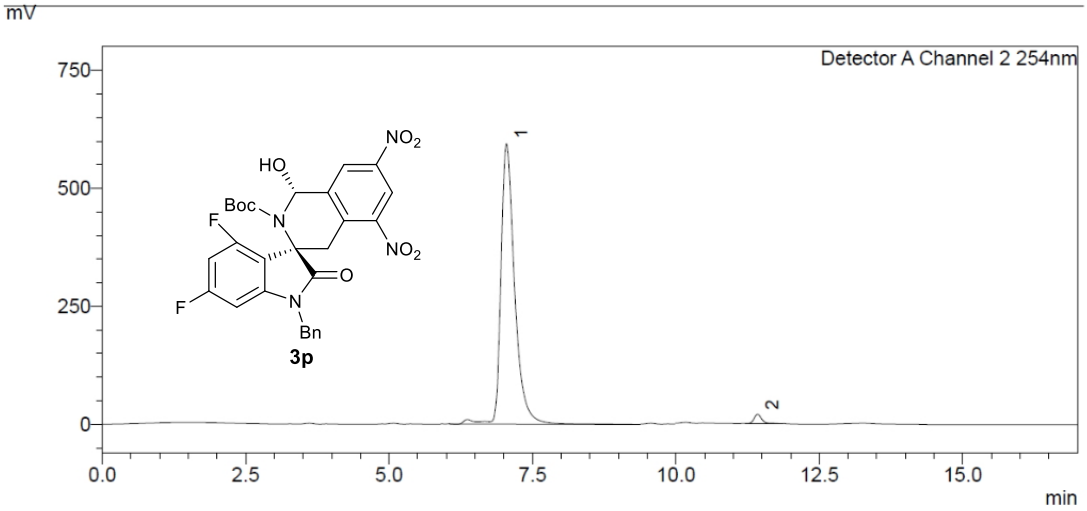

<Peak Table>

Detector A Channel 2 254nm

Peak#	Ret. Time	Area	Height	Conc.	Area%
1	7.048	9959170	593983	97.810	97.810
2	11.397	223015	14574	2.190	2.190
Total		10182185	608557		100.000

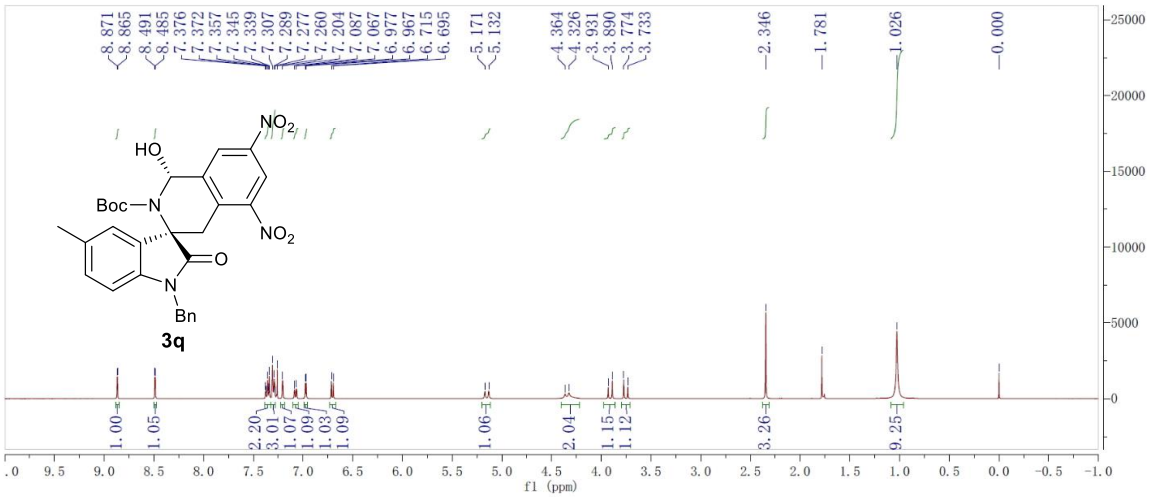
8.871
8.865
8.491
8.485
7.376
7.372
7.357
7.345
7.339
7.307
7.289
7.277
7.260
7.204
7.087
7.067
6.977
6.967
6.715
6.695
5.171
5.132
4.364
4.326
3.931
3.890
3.774
3.733
2.346
1.781
1.026
0.000
NO2
HO
Boc
N
NO2
O
N
Bn
3q
1.00
1.05
2.20
3.01
1.07
1.09
1.03
1.09
1.06
2.04
1.15
1.12
3.26
9.25
f1 (ppm)

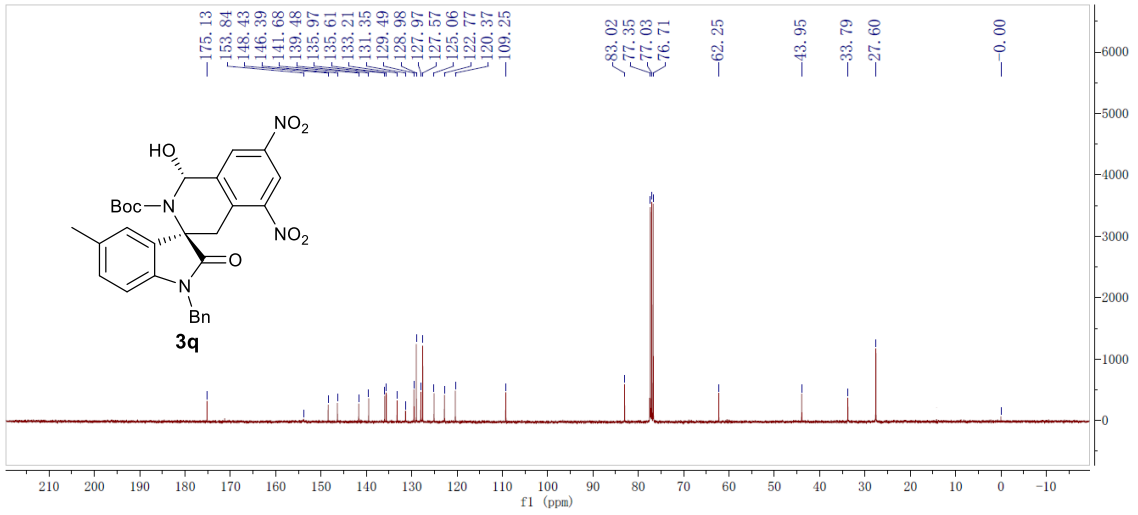
175.13
153.84
148.43
146.39
141.68
139.48
135.97
135.61
133.21
131.35
129.49
128.98
127.97
127.57
125.06
122.77
120.37
109.25
83.02
77.35
77.03
76.71
62.25
43.95
33.79
27.60
0.00
NO2
HO
Boc
N
NO2
O
N
Bn
3q
f1 (ppm)

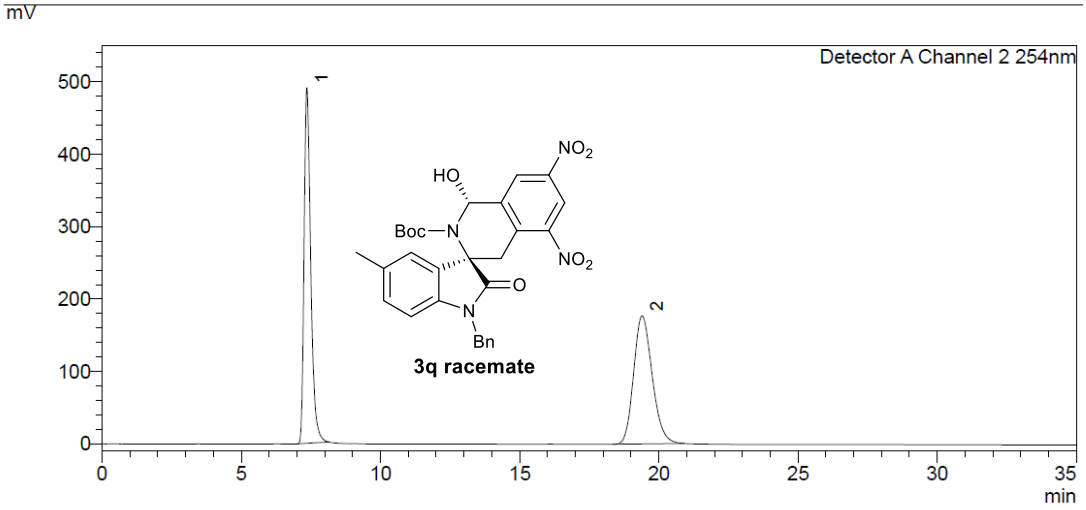

<Peak Table>

Detector A Channel 2 254nm

Peak#	Ret. Time	Area	Height	Conc.	Area%
1	7.356	8173855	491160	49.950	49.950
2	19.399	8190082	176978	50.050	50.050
Total		16363937	668138		100.000

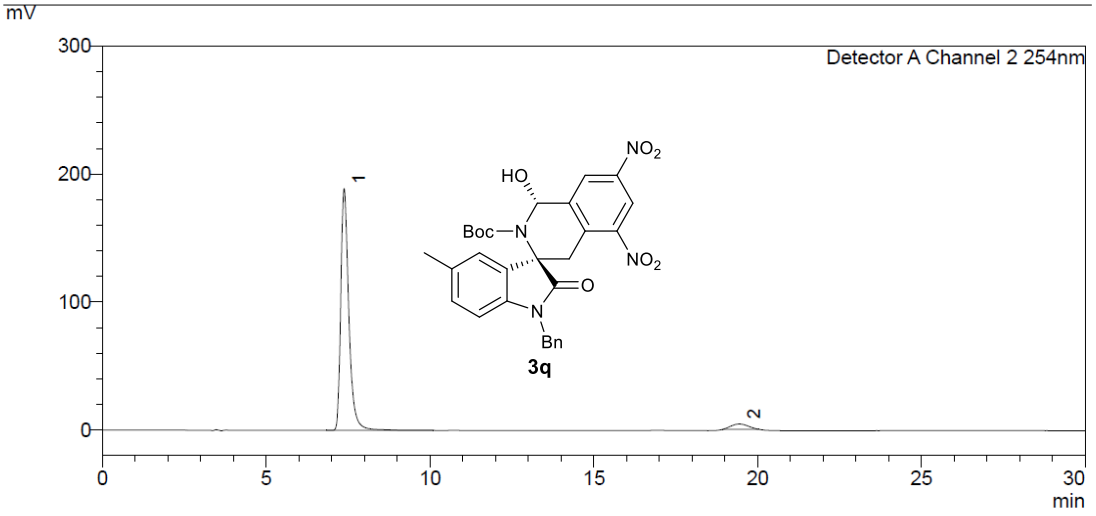

<Peak Table>

Detector A Channel 2 254nm

Peak#	Ret. Time	Area	Height	Conc.	Area%
1	7.374	3235905	188816	95.544	95.544
2	19.435	150918	4147	4.456	4.456
Total		3386822	192963		100.000

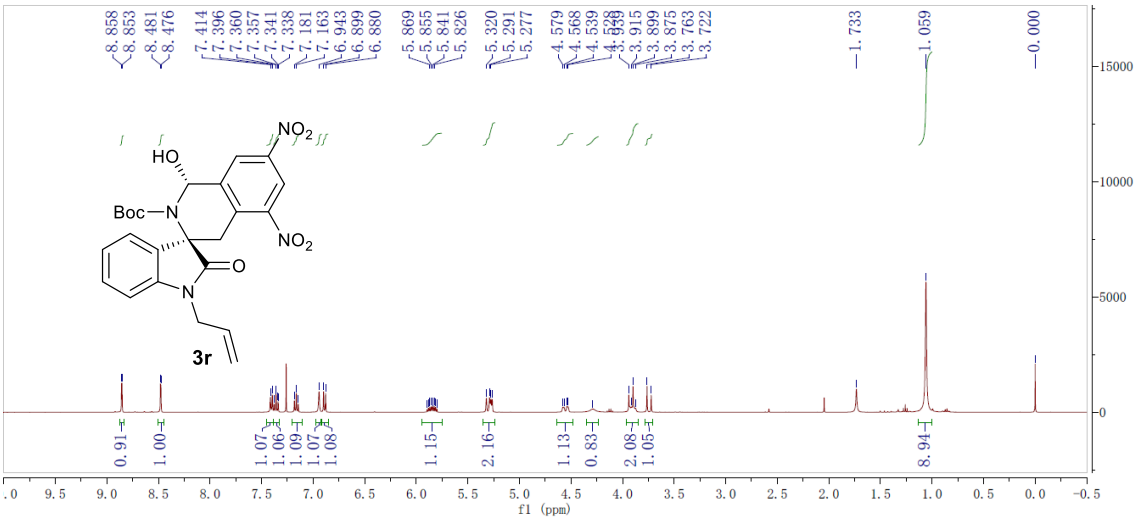
8.858
8.853
8.481
8.476
7.414
7.396
7.360
7.357
7.341
7.338
7.181
7.163
6.943
6.899
6.880
5.869
5.855
5.841
5.826
5.320
5.291
5.277
4.579
4.568
4.539
3.915
3.899
3.875
3.763
3.722
1.733
1.059
0.000
NO2
HO
Boc
N
NO2
O
N
3r
0.91
1.00
1.07
1.06
1.09
1.07
1.08
1.15
2.16
1.13
0.83
2.08
1.05
8.94
f1 (ppm)

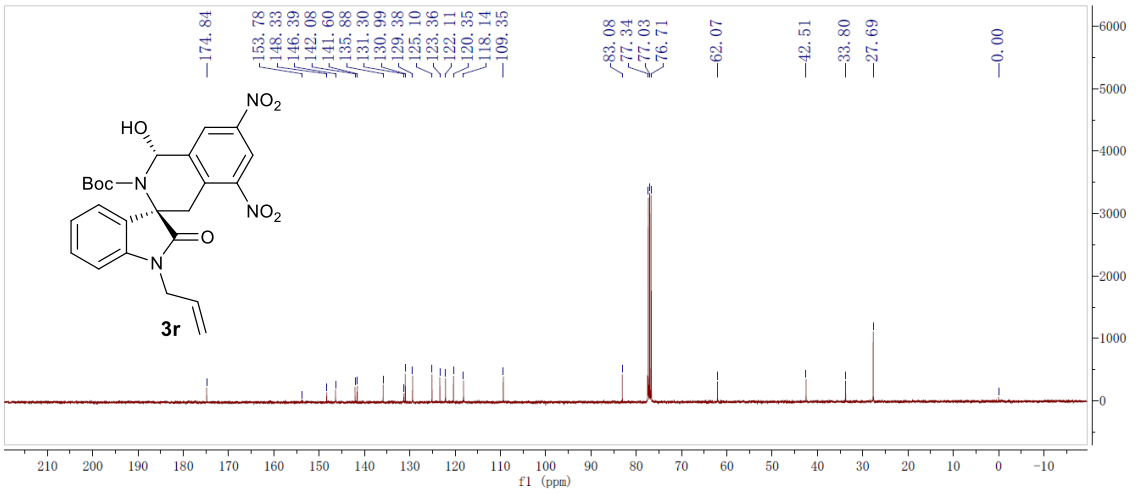
174.84
153.78
148.33
146.39
142.08
141.60
135.88
131.30
130.99
129.38
125.10
123.36
122.11
120.35
118.14
109.35
83.08
77.34
77.03
76.71
62.07
42.51
33.80
27.69
0.00
NO2
HO
Boc
N
NO2
O
N
3r
f1 (ppm)

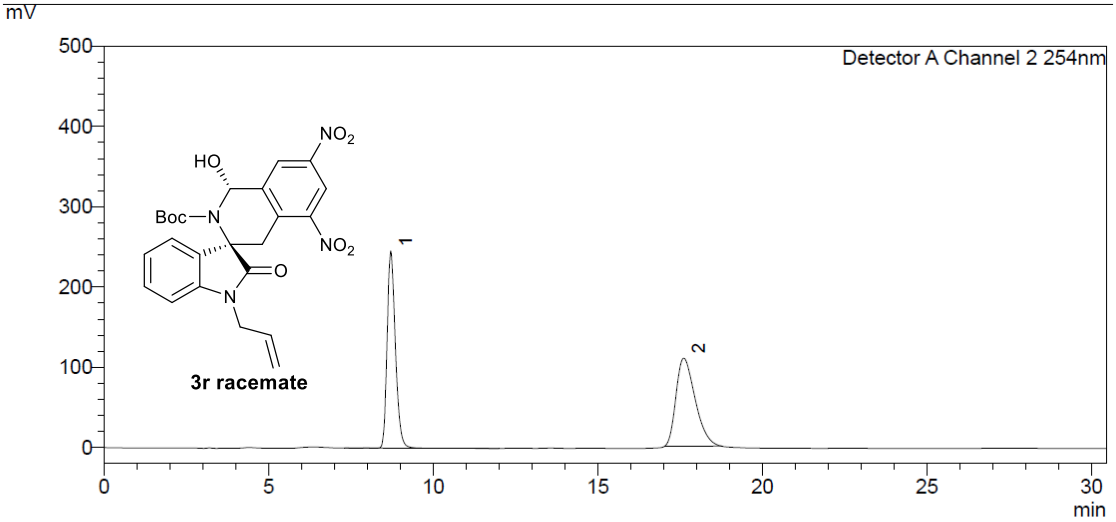

<Peak Table>

Detector A Channel 2 254nm

Peak#	Ret. Time	Area	Height	Conc.	Area%
1	8.707	4310167	245780	49.240	49.240
2	17.611	4443221	109772	50.760	50.760
Total		8753388	355553		100.000

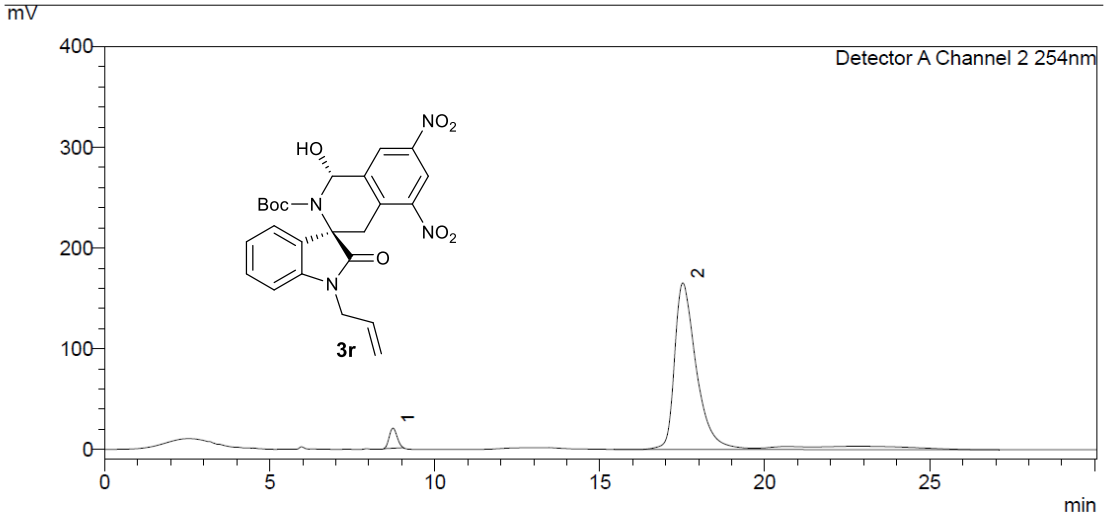

<Peak Table>

Detector A Channel 2 254nm

Peak#	Ret. Time	Area	Height	Conc.	Area%
1	8.732	328477	20049	3.732	3.732
2	17.517	8473352	165440	96.268	96.268
Total		8801830	185489		100.000

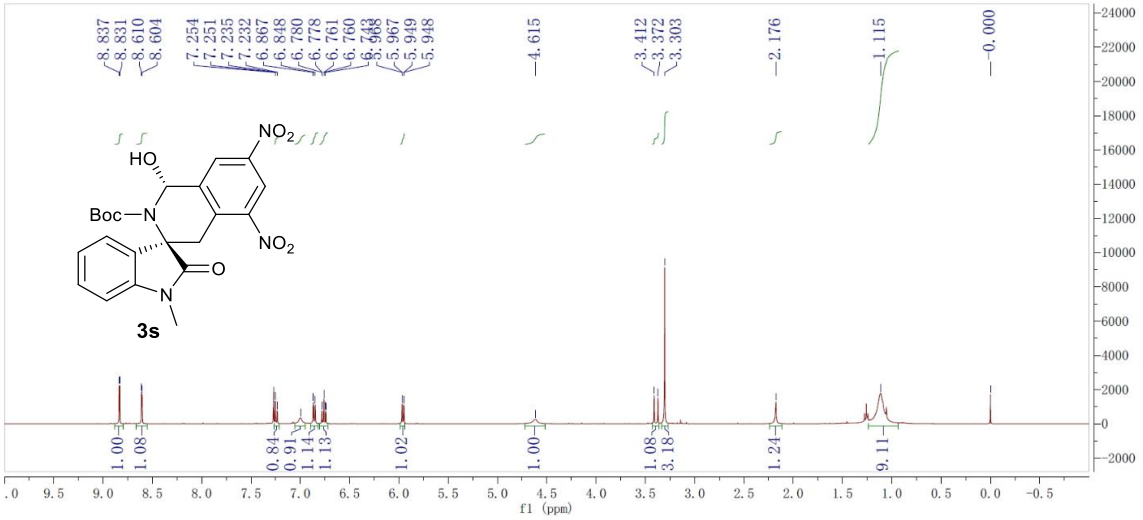
8.837
8.831
8.610
8.604
7.254
7.251
7.235
7.232
6.867
6.848
6.780
6.778
6.761
6.760
5.967
5.949
5.948
4.615
3.412
3.372
3.303
2.176
1.115
0.000
HO
Boc
N
O
NO2
NO2
3s
1.00
1.08
0.84
0.91
1.14
1.13
1.02
1.00
1.08
3.18
1.24
9.11
f1 (ppm)

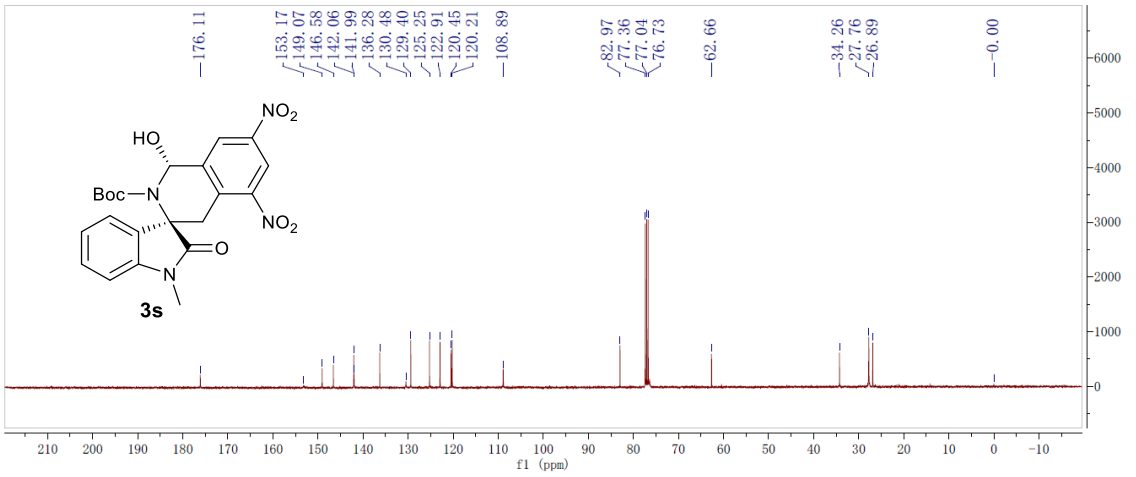
176.11
153.17
149.07
146.58
142.06
141.99
136.28
130.48
129.40
125.25
122.91
120.45
120.21
108.89
82.97
77.36
77.04
76.73
62.66
34.26
27.76
26.89
0.00
HO
Boc
N
O
NO2
NO2
3s
f1 (ppm)

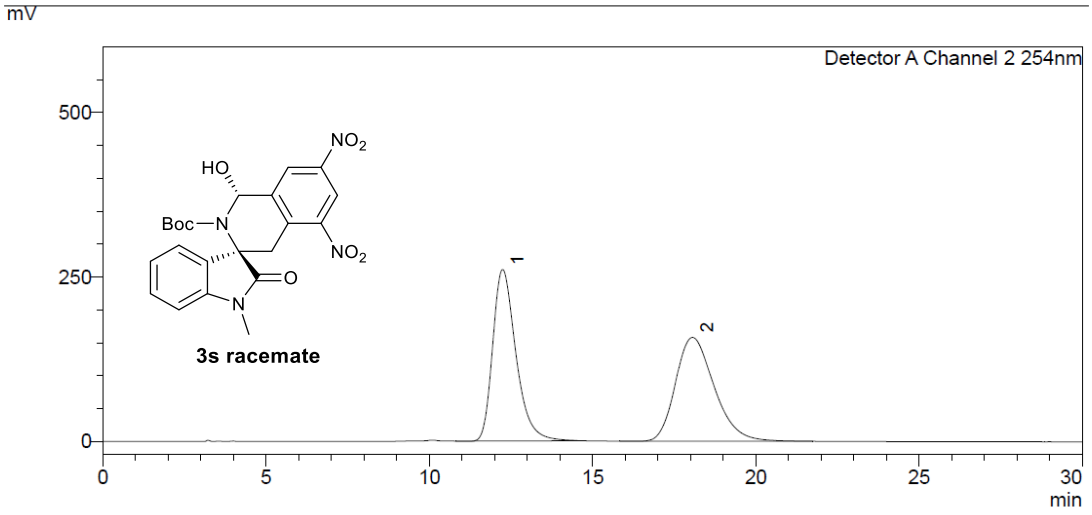

<Peak Table>

Detector A Channel 2 254nm

Peak#	Ret. Time	Area	Height	Conc.	Area%
1	12.240	12891244	260666	49.787	49.787
2	18.055	13001471	157931	50.213	50.213
Total		25892715	418597		100.000

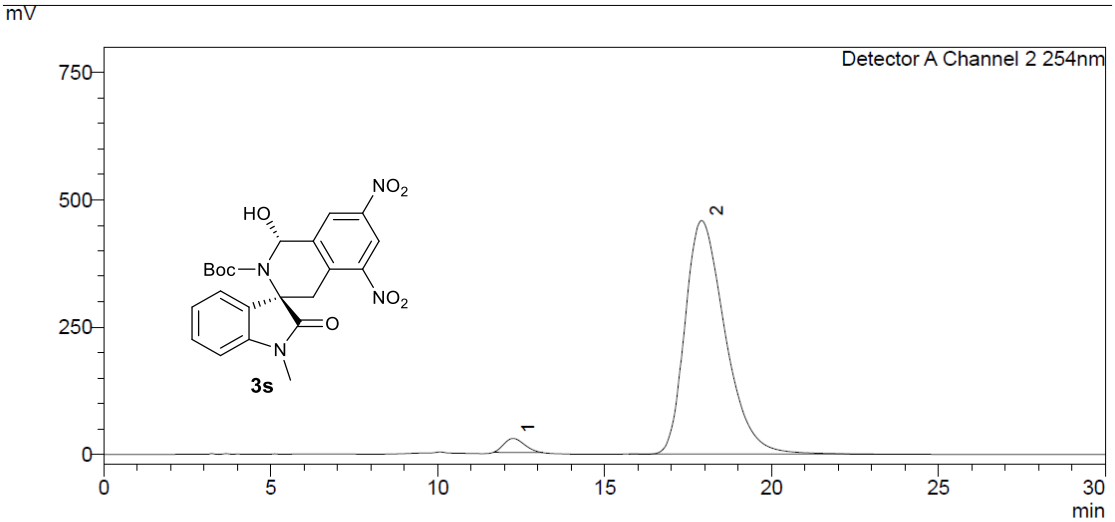

<Peak Table>

Detector A Channel 2 254nm

Peak#	Ret. Time	Area	Height	Conc.	Area%
1	12.258	1179359	27574	2.981	2.981
2	17.903	38377579	458848	97.019	97.019
Total		39556938	486423		100.000

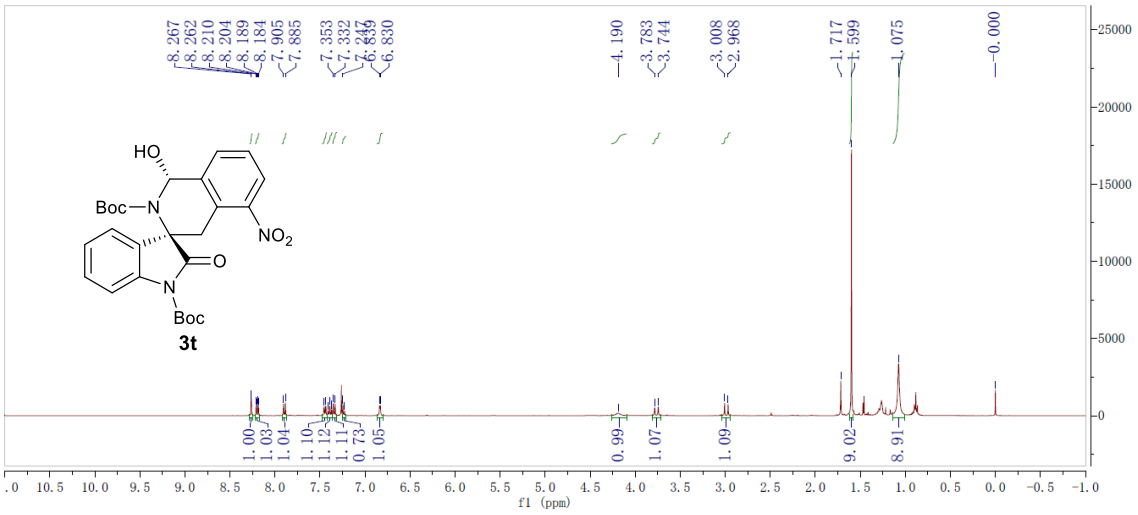
8.267
8.262
8.210
8.204
8.189
8.184
7.905
7.885
7.353
7.332
6.839
6.830
4.190
3.783
3.744
3.008
2.968
1.717
1.599
1.075
0.000
HO
Boc
N
NO2
O
N
Boc
3t
1.00
1.03
1.04
1.10
1.12
1.11
0.73
1.05
0.99
1.07
1.09
9.02
8.91
f1 (ppm)

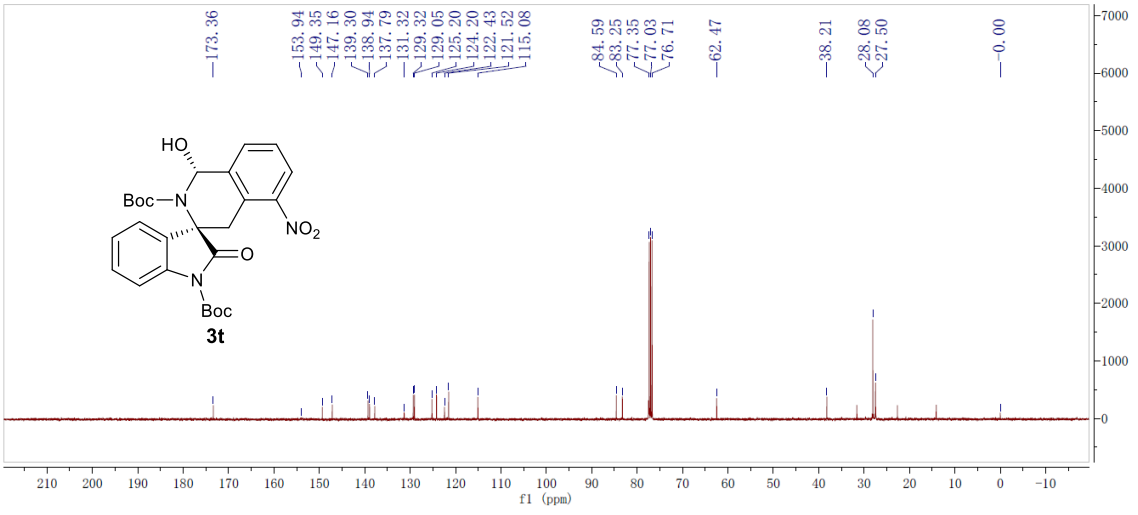
173.36
153.94
149.35
147.16
139.30
138.94
137.79
131.32
129.32
129.05
125.20
124.20
122.43
121.52
115.08
84.59
83.25
77.35
77.03
76.71
62.47
38.21
28.08
27.50
0.00
HO
Boc
N
NO2
O
N
Boc
3t
f1 (ppm)

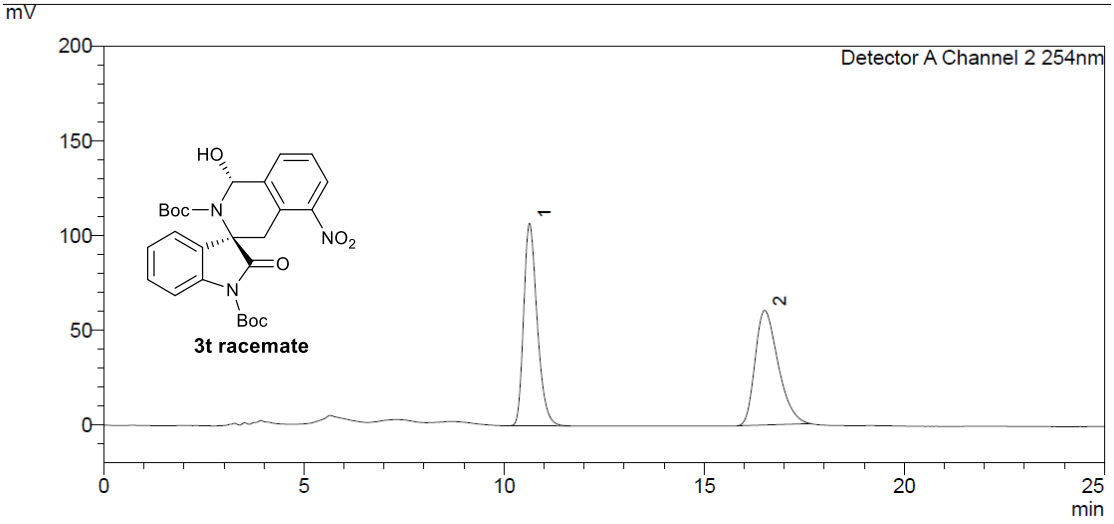

<Peak Table>

Detector A Channel 2 254nm

Peak#	Ret. Time	Area	Height	Conc.	Area%
1	10.634	2512259	106928	50.856	50.856
2	16.511	2427682	60513	49.144	49.144
Total		4939941	167440		100.000

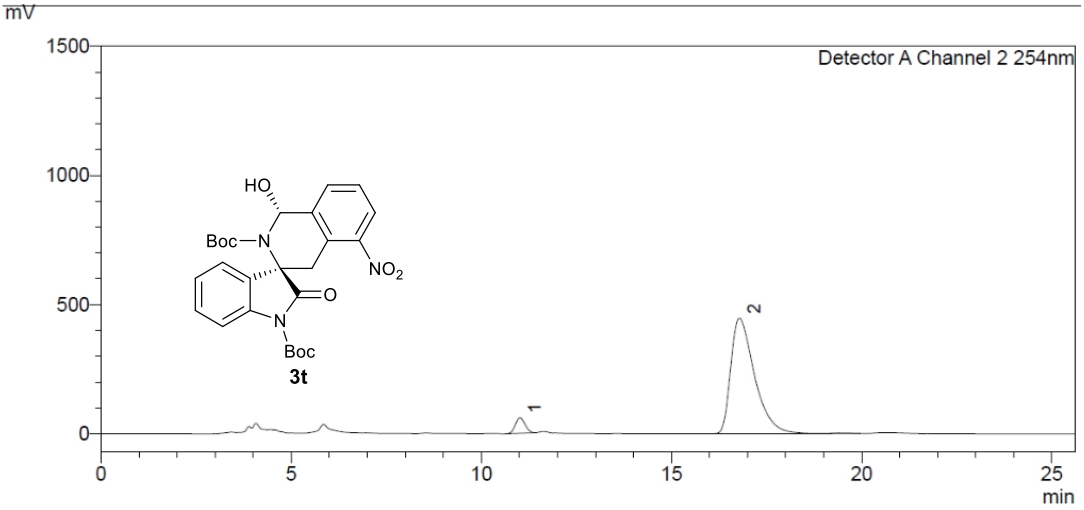

<Peak Table>

Detector A Channel 2 254nm

Peak#	Ret. Time	Area	Height	Conc.	Area%
1	11.000	1113453	140385	5.431	5.431
2	16.789	19388316	447132	94.569	94.569
Total		20501769	587517		100.000

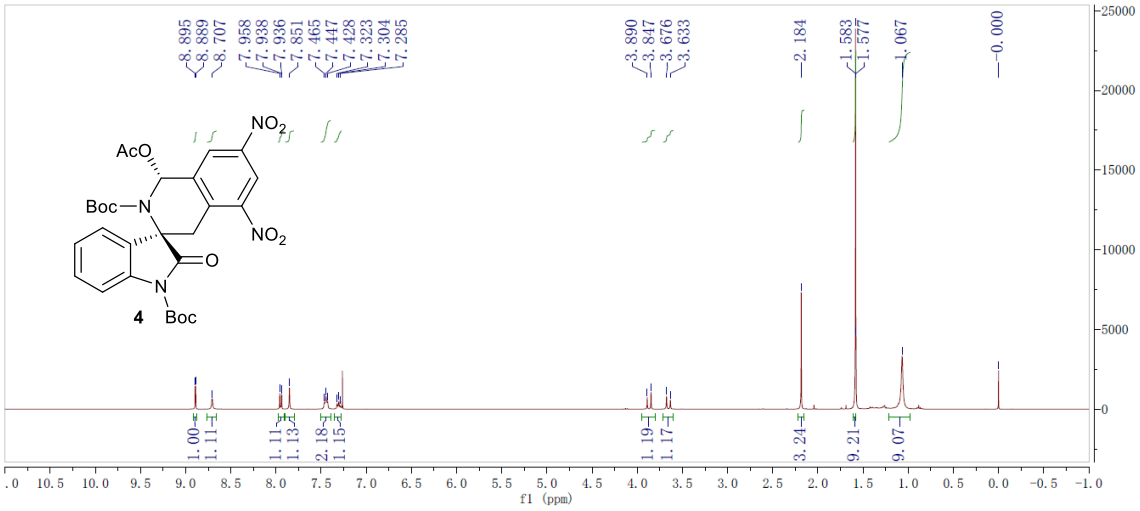
8.895
8.889
8.707
7.958
7.938
7.936
7.851
7.465
7.447
7.428
7.323
7.304
7.285
3.890
3.847
3.676
3.633
2.184
1.583
1.577
1.067
0.000
AcO
Boc
N
NO2
NO2
O
N
Boc
4
1.00
1.11
1.11
1.13
2.18
1.15
1.19
1.17
3.24
9.21
9.07
f1 (ppm)

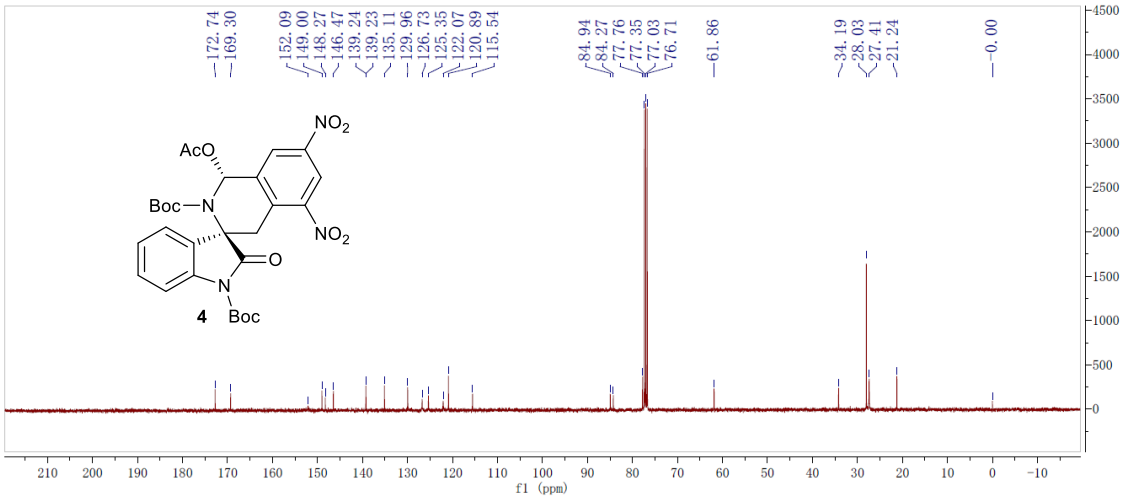
172.74
169.30
152.09
149.00
148.27
146.47
139.24
139.23
135.11
129.96
126.73
125.35
122.07
120.89
115.54
84.94
84.27
77.76
77.35
77.03
76.71
61.86
34.19
28.03
27.41
21.24
0.00
AcO
Boc
N
NO2
NO2
O
N
Boc
4
f1 (ppm)

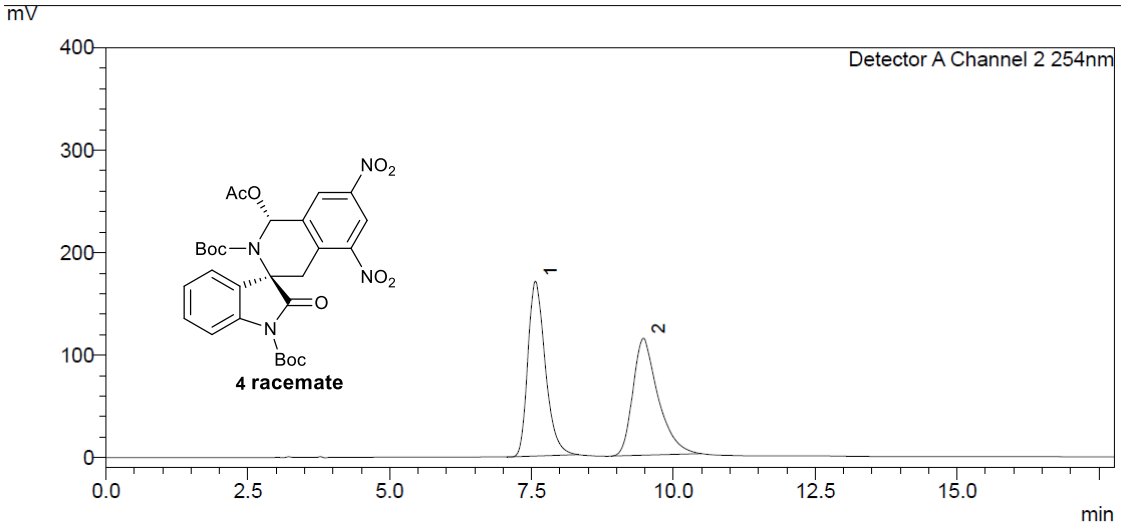

<Peak Table>

Detector A Channel 2 254nm

Peak#	Ret. Time	Area	Height	Conc.	Area%
1	7.568	3651131	170670	50.867	50.867
2	9.472	3526620	114251	49.133	49.133
Total		7177751	284921		100.000

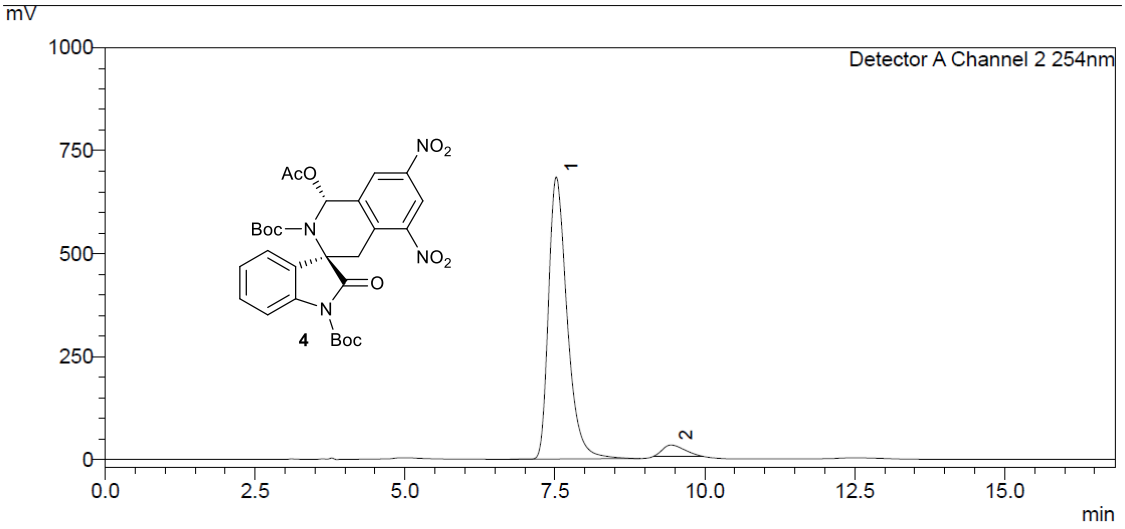

<Peak Table>

Detector A Channel 2 254nm

Peak#	Ret. Time	Area	Height	Conc.	Area%
1	7.522	14799337	684929	95.616	95.616
2	9.431	678578	27404	4.384	4.384
Total		15477916	712333		100.000

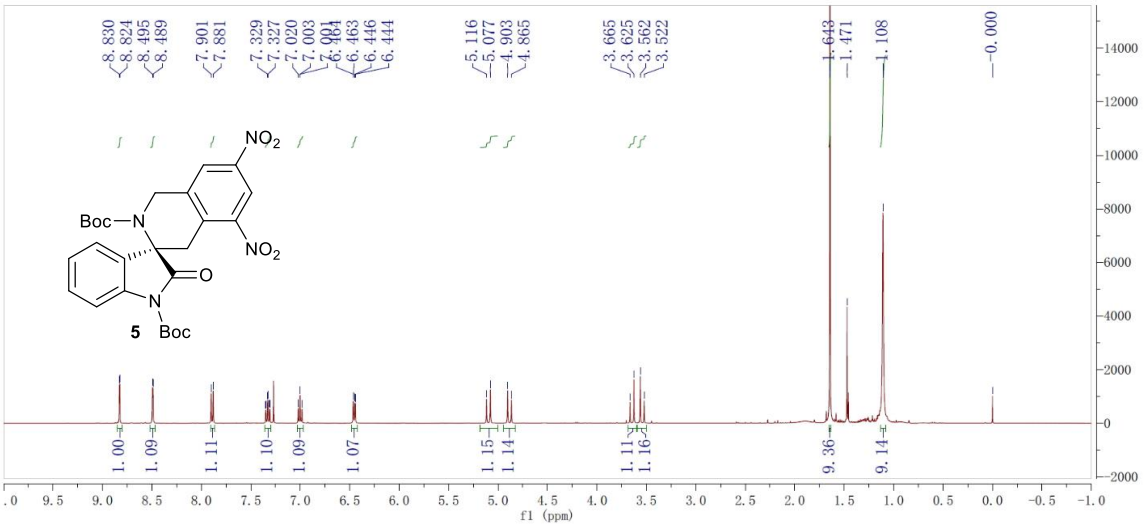
8.830
8.824
8.495
8.489
7.901
7.881
7.329
7.327
7.020
7.003
6.463
6.446
6.444
5.116
5.077
4.903
4.865
3.665
3.625
3.562
3.522
1.643
1.471
1.108
0.000
NO2
NO2
Boc
N
O
N
Boc
5
1.00
1.09
1.11
1.10
1.09
1.07
1.15
1.14
1.11
1.16
9.36
9.14
f1 (ppm)

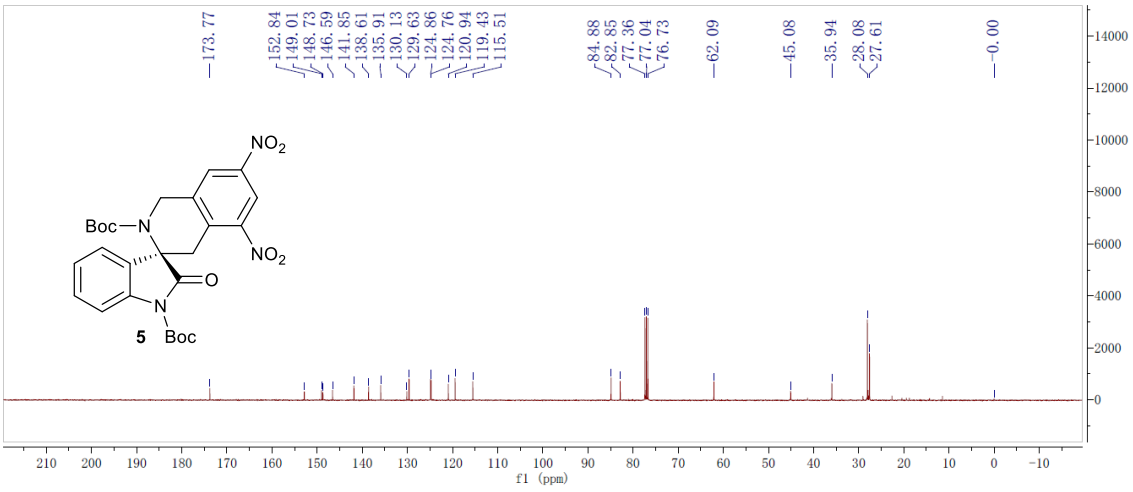
173.77
152.84
149.01
148.73
146.59
141.85
138.61
135.91
130.13
129.63
124.86
124.76
120.94
119.43
115.51
84.88
82.85
77.36
77.04
76.73
62.09
45.08
35.94
28.08
27.61
0.00
NO2
NO2
Boc
N
O
N
Boc
5
f1 (ppm)

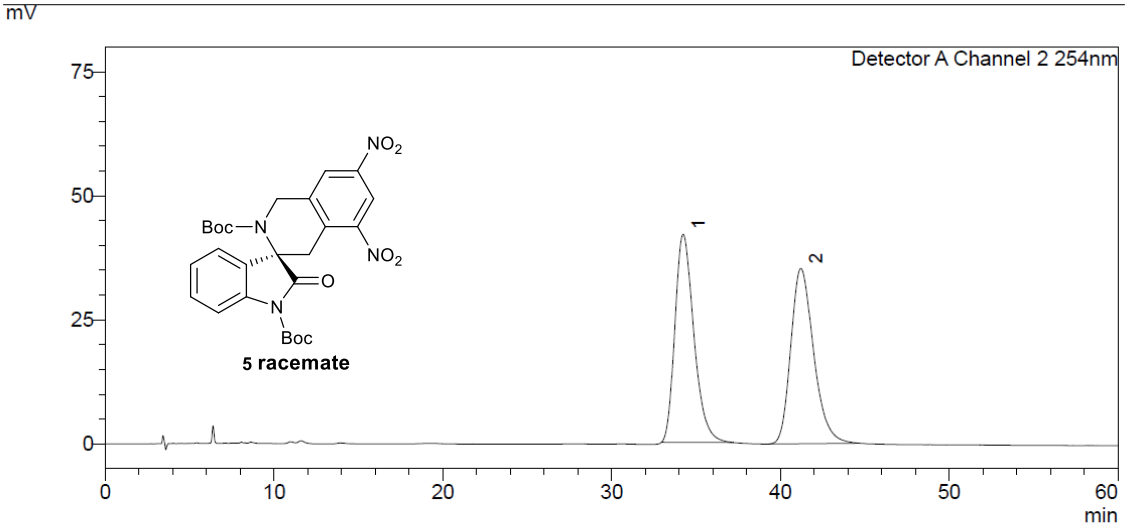

<Peak Table>

Detector A Channel 2 254nm

Peak#	Ret. Time	Area	Height	Conc.	Area%
1	34.231	3276731	41969	49.618	49.618
2	41.205	3327138	35343	50.382	50.382
Total		6603869	77312		100.000

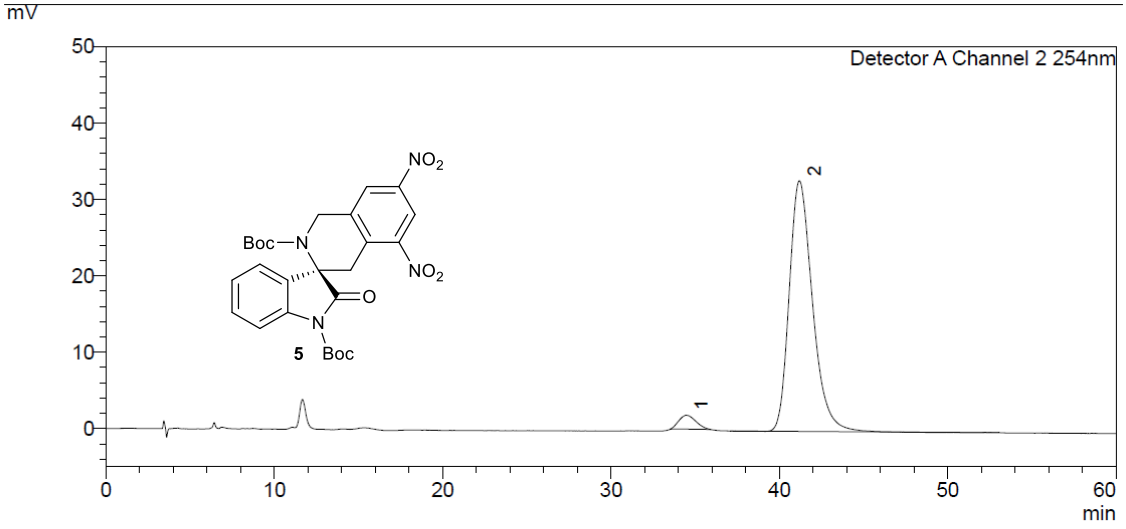

<Peak Table>

Detector A Channel 2 254nm

Peak#	Ret. Time	Area	Height	Conc.	Area%
1	34.464	127341	1815	3.885	3.885
2	41.183	3150492	32826	96.115	96.115
Total		3277832	34641		100.000

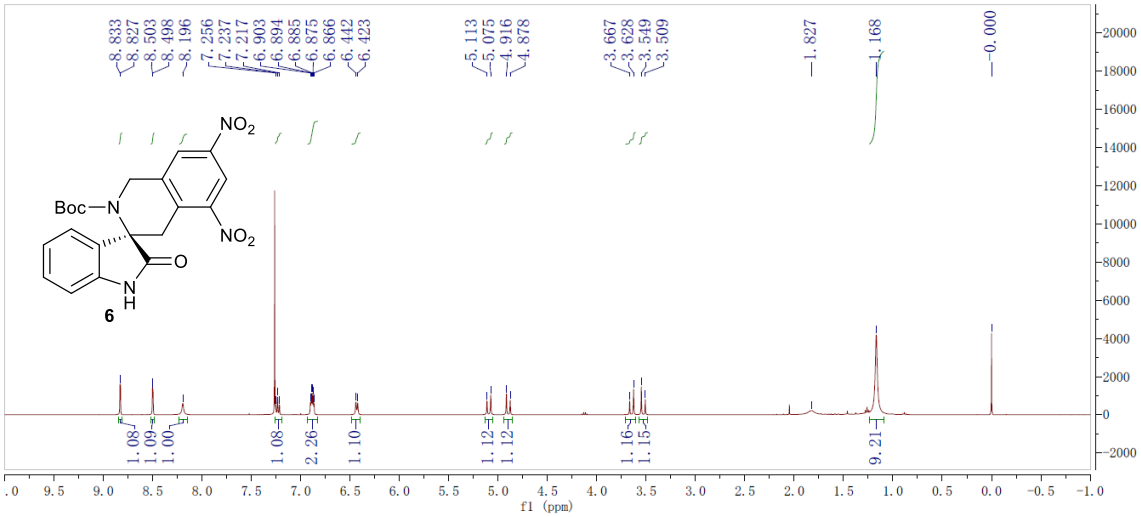
8.833
8.827
8.503
8.498
8.196
7.256
7.237
7.217
6.903
6.894
6.885
6.875
6.866
6.442
6.423
5.113
5.075
4.916
4.878
3.667
3.628
3.549
3.509
1.827
1.168
-0.000
Boc
N
NO2
NO2
O
N
H
6
1.08
1.09
1.00
1.08
2.26
1.10
1.12
1.12
1.16
1.15
9.21
f1 (ppm)

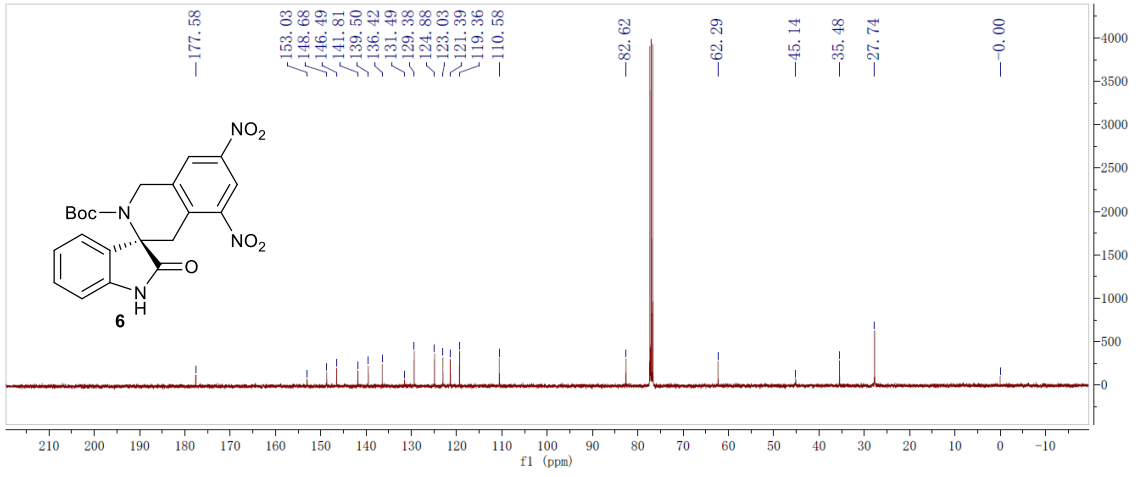
177.58
153.03
148.68
146.49
141.81
139.50
136.42
131.49
129.38
124.88
123.03
121.39
119.36
110.58
82.62
62.29
45.14
35.48
27.74
0.00
Boc
N
NO2
NO2
O
N
H
6
f1 (ppm)

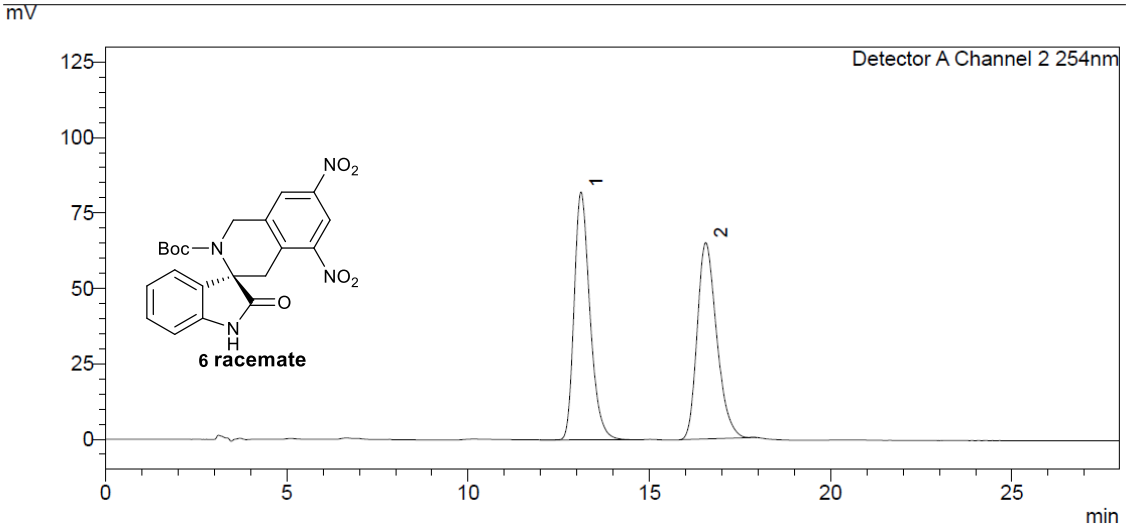

<Peak Table>

Detector A Channel 2 254nm

Peak#	Ret. Time	Area	Height	Conc.	Area%
1	13.116	2485883	82188	50.562	50.562
2	16.556	2430583	65083	49.438	49.438
Total		4916466	147270		100.000

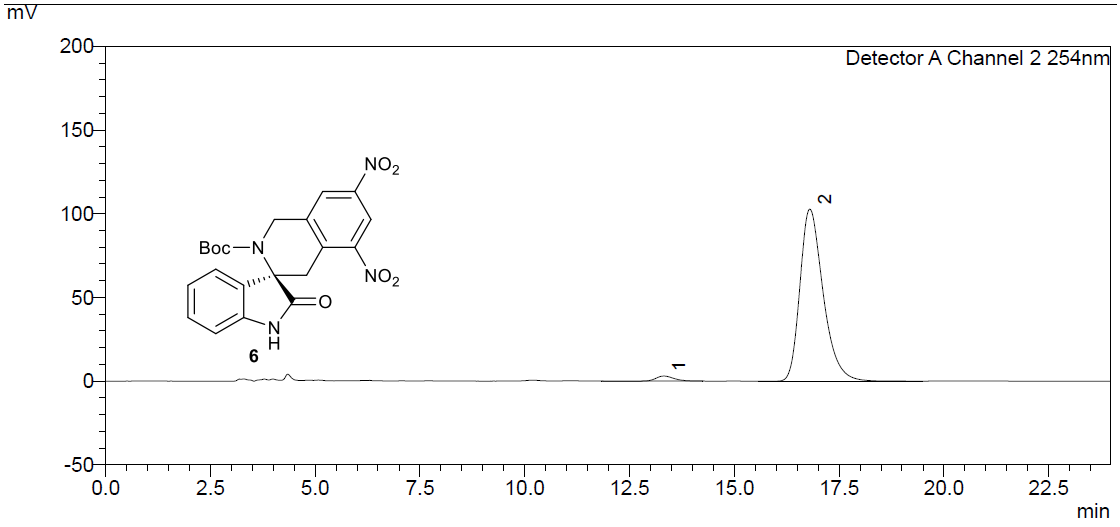

<Peak Table>

Detector A Channel 2 254nm

Peak#	Ret. Time	Area	Height	Conc.	Area%
1	13.318	87887	3046	2.169	2.169
2	16.801	3964613	102878	97.831	97.831
Total		4052500	105924		100.000

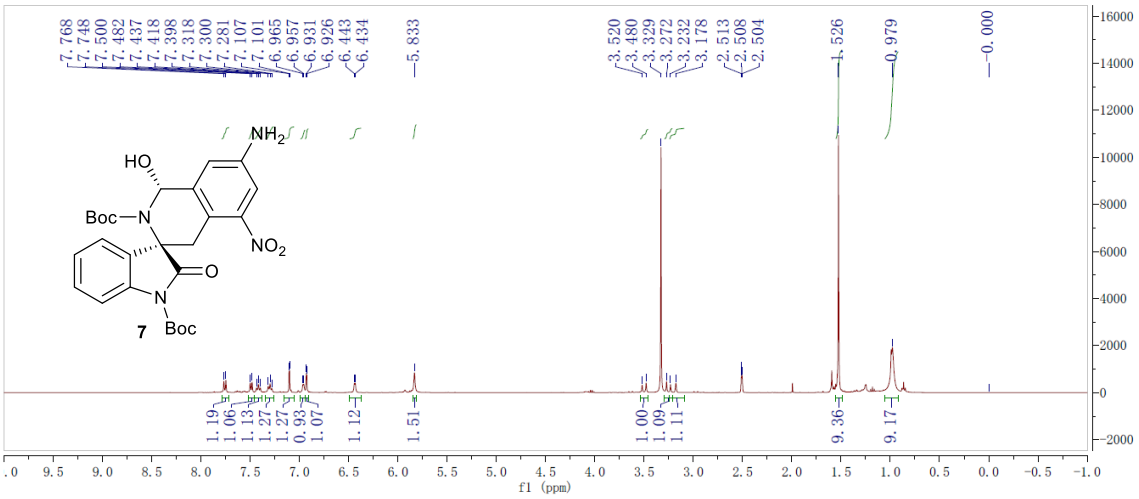
7.768
7.748
7.500
7.482
7.437
7.418
7.398
7.318
7.300
7.281
7.107
7.101
6.965
6.957
6.931
6.926
6.443
6.434
5.833
3.520
3.480
3.329
3.272
3.232
3.178
2.513
2.508
2.504
1.526
0.979
-0.000
NH2
HO
Boc
N
NO2
O
N
Boc
7
1.19
1.06
1.13
1.27
1.27
0.93
1.07
1.12
1.51
1.00
1.09
1.11
9.36
9.17
f1 (ppm)

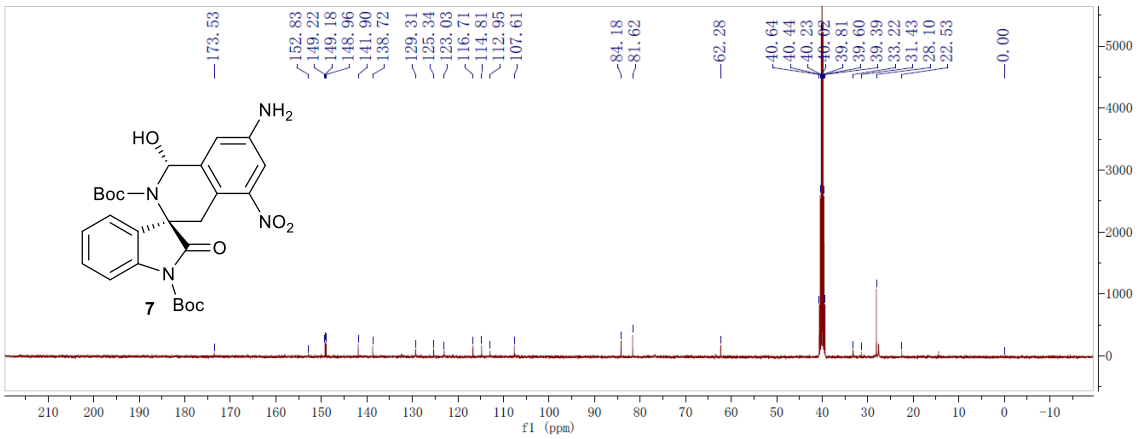
173.53
152.83
149.22
149.18
148.96
141.90
138.72
129.31
125.34
123.03
116.71
114.81
112.95
107.61
84.18
81.62
62.28
40.64
40.44
40.23
40.02
39.81
39.60
39.39
33.22
31.43
28.10
22.53
0.00
NH2
HO
Boc
N
NO2
O
N
Boc
7
f1 (ppm)

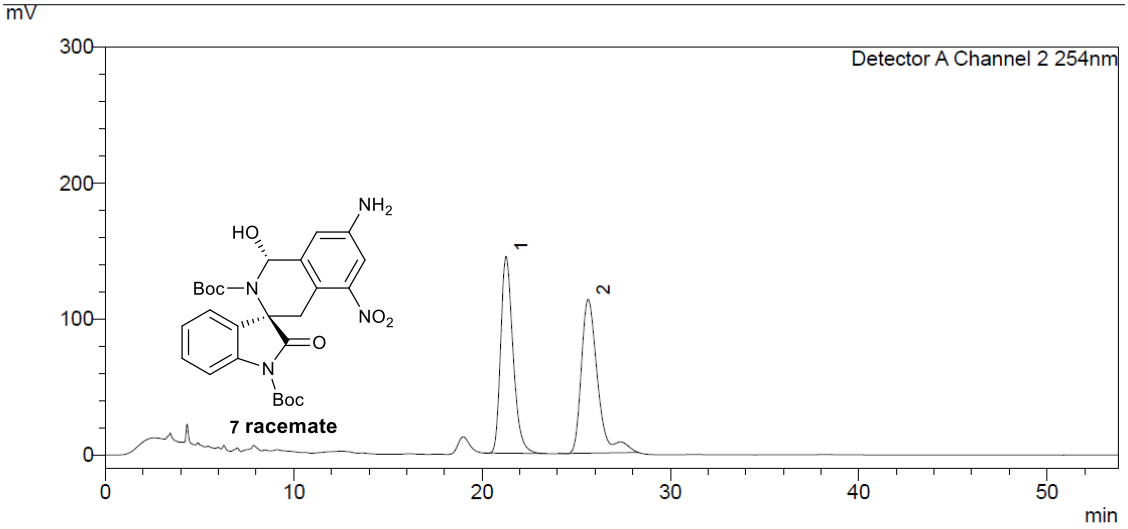

<Peak Table>

Detector A Channel 2 254nm

Peak#	Ret. Time	Area	Height	Conc.	Area%
1	21.271	6599862	144778	49.140	49.140
2	25.630	6830983	113140	50.860	50.860
Total		13430844	257918		100.000

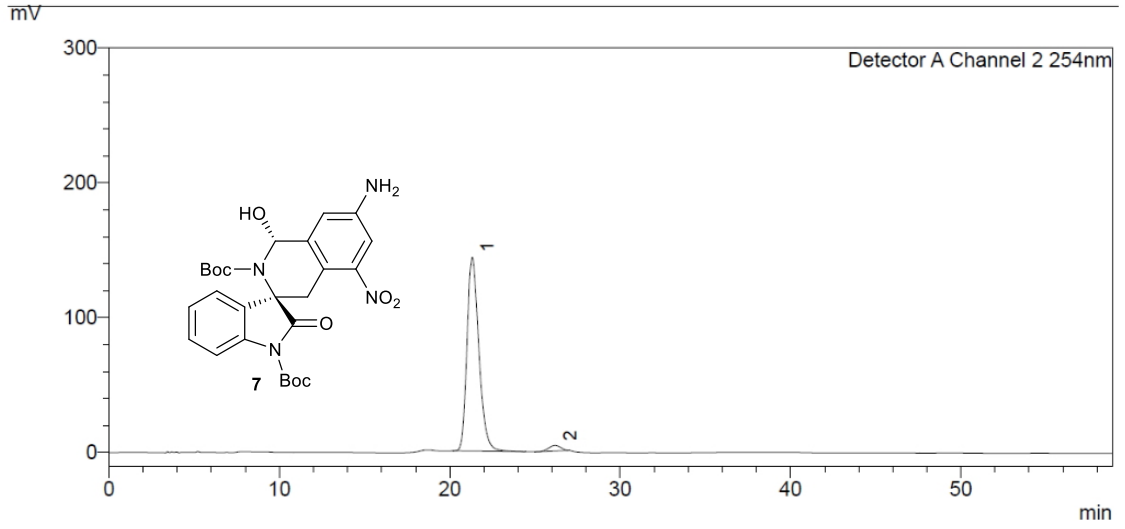

<Peak Table>

Detector A Channel 2 254nm

Peak#	Ret. Time	Area	Height	Conc.	Area%
1	21.311	6977888	143784	97.197	97.197
2	26.181	201210	4114	2.803	2.803
Total		7179098	147899		100.000

6. Preliminary screening of the Ras-GTP and cell proliferation inhibitory activities (Table S2) [a,b]

Compound	Inhibitory ratio (%)				
	Ras-GTP	MDA-MB231	A549	HCT116	Hep3B
3a	19.20	17.15	13.52	19.86	12.30
3b	29.10	17.61	20.46	21.12	16.41
3c	26.00	12.69	25.60	15.42	0.72
3d	33.00	16.18	28.80	15.26	13.05
3e	23.50	5.31	22.10	21.37	3.97
3f	25.00	13.20	18.00	20.50	15.99
3g	18.50	10.39	20.10	14.27	8.51
3h	18.00	15.66	20.80	19.56	20.50
3i	53.00	12.70	40.80	34.46	12.65
3j	74.00	25.23	50.40	55.18	17.41
3k	73.00	24.14	48.80	54.66	21.96
3l	51.00	25.61	39.60	35.62	26.21
3m	80.00	32.92	48.00	68.00	30.50
3n	82.00	25.34	56.20	63.34	26.77
3o	56.00	22.61	39.60	42.92	16.48
3p	58.00	26.82	37.80	56.16	24.64
3q	57.00	25.06	43.20	51.44	30.11
3r	61.00	26.81	37.60	45.62	17.64
3s	60.00	28.04	44.00	47.10	26.46
3t	40.50	25.28	27.30	28.61	1.15
4	28.60	22.68	19.16	18.71	23.08
5	17.40	3.52	12.44	14.01	16.84
6	13.00	20.58	7.80	12.66	6.21
7	17.60	3.76	14.56	16.79	18.41
3m'	33.40	17.04	20.80	24.46	12.65

[a] The enzymatic inhibition were determined from HTRF based assays for Ras-GTP. The cell proliferation inhibitory ratios were determined by using MTT methods; [b] Each compound was tested in triplicate; the data are presented as the mean values.

7. The superposition of binding conforms of 3m and 3m' to Ras-GTP (Figure S2)

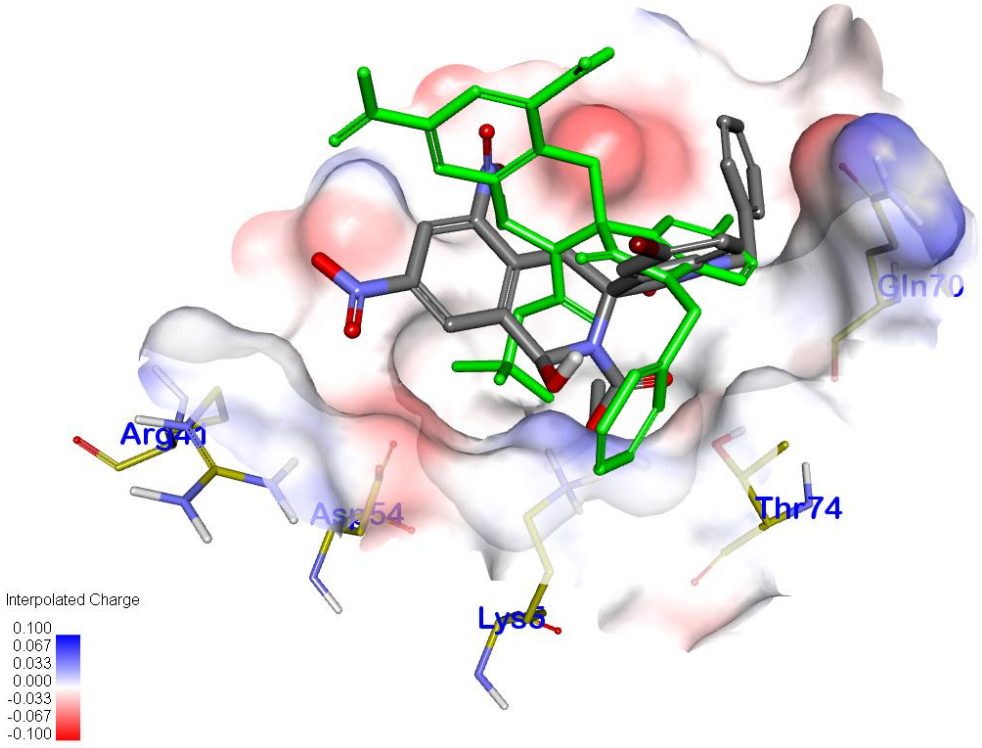

Figure S2. The potential binding modes of **3m** and **3m'** to Ras-GTP, and the enantiomer **3m'** was shown in green as a reference.

8. The cell cycle arrest induced by compound 3m (Figure S3)

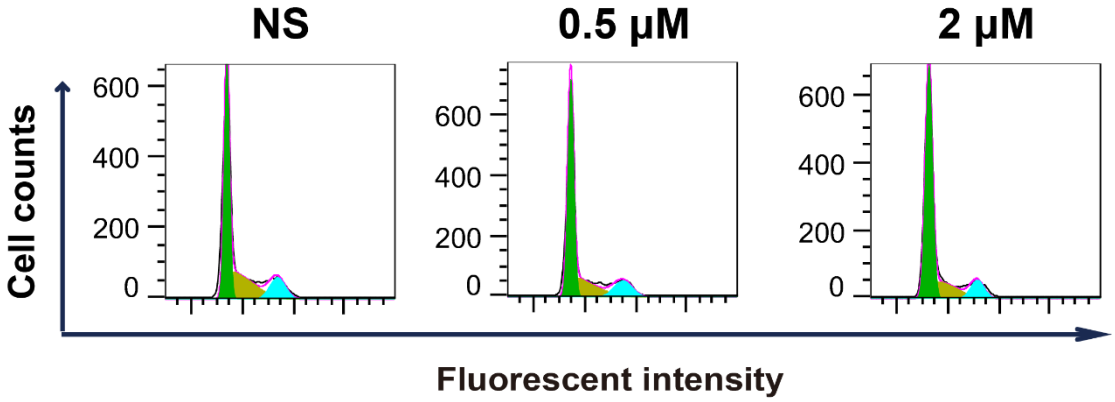

Figure S3. The flow cytometry-based analysis of cell cycles on HCT116 cells with or without **3m** treatment.

9. The results of transwell assays (Figure S4)

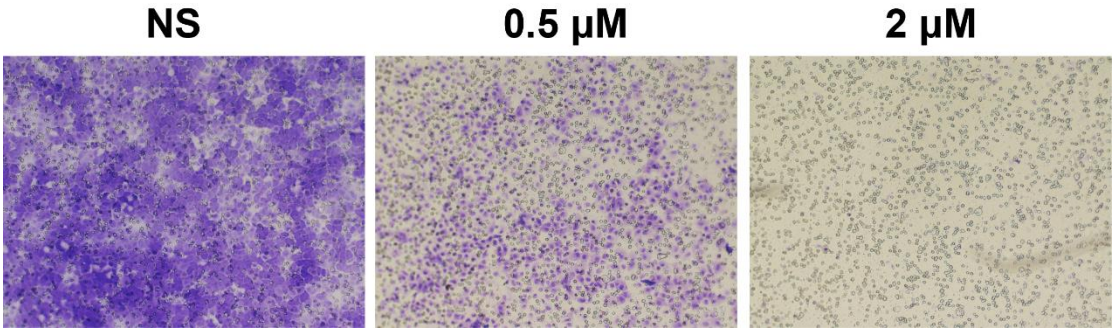

Figure S4. The transwell assays on HCT116 cells with or without **3m** treatment.

10. The WB images of cRaf, GSK3β, MMP-2, β-catenin and N-cadherin (Figure S5)

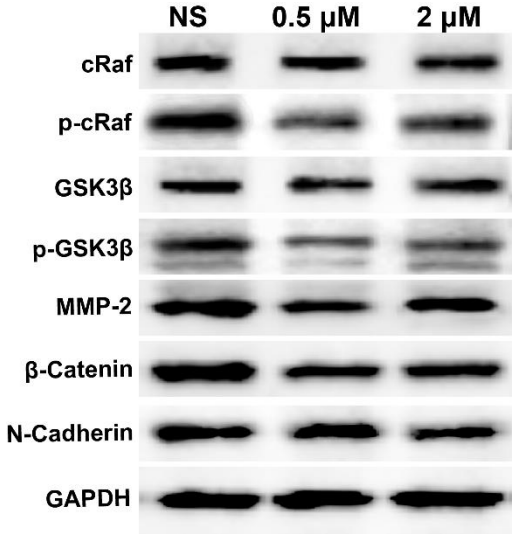

Figure S5. Compound **3m** suppressed activation of cRaf, GSK3β and the expression of MMP-2, β-catenin, N-cadherin, respectively.